Measuring Mucin Gene Expression in Human Airways—Northern Analysis and RT-PCR

Kelly Pritchard, Alinka K. Smith, Duncan F. Rogers

Introduction

Techniques to measure expression and regulation of mucin genes in human airways are aiding understanding of the pathophysiology of a number of severe respiratory conditions. Three of these conditions, namely asthma, chronic obstructive pulmonary disease (COPD) and cystic fibrosis (CF), feature hypersecretion of airway mucus in pathophysiology and clinical presentation [1-3]. Mucus is a generic term for the layer of liquid that overlies the internal surface of the airways [4,5]. The liquid is a dilute solution of proteins, lipids and electrolytes that shields the epithelium from inhaled particles and irritants. The liquid and trapped material are removed from the airways by interaction with the tips of beating cilia, a process termed mucociliary clearance. Mucins are a minor macromolecular component of the liquid (~1-2%) [6]. However, they play a pivotal role in airway homeostasis by conferring upon the mucus the viscoelastic properties essential to mucus-cilia interaction. Changes in airway mucus associated with respiratory disease, including excessive production and changes in biophysical properties, limit the effectiveness of mucociliary interaction and reduce clearance. The associated mucostasis and airway obstruction contribute to pathophysiology and, thereby, the morbidity and mortality associated with asthma, COPD and CF [1-3]. Due to the perceived importance of mucus hypersecretion in these respiratory diseases, a range of research disciplines is directed at attempting to understand the mechanisms underlying development of the hypersecretory phenotype. One possible link in the chain of pathophysiological events is alteration in the genes that encode mucins. Consequently, measurement of mucin gene expression in human airways, including comparison with controls and between diseases, is an area of increasingly active research.

Thirteen human mucin genes are currently recognised and these are designated according to human genome mapping conventions by the letters MUC followed by a number that reflects the order in which they were cloned: MUC1-4, MUC5AC, MUC5B, MUC6-9 and MUC11-12 [7-18]. Mucin gene structures for MUC1-9 are depicted in Figure 1 Most mucin genes were identified by screening from cDNA libraries using antibodies raised against purified deglycosylated core proteins of mucins [19] and were distinguished on the basis of their chromosome location and pattern of tissue expression [20]. The open reading frames (ORFs) of the mucin genes, deduced from complete and partial cDNA clones, share certain characteristic features including tandem repeats, cysteine-rich domains and extensive glycosylation. At present there are only complete cDNA sequences for MUC1, 2, 4, 5B, 7 and 9 [21-22]. MUC2, 5AC, 5B, 6, 7 and 8 are secretory mucins whereas MUC1, 3, 4 and 12 are thought to be membrane bound [10, 23-24]. Apart from MUC9 (also known as oviductin due to its

Department of Thoracic Medicine, National Heart and Lung Institute, Imperial College London, U.K.
Address reprint requests to: Dr. D.F. Rogers, Thoracic Medicine, National Heart & Lung Institute, Imperial College, Dovehouse Street, London SW3 6LY, U.K.

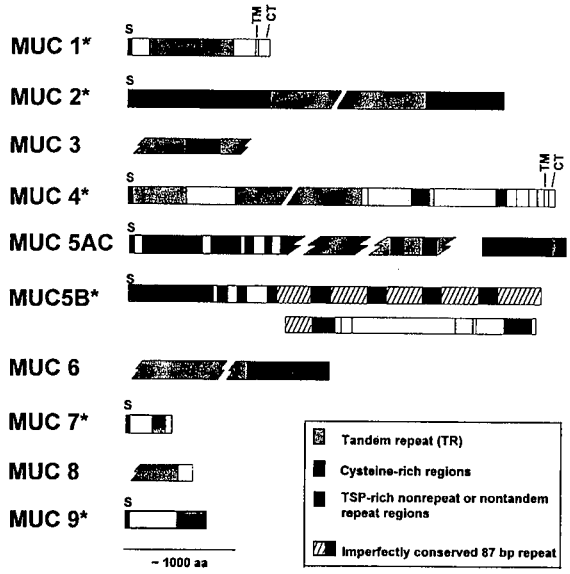

Fig. 1. Models of the first ten mucin (MUC) gene products to be described. The structures were derived either from nucleotide sequences of completely sequenced MUC genes (*) or from cDNA clones. Breaks represent long tandem repeat regions; ragged ends represent sequences awaiting elucidation. TM = proposed transmembrane domain, CT = proposed cytoplasmic tail, S = signal.

localisation to the oviduct), messenger RNA (mRNA) for many of the MUC genes is found to some extent in human adult respiratory epithelium [25], in particular MUC1, MUC2, MUC4, MUC5AC and MUC5B [26-27]. The relative contribution of different MUC genes and their protein products in healthy and diseased airways is currently receiving attention. Altered MUC gene expression has been observed in certain airway diseases. For example, MUC2 expression is upregulated in the nasal mucosa of patients with CF [28], whilst MUC1, MUC3 and MUC4 are upregulated in lung adenocarcinomas [29]. In addition, MUC1 is abundantly expressed and under-glycosylated in a number of other human cancers [30]. Various inflammatory mediators also alter MUC gene expression in human airways *in vitro*, for example TNFα [31].

Mucin mRNA from airway tissues may be examined using standard molecular techniques such as Northern blotting [32] and reverse transcription-polymerase chain reaction (RT-PCR), but there are specific problems necessitating technical modifications. The main difficulty is that MUC genes have large transcript sizes (2.4-40 kb) [33] which can lead to inefficient transfer during Northern blotting from the agarose gel to the nylon membrane prior to hybridization. MUC mRNA is also relatively sensitive to mechanical degradation. Many MUC genes (but not MUC1 or MUC7) have a high degree of polydispersity and are detected as either smears or wide bands, rather than a distinct band of predicted size [33]. The smears could be caused either by rapid turnover of mRNA, several related genes producing varied transcript lengths, alternative splicing, or were simply artifacts. Debailleul and colleagues [33] modified the method of RNA purification to reduce mechanical degradation. They concluded that the polydispersity was not an artifact but was due to allelic variations which are directly related to the variable number of tandem repeat (VNTR) polymorphisms seen at the DNA level.

The present article describes Northern analysis and RT-PCR for the study of airway mucin gene expression. The methods are used with the modifications suggested by Debailleul and colleagues [33] for large transcript sizes. Precise details of the measurement of human airways MUC gene expression by Northern blotting, including step-by-step protocols, can be found in Pritchard *et al* [34]. Total RNA is extracted from airway tissue using either a method based upon guanidinium isothiocyanate, which is relatively inexpensive, or TRIzol reagent, which is considerably more expensive, and is then analysed by either Northern blotting or RT-PCR. For Northern analysis, the RNA is electrophoresed on a denaturing agarose gel to separate RNA according to molecular weight, and is then transferred by capillary action onto a nylon membrane. The RNA on the membrane is cross-linked by UV light to stabilise it and hybridised to a specific radiolabeled cDNA probe. The membrane is then exposed to X-ray film and the RNA under investigation appears as a dark

band on the film. Glyceraldehyde-3-phosphate dehydrogenase (GAPDH) is a common gene used as an internal standard to ascertain that the RNA has not degraded, is present in sufficient amounts on the membrane to be detected, and also for quantification purposes [35-36]. For PCR, the RNA is DNAse treated to remove genomic DNA and is reverse transcribed to convert RNA into cDNA. This is followed by PCR to amplify the DNA sequence of interest. The PCR product is run on an agarose gel to visualise the PCR product. GAPDH is again used as an internal standard to check for equality of loading. For both Northern analysis and RT-PCR, densitometry is used to quantify the RNA under investigation in relation to the amount of GAPDH present.

Tissue Collection for RNA

Lung tissue can be obtained either at surgery, for example for lung carcinoma [37], or at autopsy. MUC gene expression can also be measured in cultured epithelial cells, including primary cells, taken for example at bronchoscopy by 'brushing' the airways, and respiratory epithelial cell lines, for example A549 cells [25]. The samples we obtain at surgery are from segmental bronchi (approximate size 1.5 cm long x 0.3 cm outside diameter), subsegmental bronchi (approximate size 0.5 x 0.5 cm), and parenchyma (2 x 1 cm is more than enough for RNA extraction and subsequent analysis). Occasionally, samples from larger bronchi become available. Samples are immersed for several minutes in ice cold, aerated Krebs-Henseleit solution, after which they are frozen as small segments in liquid nitrogen and stored at -70°C until required. RNA may also be extracted from tissue frozen immediately after surgery (i.e. without a Krebs-Henseleit wash). It is important that the tissue is frozen as quickly as possible (e.g. within 1-2 hours) to reduce RNA breakdown by RNAses. RNA*later* is a useful solution to put the tissue in straight away and can be stored at room temperature for one week and at 4°C for one month or longer.

RNA Extraction for Northern Analysis

For Northern analysis, total RNA can be isolated by either one of the two methods outlined below, namely the solution D method or the TRIzol method. The advantage of the solution D method is that it is cheaper than the TRIzol method. However, although more expensive, the TRIzol method is much quicker, taking only a few hours compared with approximately a day for the solution D method. Both methods have the adaptation that homogenisation, vigorous shaking and vortexing were avoided to limit mechanical degradation of large mRNA transcripts [33].

1. The solution D method

The solution D method is based on the guanidinium-phenol-chloroform procedure [38]. Tissues are ground to a fine powder in liquid nitrogen using a pestle and mortar. The tissue must not be allowed to thaw, so liquid nitrogen should be poured on continually. The powdered tissue is immediately resuspended in solution D (4 M guanidinium thiocyanate, 25 mM sodium citrate pH 7.0, 0.5% sodium *N*-lauroylsarcosine and 0.1 M 2-mercaptomethanol). The RNA is then separated out using a solution of sodium acetate, water-saturated phenol, and chloroform-isoamyl alcohol. The solution is mixed gently and left to settle on ice before centrifugation. The aqueous phase containing the RNA is transferred to a fresh tube and the RNA is precipitated with isopropanol. After centrifugation, the resulting pellets are resuspended in solution D and precipitated for a second time in isopropanol overnight. The final pellet is washed with ethanol and freeze dried in a vacuum dessicator. The optical density of an aliquot of the reconstituted pellet is measured to calculate yield according to the following equation:

[RNA] μg/ml = A_{260} × 44.19 × dilution factor s ÷ 1000

where A_{260} is the absorbance at 260 nm

dilution factor is 25 (using standard methods)

44.19 is the extinction coefficient of RNA (in the presence of excess salt or protein the absorbance can be skewed, so an A_{260}/A_{280} ratio can be used to assess the quality of the RNA; pure RNA has a ratio of ~2)

Samples are analysed on an agarose-formaldehyde gel to check for degradation. Poly $(A)^+$ RNA may then be isolated from total cellular RNA using the polyATract isolation kit.

2. The TRIzol Method

After grinding in liquid nitrogen (see above), the tissue is incubated at room temperature in TRIzol Reagent for approximately 10 minutes. After addition of chloroform and centrifugation, RNA in the upper aqueous layer is precipitated with isopropanol in a high salt buffer (0.8 M sodium citrate, 1.2 M NaCl). The latter procedure removes proteoglycan and polysaccharide contamination from the isolated RNA. After centrifugation, the pellet, containing the RNA, is washed in 75% ethanol. The supernatant should be poured off extremely carefully because the pelleted RNA is not stuck avidly to the sides of the tube. The pellet is then briefly freeze dried or air dried, taking care not to over-dry which renders the RNA difficult to redissolve. The absorption of an aliquot is used to calculate the yield (see above). The RNA is stored frozen at –70°C in diethyl pyrocarbonate (DEPC) water.

RNA Extraction for PCR

Tissues are powdered in liquid nitrogen (see above) and immediately suspended in the TRIzol reagent at room temperature. Chloroform is added and, after centrifugation, the RNA in the upper aqueous phase is precipitated with isopropanol. As above, a high salt solution is used to rid samples of proteoglycan contamination. After two further centrifugation steps, including an ethanol wash, the RNA pellet is freeze dried and carefully resuspended in nuclease-free water. Optical density was measured as above and RNA stored in 1 μg aliquots ready for PCR.

Quick Guides for Northern Analysis

1. RNA Electrophoresis

Total RNA or mRNA samples are size fractionated by agarose-formaldehyde gel electrophoresis in MOPS (morpholinosulphonic acid). After dissolving the agarose, the solution is cooled to hand-hot, formaldehyde is added and the liquid is poured into a gel cast and allowed to set. A gel 'comb' is used to form the line of slots that accommodate the samples. Gels can be covered in polythene film and stored at 4°C for later use. The RNA samples are prepared in DEPC water, gel loading buffer and ethidium bromide. It is best to plan to use a maximum of 20 μg RNA per slot to prevent loss of resolution when the gel is viewed. We tend to use 15 μg RNA per slot. Each sample is denatured by incubating at 65°C, followed by immediate cooling on ice. The samples are then pulse spun in a microcentrifuge and are loaded onto the gel, together with Orange G (a marker dye to track the electrophoretic mobility of the samples). Slow controlled loading prevents the force of the pipette blowing the sample out of the slot. It is advisable to avoid using the outermost lanes because the RNA does not transfer optimally to the nylon membrane. The samples are electrophoresed at a maximum of 5 V per cm of gel length, with the RNA running from negative to positive. Our gels are 11 cm long and we find 75 V to be optimal. A lower voltage allows for better separation but takes more than four hours to run the required length. A higher voltage can overheat the gel. After the samples have moved approximately half the length of the gel (~1.5 h for an 11 cm gel), the progress of the gel can be determined. The voltage is switched off and the gel is examined, in its casting tray, under a UV transilluminator. It is possible to see if the RNA has degraded, as indicated by smeared bands as

opposed to discrete bands. Ribosomal RNA should be visible as two distinct bands, namely 18S and 28S (Figure 2). Ideally, the intensity of the 28S rRNA should be approximately double that of the 18S rRNA. If the RNA is satisfactory, the gel can continue electrophoresis until the Orange G runs off the bottom of the gel. The large MUC mRNA should be between the 18 S band and the slots of the gel. Consequently, it is best to electrophorese the gel for as long as possible for maximum separation of these large molecules.

2. Transfer of RNA from Gel to Nylon Membrane ('Blotting')

Before transfer, the gel is soaked in 0.5 M NaOH for 20 minutes and is rinsed with RNase-free water before blotting. The RNA is blotted onto nylon membranes by overnight capillary transfer in sodium citrate solution in a transfer tank (Figure 3). The nylon membrane is wrapped in clear cellophane to prevent it drying out and is stored at 4°C until use. RNA is then covalently crosslinked to the membrane by UV irradiation, for example using a UV Stratalinker-1800 (Stratagene, U.K.). The membrane needs to be observed to check that the RNA has transferred adequately and the positions of the 18S and 28S bands are marked. The membrane can be kept wrapped in cellophane and stored at 4°C until use.

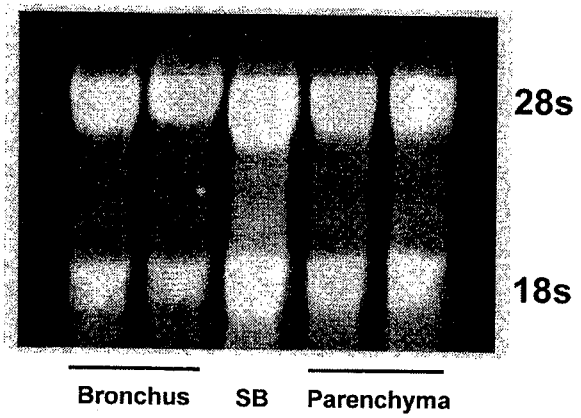

Fig. 2. Total RNA from human lung. Tissue was collected at surgery and 15 μg RNA per lane electrophoresed on agarose gel (visualised with ethidium bromide). Note the clear 28S and 18S bands, demonstrating that the RNA has not degraded.

3. Preparation of Probes

MUC probes are not currently available commercially and different research groups design their own probes [32]. A number of the probes we use were designed by Dr. Yu-Chih Liu [39]. Plasmid vectors are stored in 50% glycerol at −70°C and, when required, are grown up individually in L-Broth containing ampicillin. To obtain high quality plasmid DNA, we have found that recovery using the QIA Filter Plasmid midi kit (Quiagen, U.K.) is effective. To cut out the cloned cDNA fragments, restriction digests are performed. For cDNA fragments cloned into the pGEM-T Easy vector, the restriction enzyme ECoRI is used, whereas for those cloned into the pGEM-T vector, SacI and ApaI are used. Digests were run out on an agarose gel containing ethidium bromide, Orange G dye, and a 1 kb DNA ladder. The desired fragment size is cut out and further purified, for example using the GFX PCR DNA and Gel band purification kit (Pharmacia Biotech, U.K.). Purified probes are aliquoted to 50 ng with Tris-EDTA for each Northern reaction.

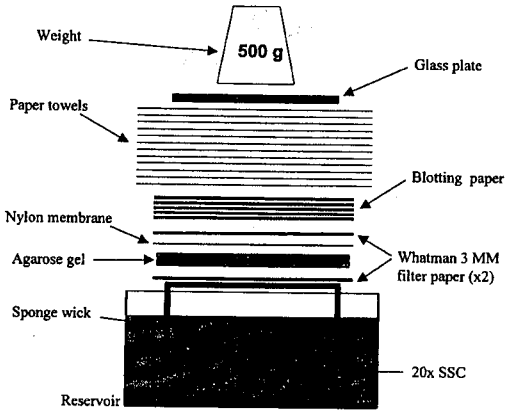

Fig. 3. Capillary transfer of RNA for Northern blotting. The system is arranged so that buffer solution is drawn from the reservoir via the wick, and passes through the filter paper, the agarose gel, the nylon membrane, the blotting paper and seeps into the paper towels. Through this action, RNA is drawn from the gel onto the membrane, where it is permanently fixed. SSC = standard sodium citrate.

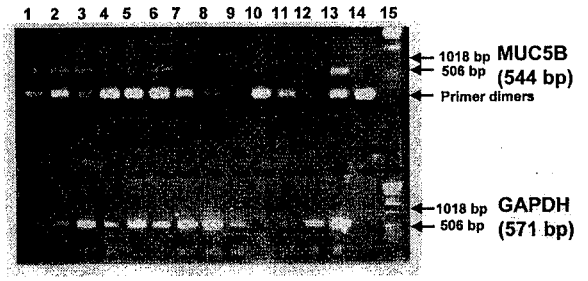

Fig. 4. PCR products for MUC5B and GAPDH in human lung. Tissue was collected at autopsy from patients with and without COPD and 15 μg RNA per lane electrophoresed on agarose gel (visualised with ethidium bromide). Lanes 1 and 2: subsegmental bronchus and parenchyma respectively (COPD patient); lanes 3-5: segmental bronchus, subsegmental bronchus and parenchyma (COPD patient); lane 6: parenchyma (non-COPD patient); lane 7: parenchyma (COPD patient); lanes 8-11: segmental bronchus and subsegmental bronchus (GAPDH only), subsegmental bronchus (MUC5B only), and parenchyma (COPD patient); lanes 12 and 13: segmental bronchus, parenchyma (non-COPD patient); lane 14: PCR negative control; lane 15: DNA size marker (1 kb 'ladder': Gibco, U.K.).

4. Hybridisations

Membranes are prehybridised with prehybridisation buffer comprising deionised formamide, Tris-HCL, Denhardt's solution, sodium dodecyl sulphate, EDTA and denatured salmon sperm DNA in a hybridisation oven, for example the Hybridiser-600 (Stratagene, U.K.). The cDNA probes were labelled with [^{32}P]dCTP. This can most easily be done utilising a commercial random-primed labelling kit, for example Ready-to-Go (Pharmacia Biotech, U.K.). Labeled probes (25-50 ng DNA), purified through a G50 Sephadex column, are added to the prehybridisation chamber and are left to hybridise overnight. Post-hybridisation washes are performed to remove non-specific binding of the cDNA probes, at increasing temperature and reduced salt concentration (increasing stringency). The blots are then exposed to film, for example Kodak X-OMAT. Optimal exposure time can be judged from the level of radioactivity of the blot after the post hybridisation washes. For example, a high level of radioactivity requires a shorter exposure time. GAPDH is more strongly expressed than MUC genes and in general needs approximately four days exposure, depending upon the strength of the radioactivity on the membrane. MUC probes are used separately and the film is exposed for up to 10 days. Autoradiographs are quantitated by densitometry, for example by use of GelWorks ID Intermediate (U.K.) with the relative amounts of RNA calculated as a ratio of GAPDH or, in the case of some total RNA blots, 18s ribosomal RNA. For re-probing, membranes are stripped in stripping buffer (comprising formamide and sodium orthophosphate in RNase free water) for at least 1 hour at 65°C, then rinsed twice with 2x standard sodium citrate at 25°C for 10 minutes.

Quick Guides for Semi-Quantitative RT-PCR

We have used the following methodology to successfully measure MUC5AC mRNA in airway tissue taken at surgery for lung carcinoma [37]. Figure 4 is an example of a gel obtained from PCR of MUC5B from human airway tissue.

1. DNase treatment

Genomic contamination in RNA samples is reduced using DNase I and first strand buffer. DNase activity is stopped by addition of EDTA and incubation at 65°C for 10 min.

2. Preparation of cDNA

The DNase I treated RNA samples are reverse-transcribed using reverse transcription mix comprising Avian Myeloblastosis Virus (AMV) reverse transcriptase, magnesium chloride, reverse transcription buffer, dNTPs (dATP, dGTP, dCTP, dTTP), recombinant ribonuclease inhibitor (RNasin), random hexa primers and dithiothreitol (if DNase treated) in nuclease free water. After incubation, the AMV reverse transcriptase is inactivated at 95°C for 4 min and the cDNA diluted in water and stored at 4°C.

3. Primer Design

Individual research groups have been designing their own primers for some time. After

Table. Comparison of the expense and labor between WB and plasma lactate analysis

Human MUC5AC	sense primer	CGA CAA CTA CTT CTG CGG TGC
	antisense primer	GCA CTC ATC CTT CCT GTC GTT
Human MUC5B	sense primer	CAG GGC ATT TGG ACA GTT TTT C
	antisense primer	CAG TGG CAG AGG CCG TGC AGT A
Human GAPDH	sense primer	ATT CCA TGG CAC CGT CAA GGC T
	antisense primer	TCA GGT CCA CCA CTG ACA CGT

publication, others can then use them. We have successfully used the following primers for MUC5AC and MUC5B (primers for GAPDH are included for completeness) (Table)

Primers were designed using Oligo 4 and Primer Premier 4.0 (PREMIER Biosoft International, Palo Alto, U.S.A.) once the correct sequences for the genes had been obtained from Genbank http://www.ncbi.nlm.nih.gov/Entrez/nucleotide.html). The primers for human MUC5B were previously published in Borchers *et al* [40]. All mucin primers were designed to cross intron-exon boundaries in order to detect genomic contamination.

4. Polymerase Chain Reaction (PCR)

Semi-quantitative PCR can be performed in a variety of commercially available systems, for example the OmniGene thermocycler (Hybaid, U.K.). cDNA samples are to the PCR mix, which comprises NH_4 buffer, dNTPs, $MgCl_2$, Taq DNA polymerase, and the appropriate upstream and downstream primers. The correct volume is made up using distilled water. Each sample is covered with a drop of mineral oil to prevent evaporation. On occasion a 'hot start' can be used to reduce primer dimers (see below).

We have found the following cycle parameters to be effective: 94°C for 30 sec, specific annealing temperature for 30 sec, 72°C for 30 sec. Annealing temperatures and PCR product size are 58°C (336 bp) for MUC5AC, 60°C (544 bp) for MUC5B, and 58°C (571 bp) for GAPDH. The number of amplification cycles used is the minimum necessary to achieve exponential amplification where product formation is proportional to the starting cDNA. This is determined by performing cycle profiles with each individual set of primers. After amplification each sample was heated to 72°C for 10 min. If a hot start is used, cDNA is added to the PCR mix containing all components except Taq DNA polymerase. After initially heating the samples at 94°C for 5 min, Taq DNA polymerase is then added to each sample in nuclease-free water. From here on amplification is performed as above. To visualise the PCR, a sample of each reaction mixed with Orange G is size fractionated on an agarose gel containing ethidium bromide. Quantification of mucin gene expression is performed as for Northern analysis (see above).

Conclusions

The perceived importance of changes in MUC gene expression in pathophysiology of respiratory diseases such as asthma, COPD and CF has driven development of techniques to measure MUC mRNA levels in human lung tissues. Progress has been hampered by the technical difficulties associated with the large transcript sizes of MUC genes [33]. Many of these problems have been overcome, for example by initiating careful treatment of the samples by avoiding such procedures as vigorous shaking and homogenisation. Consequently, we and other groups Worldwide are now making progress in measuring the expression of MUC genes in

human airway tissue. We predict that over the next five to ten years information will become available on the expression and distribution of MUC genes in normal human airways and in hypersecretory respiratory conditions. The hope is that this information will broaden our understanding of pathophysiology with a view to delineating differences and similarities between diseases. This in turn should allow rationalisation of experimental systems to model different diseases and of drug design for therapy of airway mucus hypersecretion.

References

1. Liu YC, Khawaja AM, Rogers DF. Pathophysiogy of Airway Mucus Secretion in Asthma. In Barnes PJ, Rodger IW, Thomson NC, eds. Asthma. Basic Mechanisms and Clinical Management, pp 205-27. London: Academic Press, 1997.
2. Rogers DF. Mucus pathophysiology in COPD: differences to asthma, and pharmacotherapy. Monaldi Arch Chest Dis 2000; 55: 324-32.
3. Puchelle E, Zahm JM, de Bentzmann S, *et al.* Mucus and Airway Epithelium Alterations in Cystic Fibrosis. In Rogers DF, Lethem MI, eds. Airway Mucus: Basic Mechanisms and Clinical Perspectives, pp 301-26. Basel: Birkhäuser Verlag, 1997.
4. Widdicombe JH,.Widdicombe JG. Regulation of human airway surface liquid. Respir Physiol 1995; 99: 3-12.
5. Widdicombe JG. Airway Surface Liquid: Concepts and Measurements. In Rogers DF, Lethem MI, eds. Airway Mucus: Basic Mechanisms and Clinical Perspectives, pp 1-17. Basel: Birkhäuser Verlag, 1997.
6. Thornton DJ, Davies JR, Carlstedt I, *et al.* Structure and Biochemistry of Human Respiratory Mucins. In Rogers DF, Lethem MI, eds. Airway Mucus: Basic Mechanisms and Clinical Perspectives , pp 19-39. Basel: Birkhäuser Verlag, 1997.
7. Gendler SJ, Lancaster CA, Taylor-Papadimitriou J, Duhig T, Peat N, Burchell J et al. Molecular cloning and expression of human tumor-associated polymorphic epithelial mucin. J Biol Chem 1990; 265: 15286-93.
8. Gum JR, Jr., Hicks JW, Toribara NW, *et al.* Molecular cloning of human intestinal mucin (MUC2) cDNA. Identification of the amino terminus and overall sequence similarity to prepro-von Willebrand factor. J Biol Chem 1994; 269: 2440-6.
9. Gum JR, Jr., Ho JJ, Pratt WS, *et al.* Vinall LE et al. MUC3 human intestinal mucin. Analysis of gene structure, the carboxyl terminus, and a novel upstream repetitive region. J Biol Chem 1997; 272: 26678-86.
10. Williams SJ, Munster DJ, Quin RJ, *et al.* The MUC3 gene encodes a transmembrane mucin and is alternatively spliced. Biochem Biophys Res Commun 1999; 261: 83-9.
11. Porchet N, Nguyen VC, Dufosse J, *et al.* Molecular cloning and chromosomal localization of a novel human tracheo-bronchial mucin cDNA containing tandemly repeated sequences of 48 base pairs. Biochem Biophys Res Commun 1991; 175: 414-22.
12. Guyonnet D, V, Audie JP, Debailleul V, *et al.* Characterization of the human mucin gene MUC5AC: a consensus cysteine-rich domain for 11p15 mucin genes? Biochem J 1995; 305: 211-9.
13. Meerzaman D, Charles P, Daskal E, *et al.* Cloning and analysis of cDNA encoding a major airway glycoprotein, human tracheobronchial mucin (MUC5). J Biol Chem 1994; 269: 12932-9.
14. Toribara NW, Ho SB, Gum E, *et al.* The carboxyl-terminal sequence of the human secretory mucin, MUC6. Analysis Of the primary amino acid sequence. J Biol Chem 1997; 272: 16398-403.
15. Bobek LA, Tsai H, Biesbrock AR, *et al.* Molecular cloning, sequence, and specificity of expression of the gene encoding the low molecular weight human salivary mucin (MUC7). J Biol Chem 1993; 268: 20563-9.
16. Shankar V, Pichan P, Eddy RL, Jr., *et al.* Chromosomal localization of a human mucin gene (MUC8) and cloning of the cDNA corresponding to the carboxy terminus. Am J Respir Cell Mol Biol 1997; 16: 232-41.
17. Lapensee L, Paquette Y, Bleau G. Allelic polymorphism and chromosomal localization of the human oviductin gene (MUC9). Fertil Steril 1997; 68: 702-8.
18. Williams SJ, Wreschner DH, Tran M, *et al.* Muc13, a novel human cell surface mucin expressed by epithelial and hemopoietic cells. J Biol Chem 2001; 276: 18327-36.
19. Gendler SJ,.Spicer AP. Epithelial mucin genes. Annu Rev Physiol 1995; 57: 607-34.
20. Pigny P, Guyonnet-Duperat V, Hill AS, *et al.* Human mucin genes assigned to 11p15.5: identification and

organization of a cluster of genes. Genomics 1996; 38: 340-52.

21. Moniaux N, Nollet S, Porchet N, *et al.* Complete sequence of the human mucin MUC4: a putative cell membrane-associated mucin. Biochem J 1999; 338: 325-33.
22. Desseyn JL, Buisine MP, Porchet N, *et al.* Genomic organization of the human mucin gene MUC5B. cDNA and genomic sequences upstream of the large central exon. J Biol Chem 1998; 273: 30157-64.
23. Hanisch FG, Muller S. MUC1: the polymorphic appearance of a human mucin. Glycobiology 2000; 10: 439-49.
24. Crawley SC, Gum JR, Jr., Hicks JW, *et al.* Genomic organization and structure of the 3' region of human MUC3: alternative splicing predicts membrane-bound and soluble forms of the mucin. Biochem Biophys Res Commun 1999; 263: 728-36.
25. Berger JT, Voynow JA, Peters KW, *et al.* Respiratory carcinoma cell lines. MUC genes and glycoconjugates. Am J Respir Cell Mol Biol 1999; 20: 500-10.
26. Rose MC, Gendler SJ. Airway Mucin Genes and Gene Products. In Rogers DF, Lethem MI, eds. Airway Mucus: Basic Mechanisms and Clinical Perspectives, 41-66. Basel: Birkhäuser Verlag, 1997.
27. Reid CJ, Gould S, Harris A. Developmental expression of mucin genes in the human respiratory tract. Am J Respir Cell Mol Biol 1997; 17: 592-8.
28. Li D, Wang D, Majumdar S, *et al.* Localization and up-regulation of mucin (MUC2) gene expression in human nasal biopsies of patients with cystic fibrosis. J Pathol 1997; 181: 305-10.
29. Nguyen PL, Niehans GA, Cherwitz DL, *et al.* Membrane-bound (MUC1) and secretory (MUC2, MUC3, and MUC4) mucin gene expression in human lung cancer. Tumour Biol 1996; 17: 176-92.
30. Agrawal B, Krantz MJ, Reddish MA, *et al.* Cancer-associated MUC1 mucin inhibits human T-cell proliferation, which is reversible by IL-2. Nat Med 1998; 4: 43-9.
31. Levine SJ, Larivee P, Logun C, *et al.* Tumor necrosis factor-alpha induces mucin hypersecretion and MUC-2 gene expression by human airway epithelial cells. Am J Respir Cell Mol Biol 1995; 12: 196-204.
32. Porchet N, Aubert JP. Northern blot analysis of large mRNAs. Methods Mol Biol 2000; 125: 305-12.
33. Debailleul V, Laine A, Huet G, *et al.* Human mucin genes MUC2, MUC3, MUC4, MUC5AC, MUC5B, and MUC6 express stable and extremely large mRNAs and exhibit a variable length polymorphism. An improved method to analyze large mRNAs. J Biol Chem 1998; 273: 881-90.
34. Pritchard K, Smith AK, Rogers DF. Measurement of airway mucin gene expression. In Rogers DF, Donnelly LE, eds. Human Airway Inflammation. Sampling Techniques and Analytical Protocols, 285-94. Totowa: Humana Press, 2001.
35. Thellin O, Zorzi W, Lakaye B, *et al.* Housekeeping genes as internal standards: use and limits. J Biotechnol 1999; 75: 291-5.
36. Suzuki T, Higgins PJ, Crawford DR. Control selection for RNA quantitation. Biotechniques 2000; 29: 332-7.
37. Pritchard K, Tetlow M, Nicholson A, *et al.* Expression of mucin gene MUC5AC in human airways. Am J Respir Crit Care Med 2001; 163 (suppl): A408.
38. Chomczynski P, Sacchi N. Single-step method of RNA isolation by acid guanidinium thiocyanate-phenol-chloroform extraction. Anal Biochem 1987; 162: 156-9.
39. Liu YC. Airway Mucus Secretion: Control Mechanisms, Pharmacological Regulation and Mucin Gene Expression. PhD Thesis 1999. London, University of London.
40. Borchers MT, Wert SE, Leikauf GD. Acrolein-induced MUC5ac expression in rat airways. Am J Physiol 1998; 274: L573-81.

Impact of Feeding Status on Biochemical and Respiratory Parameters in Ventilator-Dependent Patients

Ching-Hsiung Lin, Hui-Chen Lo*, Bo-Chin Chiou*

Meeting the adequate nutritional requirements of ventilator-dependent patients is still a challenge, because of the variety and severity of the diseases of these patients and the lack of reliable nutritional support guidelines. The objective of this study was to compare the energy requirement, biochemical data, and respiratory parameters in ventilator-dependent patients fed with different amounts of calories. Twenty-eight patients who had been on mechanical ventilation more than 14 days, with various primary diagnoses, and on continuous nasogastric tube feeding, were recruited. Resting energy expenditure (REE) was measured by indirect calorimetry (IC). Total energy expenditure (TEE) was defined as 1.2-fold of REE. Degree of feeding (DF) was defined as the ratio of actual calories provided to TEE. Our results showed that there were 5 patients (group A) with under- (DF < 0.9) or appropriate feeding (0.9 ≤ DF ≤ 1.1), and 23 patients (group B) with overfeeding (DF > 1.1) in this study. There were no significant differences in the serum levels of glucose, albumin, blood urea nitrogen, creatinine, prealbumin, transferrin, C-reactive protein, and nitrogen balance between group A and group B. The results of the complete blood count, blood gas, nutrient intake, tidal volume, respiratory rate, and minute ventilation were not significantly different between two groups. However, the proportional contribution of the energy substrate from carbohydrates was significantly greater in patients with overfeeding. In addition, patients with overfeeding had significantly lower carbon dioxide production, oxygen consumption, and REE, and had significantly higher levels of respiratory quotient (RQ) and non-protein RQ than the other patients. These results suggest that most of the ventilator-dependent patients in this study were overfed and had decreased fat oxidation. The use of IC may reduce the incidence of inappropriate feeding. Even though we found there were no significant effects of overfeeding in the biochemical data and respiratory parameters, the risks of overfeeding and the waste of medical resources are still worthy of consideration. ***(Thorac Med 2002; 17:10-18)***

Key words: ventilator-dependent, resting energy expenditure, indirect calorimetry, respiratory parameter

Division of Chest Medicine, Department of Internal Medicine, Department of Medical Education and Research, Laboratory of Biochemical Nutrition*, Changhua Christian Hospital, Changhua, Taiwan
Address reprint requests to: Dr. Ching-Hsiung Lin, Changhua Christian Hospital, 135 Nanshiao Road, Changhua, 500, Taiwan

Introduction

Providing adequate nutrition is important for ventilator-dependent patients in order to maintain their muscle strength and immune function, which are crucial in facilitating ventilator weaning. However, the energy requirement of these patients is difficult to predict, because of the variety and severity of diseases, the different degrees of stress, and the variations in individuals [1]. Indirect calorimetry (IC) is a method used to determine energy expenditure by measuring oxygen consumption and carbon dioxide production. It has been observed that critically ill patients are usually fed with amounts of calories significantly different from the resting energy expenditure (REE) determined by IC [2].

The deleterious effects of overfeeding and underfeeding have been documented in many studies. Underfeeding results in malnutrition, which increases the risk of infection, blunts respiratory drive, decreases respiratory muscle strength, and prolongs dependence on the mechanical ventilator [3]. In contrast, overfeeding causes hyperlipidemia, hyperglycemia, hepatic dysfunction, carbon dioxide retention, acidosis, azotemia, and the inability to wean from the ventilator [4]. The use of IC can allow clinicians to assess the patient's energy needs more accurately than using conventional predicting equations [5], such as the Harris-Benedict equation [6].

The respiratory care unit (RCU) in our hospital is open for ventilator-dependent patients who have failed ventilator weaning after several trials. Patients in this unit were transferred from our medical and surgical intensive care units, or from other medical centers. Most of the patients had been on ventilator for more than 21 days. The goal of this unit is to help patients wean from the ventilator; however, if this is not possible, the goal is to optimize their physical function and quality of life. Appropriate nutritional support is one of the key factors that affect their course of physical rehabilitation and weaning. Therefore, the objective of this study was to investigate the effects of feeding status on energy utilization and clinical outcome, such as that revealed in biochemical data and respiratory parameters, in ventilator-dependent patients.

Materials and Methods

Subjects. Twenty-eight clinically stable patients who had been on mechanical ventilation over two weeks in the RCU, and who were on continuous nasogastric tube feeding, were recruited into this study. Ethical approval from the Institutional Review Board of Chunghua Christian Hospital, and informed consent from the patients' families, were obtained. Patients were excluded from the study if they had oral intake or total parenteral nutrition, if there was no informed consent, or if they had an unstable hemodynamic status. In addition, patients with clinical conditions, such as a fraction of inspired oxygen (FiO_2) over 0.6, positive end-expiratory pressure over 5 cm H_2O, seizure, incompetent endotracheal tube cuff, or chest tube insertion, which interfered with the results of the IC measurement, were also excluded. The gender, age, total hospital length of stay (LOS), total days on ventilator before IC measurement (LOV), APACHE II score, body height (BH), body weight (BW), and body mass index (BMI), were recorded.

Biochemical data. Arterial and venous blood samples were obtained at 10 o'clock in the morning on the day of the IC measurement. Complete blood counts, including white blood cells, red blood cells, hemoglobin, hematocrit, and platelets, were measured using a hematology analyzer (GEN'S, Coulter Inc., FL, USA). Arterial blood samples were collected using heparin-rinsed syringes to measure the blood gases (Omni 4, AVL Inc., Switzerland). Concentrations of glucose, albumin, glutamate oxaloacetate transaminase (GOT), glutamate pyruvic transaminase (GPT), blood urea nitrogen

(BUN), and creatinine in serum were measured using an automatic analyzer (Hitachi 747, Japan). Serum levels of prealbumin, transferrin, C-reactive protein (CRP), and free thyroxin (T_4), were measured using the immunonephlometric method.

Urine samples were collected for 24 hours, starting from the day before the IC measurement. The total volume of 24-hour urine was recorded. The concentrations of creatinine and urea nitrogen were analyzed and the creatinine clearance (C_{CR}) was calculated. The total nitrogen balance was calculated by grams of nitrogen intake subtracted from grams of urinary urea nitrogen and 4.

Parameters from the ventilator and indirect calorimetry. Tidal volume, respiratory rate, minute ventilation (MV), inspired and expired tidal volume, positive end-expiratory pressure (PEEP), and FiO_2 were recorded from ventilators during IC measurement. REE was measured by an open-circuit indirect calorimetry (Deltatrac II MBM-200 metabolic monitor, Datex-Engstrom Co., Finland). Oxygen consumption (VO_2) and carbon dioxide production (VCO_2) were obtained. REE, respiratory quotient (RQ), and non-protein RQ (npRQ) were calculated. The equations used by this metabolic monitor are as follows: REE = 5.50 x VO_2 + 1.76 x VCO_2 - 1.99 x urinary nitrogen excretion (U_N, g/24h); RQ = VCO_2/VO_2; and npRQ = (1.44 x VCO_2 – 4.890 x U_N)/ (1.44 x VO_2 – 6.04 x U_N). Before IC measurement, the monitor was warmed up for at least 30 minutes and then calibrated using standard gas, which contained 95% O_2 and 5% CO_2. In addition, the ventilator setting was not altered for at least 90 minutes before IC measurement. Stable and steady-state measurement was obtained for at least 20 minutes for each patient. Steady state is defined as minute-to-minute variations of VO_2, VCO_2, and RQ less than 10%.

Nutrient intake and energy utilization. The total caloric intake was calculated, and included the calories from tube feeding and intravenous infusion. The amount of calories provided was based on the Harris-Benedict equation or on the kilograms of body weight multiplied by 25 to 35 kcal/kg, which was suggested by the dieticians. Each patient had been fed with the suggested amount of calories for over 14 days when included into this study. The 24-hour consumption of carbohydrates, protein, and fat were also calculated. The amounts and proportional contributions of carbohydrates, protein, and fat oxidized were obtained from the IC. Total energy expenditure (TEE) was defined as 1.2-fold of REE. Degree of feeding (DF) was defined as the ratio of calories provided to TEE, as suggested by McClave et al [7]. Patients were classified as underfed when DF was less than 0.9, as appropriate feeding when DF was between 0.9 and 1.1, and as overfed when DF was greater than 1.1 [7]. Because most of the patients recruited were overfed, we combined patients with underfeeding and appropriate feeding into group A. Patients with overfeeding were assigned into group B.

Statistical analysis. Values are expressed as mean ± SD. The Wilcoxon Rank Test was used to determine the significant difference of each parameter between groups. The correlation analysis was processed using the Sperman correlation method to assess the relationships between caloric intake and DF with biochemical data and parameters from the ventilator and the IC in ventilator-dependent patients. Statistical significance was assumed at $P<0.05$.

Results

Subject characteristics. The distribution of DF is shown in Figure 1. The number of patients with underfeeding, appropriate feeding, and overfeeding were 2, 3, and 23, respectively. The gender, age, LOS, LOV, APACHE II score, BH, BW, and BMI are listed in Table 1. In this study, we recruited 16 males and 12 females. The primary diagnosis of these 28 patients was classified into: (1) neuromuscular disease (n=12),

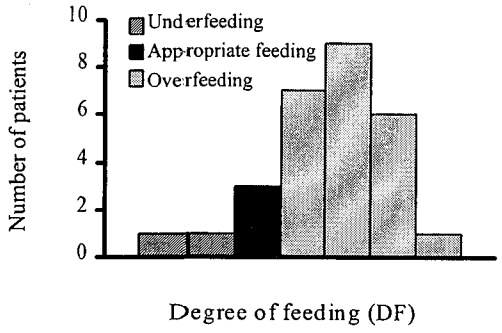

Fig. 1. Distribution of degree of feeding (DF) in ventilator-dependent patients. Patients with DF < 0.9 were classified as "underfeeding", with 0.9≦DF≦1.1 were classified as "appropriate feeding",and with DF > 1.1 were classified as "overfeeding".

(2) acute lung injury, such as pneumonia or acute respiratory distress syndrome (n=3), (3) chronic lung disease, such as asthma, chronic obstructive pulmonary disease, bronchiectasis, pulmonary tuberculosis with destructive lung (n=7), (4) postoperative (n=4), and (5) other medical illnesses (n=2). There were no significant differences in gender distribution, age, LOS, LOV, APACHE II score, BH, BW, or BMI between groups.

Biochemical data. The biochemical data are shown in Table 2. Serum concentrations of glucose, albumin, prealbumin, transferrin, GOT, GPT, BUN, creatinine, and CRP were not significantly different between the two groups. In addition, the levels of urinary urea nitrogen, creatinine clearance, and daily nitrogen balance were not significantly different between the groups. However, the serum concentration of free T_4 was significantly greater in group A than in group B.

There were no significant differences in the numbers of red blood cells, white blood cells or platelets, as well as in the levels of hemoglobin and hematocrit in the whole blood between these two groups (data not shown). In addition, there were no significant differences in the levels of arterial blood pH, $PaCO_2$, PaO_2, base excess, and bicarbonate ion between these two groups (data not shown).

Parameters from the ventilator and indirect calorimetry. Tidal volume, respiratory rate, and MV were not significantly different between groups (Table 3). However, VCO_2, VO_2, and REE were significantly greater, and RQ and npRQ were significantly lower in group A than in group B (Table 3). The inspired and expired tidal volume, PEEP, and inspired oxygen fraction were not significantly different between these two groups (data not shown).

Nutrient intake and energy utilization. Total caloric intake was 1611 ± 368 and 1943 ± 234 kilocalories in groups A and B, respectively. The daily consumption of carbohydrates, protein, and fat were 242.9 ± 23.5, 74.7 ± 7.2, and 57.7 ± 5.6 in group A and 258.5 ± 41.2, 79.5 ± 12.7, and 61.4 ± 9.8 grams in group B, respectively. There were no significant differences in the amounts of calories, carbohydrates, protein, and fat intake between these two groups. The amounts of carbohydrates and protein oxidized in 24 hours

Table 1. Subject characteristics in ventilator-dependent patients[1]

	Group A	Group B	p-value
Age (yr)	70.2 ± 16.8	73.3 ± 14.6	NS
LOS (day)	365.6 ± 271.4	299.3 ± 177.0	NS
LOV (day)	302.9 ± 275.4	286.5 ± 171.6	NS
APACHE II score	24.4 ± 8.4	22.0 ± 6.1	NS
Body height (cm)	162.4 ± 10.3	161.4 ± 9.2	NS
Body weight (kg)	55.9 ± 3.5	56.2 ± 8.4	NS
Body mass index	21.3 ± 1.3	21.7 ± 4.0	NS

[1]Values are means ± SD. NS, not significant; LOS, total hospital length of stay; LOV, total days on ventilator before indirect calorimetry measurement.

Table 2. Biochemical data in ventilator-dependent patients[1]

	Group A	Group B	p-value
Glucose (mg/dl)	154.2 ± 23.9	162.1 ± 75.3	NS
Albumin (g/dl)	3.3 ± 0.2	3.1 ± 0.3	NS
Prealbumin (mg/dl)	21.1 ± 4.0	18.4 ± 6.6	NS
Transferrin (mg/dl)	205.4 ± 48.0	183.4 ± 52.1	NS
GOT (IU/l)	34.4 ± 18.7	27.4 ± 15.3	NS
GPT (IU/l)	30.4 ± 22.4	26.0 ± 14.4	NS
BUN (mg/dl)	22.0 ± 8.2	22.2 ± 10.2	NS
Creatinine (mg/dl)	1.06 ± 0.21	0.96 ± 0.37	NS
CRP (mg/dl)	2.0 ± 2.0	4.0 ± 5.6	NS
Free T_4 (ng/dl)	1.4 ± 0.1	1.2 ± 0.2	0.0366
UUN (mg/dl)	434.2 ± 218.3	480.0 ± 174.2	NS
CCR (ml/min)	44.6 ± 8.5	42.6 ± 17.2	NS
NB (g/24h)	- 1.81 ± 2.82	0.82 ± 1.79	NS

[1]Values are means ± SD. NS, not significant; GOT, glutamate oxaloacetate transaminase; GPT, glutamate pyruvic transaminase; BUN, blood urea nitrogen; CRP, C-reactive protein; T_4, thyroxin; UUN, urinary urea nitrogen; CCR, creatinine clearance; NB, nitrogen balance.

Table 3. Parameters from ventilator and indirect calorimetry in ventilator-dependent patients[1]

	Group A	Group B	p-value
Tidal volume (ml)	691 ± 54.7	695 ± 93.5	NS
Respiratory rate	12.0 ± 2.35	14.5 ± 5.30	NS
MV (l/ml)	8.49 ± 1.44	9.40 ± 2.61	NS
VCO_2 (ml/min)	178.7 ± 21.0	152.0 ± 17.8	0.0128
VO_2 (ml/min)	205.7 ± 19.5	163.6 ± 17.9	0.0027
REE (kcal/24h)	1429 ± 139	1150 ± 127	0.0033
RQ	0.864 ± 0.034	0.927 ± 0.049	0.0082
npRQ	0.880 ± 0.048	0.962 ± 0.065	0.0096

[1]Values are means ± SD. MV, minute ventilation; VCO_2, carbon dioxide production; VO_2, oxygen consumption; REE, resting energy expenditure; RQ, respiratory quotient; npRQ, non-protein respiratory quotient.

were not significantly different between the two groups (Table 4). However, the amount of fat oxidized in 24 hours was significantly lower in group B than in group A. The proportional contribution of the energy substrate from protein was not significantly different between these two groups. However, the proportional contribution of the energy substrate from carbohydrates was significantly greater in group B than in group A (Table 4).

Correlations. Most of the biochemical data we measured had no significant correlation with caloric intake or DF in ventilator-dependent patients (data not shown), except that the nitrogen balance had significantly positive correlations with caloric intake and DF ($r = 0.6188$, $p = 0.0004$ and $r = 0.4948$, $p=0.0074$, respectively). Tidal volume, respiratory rate, and MV had no significant correlation with caloric intake or DF in ventilator-dependent patients (Table 5). Most of the parameters from IC had no significant correlation with the caloric intake or DF in ventilator-dependent patients, except that VCO_2, VO_2, and REE had significantly negative correlations with DF (Table 5).

Discussion

To adequately meet the nutritional requirements of ventilator-dependent patients is

Table 4. Energy utilization in ventilator-dependent patients[1]

	Group A	Group B	p-value
Carbohydrate			
g/24 h	176.1 ± 50.4	194.3 ± 49.8	NS
%	51.5 ± 11.1	71.0 ± 16.3	0.0117
Protein			
g/24 h	53.4 ± 16.5	51.1 ± 8.6	NS
%	15.7 ± 4.0	18.9 ± 3.6	NS
Fat			
g/24 h	48.9 ± 21.9	12.5 ± 20.2	0.0048
%	32.8 ± 14.3	10.1 ± 16.9	0.0099

[1]Values are means ± SD. NS, not significant.

Table 5. Correlation coefficients between provided calories and degree of feeding with parameters from ventilator and indirect calorimetry in ventilator-dependent patients[1]

	Calories intake		Degree of feeding	
	r	p	r	p
Tidal volume (ml)	0.2928	NS	0.0120	NS
Respiratory rate	0.1449	NS	0.0403	NS
MV (l/ml)	0.1177	NS	0.0625	NS
VCO_2 (ml/min)	0.1489	NS	-0.6058	0.0006
VO_2 (ml/min)	0.1496	NS	-0.6216	0.0004
REE (kcal/24h)	0.1627	NS	-0.6205	0.0004
RQ	0.1228	NS	0.2159	NS
npRQ	0.1400	NS	0.2378	NS

[1]Values are the corresponding coefficient (r) and p-values. MV, minute ventilation; VCO_2, carbon dioxide production; VO_2, oxygen consumption; REE, resting energy expenditure; RQ, respiratory quotient; npRQ, non-protein respiratory quotient.

still a challenge for clinicians. In order to improve physical functioning and to facilitate the ventilator weaning, we used IC to assess energy requirement and to investigate the effects of degree of feeding on energy utilization and clinical outcome in ventilator-dependent patients. Our results revealed that most of the patients in our RCU were overfed when providing the energy suggested by the Harris-Benedict equation or by the 25 to 35 kilocalories per kilogram of body weight, which are the common approaches used by dieticians.

There are several factors that augment the difficulty in predicting the energy requirement in ventilator-dependent patients, for example, the previous nutritional status, clinical conditions, and the unique response to a given injury in an individual patient [7]. It has been shown that burn patients had a 50% increased REE, patients with sepsis alone, and without fever, had a 30-60% increased REE [8], and patients with malnutrition had a lower metabolic rate and REE to preserve their energy [3]. As reported by McClave et al, REE is decreased in elderly persons, but increased in ICU patients for hypermetabolism [9]. In using IC to measure energy requirements, we found that about 80% of the patients in our RCU were overfed. These overfed patients had lower VCO_2, VO_2, and REE, but similar body weight when compared to patients with underfeeding and appropriate feeding. In addition, VCO_2, VO_2, and REE were negatively correlated with the degree of feeding in our patients. We believe that the high prevalence of overfeeding in

our RCU was mainly because most of our patients were over 50 years old, in a stable clinical condition, and accompanied with malnutrition, or with edema, which artificially increases the body weight. Therefore, the body weight-based predicting formulas usually overestimate the energy requirements in ventilator-dependent patients. This study confirmed the importance of IC for evaluating the energy requirements in ventilator-dependent patients.

The deleterious effects of overfeeding have been reported. For example, overfeeding protein leads to azotemia, hypertonic dehydration, and metabolic acidosis; overfeeding carbohydrates leads to hyperglycemia, hypertriglyceridemia, and hepatic steatosis; and overfeeding fat leads to hypertriglyceridemia and fat-overload syndrome [10]. Thyroxin is related to increases in metabolism and energy expenditure. In this study, we found that patients with lower levels of free thyroxin had lower levels of REE. However, we did not find significant effects of overfeeding in most of the biochemical data. This is possibly due to the fact that the degree of overfeeding in our patients was not severe enough to show the deleterious effects of overfeeding. For instance, the highest DF was 1.9 in one of our patients.

Patients with enteral overfeeding usually have accompanying diarrhea, intestinal ileus, malassimilation, and intolerance [11]. These gastrointestinal complications may result in the incomplete digestion and absorption of the provided calories. Therefore, the efficiency of energy utilization in patients with enteral tube feeding is an important issue to be considered during the management of nutritional support. Using the IC instrument, we can observe the energy utilization. In our patients, the amounts of oxidized carbohydrates and protein were not affected by the feeding status. However, overfeeding significantly decreased the amount of oxidized fat. In addition, the proportional contribution of substrate oxidation from carbohydrates was significantly increased, whereas that from lipids was significantly decreased in patients with overfeeding. Taken together, these results suggest that our overfed patients had the tendency to spare the fat as an energy source.

RQ and npRQ are the parameters obtained from IC. Traditionally, RQ and npRQ were used to determine substrate utilization [12]. However, McClave et al indicated that RQ and npRQ should only be used to confirm the test validity [13]. Nevertheless, we still found that the patients with a lower RQ and npRQ had a greater amount of fat being oxidized. The values of RQ in our patients were from 0.83 to 1.04, which is in the physiologic range (0.67 to 1.3). In addition, stable and steady-state measurement was obtained for at least 20 minutes, and the minute-to-minute variations of VCO_2, VO_2, and RQ were less than 10% for each patient. Therefore, the IC measurement was valid in this study.

Traditionally, excess caloric intake induces high CO_2 production and increased MV [14, 15]. However, an impressive study with 213 mechanically ventilated patients showed that degree of feeding correlates inversely with MV [7]. They explained that those who are underfed may develop respiratory muscle dysfunction, which results in increased MV. In our study, we did not show the relationship between degree of feeding and MV, which is possibly due to the fact that the patients in our RCU were not extremely overfed or underfed with enteral nutrition.

Our results indicated that over 80% (23/28) of our patients were overfed. We calculated the cost of the enteral formula, based on the standard reimbursement of the Bureau of National Health Insurance, and found that the average cost for overfed calories was $3.91 NT dollars per patient per day in our RCU. This cost extrapolated over 28 patients for 365 days would be $39,960 NT dollars. Considering the expense of the hospital, the average cost of overfed calories was $56.27 NT dollars per patient per day. And, this cost extrapolated over 28 patients for 365 days would be $575,079 NT dollars. From this point of view,

we believe that the use of IC may help clinicians provide adequate nutritional support for ventilator-dependent patients and avoid the potential waste of medical resources.

In summary, this study reveals that most of the patients in our RCU were overfed when providing energy as suggested by the Harris-Benedict equation or by the 25 to 35 kilocalories per kilogram of body weight, which are the common approaches used by dieticians. In addition, these overfed patients had decreased VCO_2, VO_2, REE, and fat oxidation. Therefore, it is important to use IC to evaluate the energy requirements of ventilator-dependent patients. Even though we did not find any significant effects of overfeeding in the biochemical data and respiratory parameters, the risks of overfeeding and waste of medical resources are worthy of consideration.

References

1. Cutts ME, Dowdy RO, Ellersieck MR, *et al.* Predicting energy needs in ventilator-dependent critically ill patients: effect of adjusting weight for edema or adiposity. Am J Clin Nutr 1997; 66: 1250-6.
2. Makk LJ, McClave SA, Creech PW, *et al.* Clinical application of the metabolic cart to the delivery of total parenteral nutrition. Crit Care Med. 1990; 18: 1320-7.
3. Spector N. Nutritional support of the ventilator-dependent patient. Nurs Clin North Am. 1989; 24: 407-14.
4. Takiguchi SA. Report of a hidden case of overfeeding. Heart Lung 1990; 19: 639-40.
5. Richard DB. The measurement of energy expenditure: Instrumentation, Practical Considerations, and Clinical Application. Respir care 1990; 35: 640-59.
6. Frankenfield DC, Muth ER, Rowe WA. The Harris-Benedict studies of human basal metabolism: History and limitations. J Am Diet Assoc 1998; 98: 439-45.
7. McClave SA, Lowen CC, Kleber MJ , *et al.* Are patients fed appropriately according to their caloric requirements? J Parent Enter Nutr 1998; 22: 375-81.
8. Long CL, Schaffel N, Geiger JW, *et al.* Metabolic response to injury and illness: estimation of energy and protein needs from indirect calorimetry and nitrogen balance. J Parenter Enteral Nutr 1979; 3: 452-6.
9. McClave SA, McClain CJ, Snider HL. Should indirect calorimetry be used as part of nutritional assessment? J Clin Gastroenterol 2001; 33: 14-9.
10. Klein CJ, Stanek GS, Wiles CE 3rd. Overfeeding macronutrients to critically ill adults: metabolic complications. J Am Diet Assoc1998; 98: 795-806.
11. McClave SA,Sexton LK, Spain DA, *et al.* Enteral feeding in the intensive care unit: Factors impeding adequate delivery. Crit Care Med 1999; 27: 1252-6.
12. Matarese LE. Indirect calorimetry: technical aspects. J Am Diet Assoc. 1997; 97: S154-60.
13. McClave SA, Lowen CC, Kleber MJ, *et al.* Is the respiratory quotient a useful indicator of over or underfeeding? J Parenter Enteral Nutr 1997; 21: S11.
14. Covelli HD, Black JW, Oleson MS, *et al.* Respiratory failure induced by high carbohydrate loads. Ann Intern Med 1981; 95: 579-80.
15. Dark Ds, Pingleton SK, Kerby GR. Hypercapnia during weaning: a complication of nutritional support. Chest 1985; 88: 141-43.

餵食狀況對呼吸器依賴患者血液生化值及呼吸參數之影響

林慶雄　羅慧珍*　邱伯勤*

背景：呼吸器依賴患者由於疾病的多樣性和不同的嚴重度，且目前尚無對此類患者營養支持的標準，故如何提供此類患者適當的熱量，對醫療人員而言仍是一大挑戰。本研究旨在了解呼吸器依賴患者的熱量需求，以及在不同的熱量給予下血液生化值及呼吸參數之變化。

方法：本研究包括 28 位使用呼吸器超過 14 天、具不同臨床診斷且以鼻胃管連續灌食的患者。我們以間接熱量測定儀測量患者的休息狀態熱能消耗(REE)。患者的總熱量需求(TEE)定義為 1.2 倍 REE。餵食狀況(degree of feeding, DF)定義為實際餵食熱量與 TEE 之比率。

結果：結果顯示有 5 位患者屬於過低熱量餵食(<0.9 倍 DF, A 組)或適當熱量餵食(0.9 至 1.1 倍 DF, A 組)，而有 23 位屬於過度熱量餵食(>1.1 倍 DF, B 組)。血清中血糖、白蛋白、尿素氮、肌酸酐、前白蛋白、運鐵蛋白和 C 反應蛋白質濃度及氮素平衡在 A 組及 B 組間並無顯著差異。兩組的全血球計數、動脈血液氣體分析、潮氣容積、呼吸速率、每分鐘通氣量與患者實際餵食熱量也沒有顯著差異。然而過度熱量餵食者醣類利用百分率顯著增加，而脂肪利用百分率顯著下降。此外，過度熱量餵食者其二氧化碳產生量、氧氣消耗量及 REE 顯著低於過低或適當熱量餵食者，但是他們的呼吸商及非蛋白質呼吸商卻顯著較高。

結論：本中心的患者大部分有過度熱量供給的現象，且這些患者的脂肪氧化作用顯著降低。因此使用間接熱量測定儀可減低不當餵食的機率。本研究未發現過度熱量餵食對血液生化值及呼吸參數的顯著影響，但是經由腸道過度熱量餵食的潛在危險及造成的醫療資源浪費仍不可忽視。***(胸腔醫學 2002; 17: 10-18)***

關鍵詞：呼吸器依賴，休息熱量消耗，間接熱量測定，呼吸參數

財團法人彰化基督教醫院　內科部胸腔內科　教學研究部營養生化研究室*
索取抽印本請聯絡：林慶雄醫師，彰化市 500 南校街 135 號

A Comparison of the Efficacy and Safety of Salmeterol Accuhaler and Ipratropium in Patients with Chronic Obstructive Pulmonary Disease

Hsin-Hung Pan, Jeng-Yuan Hsu, Chi-Der Chiang

Background: At the present time, bronchodilator medications, including anticholinergics and long-acting β2-agonists, are central to symptom management in chronic obstructive pulmonary disease, but few studies have compared the Salmeterol accuhaler with the Ipratropium metered-dose inhaler alone.

Objectives: To compare their efficacy and safety, 50mcg bid with the Salmeterol accuhaler, and 40mcg qid with the Ipratropium metered-dose inhaler, were administered over two three-month treatment periods to patients with chronic obstructive pulmonary disease.

Methods: Thirty-five patients with well-controlled chronic obstructive pulmonary disease were randomized to undergo three months of a crossover and comparative study with two episodes of the treatment modalities. Either the Salmeterol accuhaler 50mcg bid or the Ipratropium metered-dose inhaler 40mcg qid were administered daily. Then, the forced expiratory volume in one second (FEV1), systolic blood pressure, diastolic blood pressure, heart rate, and device usage, were compared.

Results: Both the Salmeterol accuhaler 50 mcg bid, and the Ipratropium metered-dose inhaler 40 mcg qid, demonstrated clinical efficacy in increasing FEV1 and forced vital capacity (FVC). The Salmeterol group showed the same improvement in net change of FEV1 and FVC as the Ipratropium group after 3 months' use, with no statistical difference. No significant changes in pulse rate, or systolic and diastolic pressure were found between the two groups.

Conclusion: The Salmeterol accuhaler was equal to the Ipratropium metered-dose inhaler in improving lung function at the recommended doses over the 3-month period, but the accuhaler was easier to use than the metered-dose inhaler.. ***(Thorac Med 2002; 17: 19-25)***

Key words: Salmeterol, Ipratropium, chronic obstructive pulmonary disease

Chest Division, Department of Internal Medicine, Taichung Veterans General Hospital
Address reprint requests to: Dr. Jeng-Yuan Hsu, Division of Chest Medicine, Department of Internal Medicine, Taichung Veterans General Hospital, No.160, Section 3, Chung-Kan Road, Taichung City, Taiwan

Introduction

Chronic obstructive pulmonary disease (COPD) is defined as a disease that is characterized by the presence of a not fully reversible airflow obstruction, due to chronic bronchitis or emphysema, and is generally progressive [1]. The goals of pharmacotherapy when dealing with this disorder are to induce bronchodilation and to facilitate expectoration in order to improve symptoms, prevent recurrent exacerbations, and thereby enhance the quality of life [2]. Both inhaled $ß_2$-agonists and anticholinergic medications are considered to be initial bronchodilator therapy for patients with COPD [3-5]. Randomized clinical trials have demonstrated that these medications can improve lung function and reduce the severity of breathlessness in such patients [6-8].

Salmeterol is a selective beta2-receptor agonist. This novel compound has produced sustained inhibition in both PGF2 α -pre-contracted and electrically-stimulated isolated guinea-pig trachea [9]. Salmeterol also provides protection against histamine-induced broncho-constriction in healthy subjects for at least 12 hours [10-12]. This study was designed to investigate the efficacy of the Salmeterol accuhaler, 50 mcg bid, versus the Ipratropium metered-dose inhaler (MDI), 40 mcg qid, in patients with moderate to severe chronic obstructive pulmonary disease.

Materials and Methods

We selected forty patients with moderate to severe COPD (our definition of COPD was consistent with the criteria proposed by the American Thoracic Society), aged 40 to 75 years old. The patients fulfilled the following criteria: Predicted Lung Function: 1, an FEV1 $\leq$60% of the predicted values; 2, FEV1/FVC $<$70%; and 3, an improvement in FEV1 of $<$12% following 200μg of inhaled short-acting β2-agonists. Symptoms and/or Diurnal Variation: out of a total score of 4 in the last 7 days of the run-in period, having a total symptom score (daytime plus nighttime) of at least 2 or more (daytime symptom score: 0= no symptoms during the day, 1= symptoms for one short period during the day, 2= symptoms for two or more short periods during the day, 3= symptoms for most of the day which do not affect your normal daily activities, 4= symptoms for most of the day which do affect your normal daily activities, 5= symptoms so severe that you cannot go to work or perform normal daily activities; nighttime symptom score: 0= no symptoms during the night, 1= symptoms causing you to wake once or wake early, 2= symptoms causing you to wake twice or more [including waking early], 3= symptoms causing you to be awake for most of the night, 4= symptoms so severe that you do not sleep at all.) The patients had to be willing to give informed consent to participate in the study. The exclusion criteria were as follows: older than 75 years and younger than 40; clinical or laboratory evidence of serious uncontrolled systemic disease; cardiovascular disease; having had a lower respiratory tract infection within the previous 28 days; diabetes; having been hospitalized for any aspect of chronic airway disease within the past 28 days; requiring a maintenance dose of oral steroids >10mg; having required a booster course of steroids within the previous 28 days; pregnant or lactating; having a known hypersensitivity to beta-receptor agonists; being treated with a non-selective beta-receptor antagonist (beta-blocker) medication; currently receiving other research medication or having taken other research medication in the last month; and incapable of using the study medications. Concurrent medications permitted: methylxanthines; inhaled steroids, dosage $\leq$ 400μg daily; sodium cromoglycate; nedocromil sodium; ketotifen. Oral/parenteral/rectal beta agonists were not permitted. Females of childbearing age could be included in the study if, in the opinion of the supervising physician, they were taking adequate

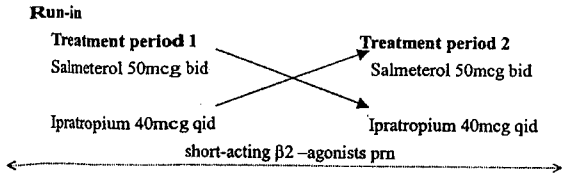

	1M	1 M	1 M	1 M	1M	1M	1M	
Visit Numbers*	1	2	3	4	5	6	7	8
BP/HR	×	×	×	×	×	×	×	×
Lung function		×			×			×
Adverse events		×	×	×	×	×	×	×

*First month: run-in period; 2-4 months: first treatment period; 5-7 months: second treatment period
BP: blood pressure
HR: heart rate
M: month

Fig.1. Study Plan

contraceptive precautions.

This study was a randomized, crossover, and comparative study. There were two 3-month treatment periods (Figure 1). Patients began the run-in period having replaced any medication not permitted by the protocol with inhaled short-acting β2-agonists prn. The run-in period acted as a baseline period. Following the run-in period, if eligible, the patient was randomized to receive either Salmeterol or Ipratropium for three months. After three months, they crossed over to receive the other drug for another three months. Rescue inhaled short-acting β2-agonists were provided for use whenever necessary throughout the treatment period

Each patient attended the hospital/clinic on 8 occasions before, during, and after the 6 months' treatment period. At each clinic after the run-in and treatment periods, the physician and the patient made independent assessments of the efficacy of the treatment since the previous visit. Measurements of forced expiratory volume, body weight, systolic blood pressure, diastolic blood pressure, heart rate, and device usage, were recorded.

For each treatment period, data was analyzed for months 1-3, and months 4-6. A minimum of 15 days' data from the run-in period and a minimum of 2 months' data from the treatment period were required for inclusion in the analysis. Statistical comparisons among the treatment groups were performed using a Wilcoxon rank test, except for compliance of device usage, which was compared using the Mantel-Haenszel chi-square test.

Results

Of the 40 patients recruited for the study, five were excluded before randomization because

Table 1. Demographic and baseline characteristics of patients

	Sequence I (Salmeterol/Ipratropium)				Sequence II (Ipratropium/Salmeterol)				p-value[a]
	N	mean	sd	median	N	mean	sd	median	
Age (yr)	18	68.17	6.05	70.5	17	70	3.71	70	0.607
Body weight (kg)	18	58.44	12.91	55	17	63.06	16.21	58	0.508
Body height (cm)	18	161.28	5.28	160	17	162.29	7.11	163	0.427
COPD duration years (yr)	17	7.06	11.16	2.5	15	5.5	5.05	4	0.761
Diastolic B.P. (mmHg)	17	131.47	19.17	138	17	132.41	21.89	125	0.973
Systolic B.P. (mmHg)	17	79.53	8.47	82	17	79.18	10.08	80	0.823
Heartbeat (/min)	17	88.35	15.4	87	17	81.94	10.57	83	0.184
FVC (L)	16	1.98	0.59	1.99	16	2.01	0.62	2.04	0.880
FEV1 (L/sec)	16	0.92	0.27	0.87	16	0.94	0.31	0.89	0.955

a. Test statistics based on Wilcoxon rank sum test
N: number
Sd: standard deviation
B.P: blood pressure
FVC: forced vital capacity
FEV1: forced expiratory volume in one second

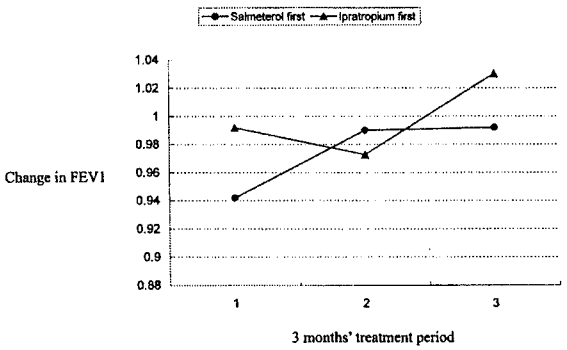

Fig. 2. The salmeterol group yielded a small improvement in net change in FEV1 as compared to the Ipratropium group after 3 months' use.
*1-1st visit, 2-4th visit, 3-7th visit

of ineligibility. Of the remaining 35 patients, 18 received Salmeterol, then Ipratropium (Group I), and 17 were treated with Ipratropium, then Salmeterol (Group II). The characteristics of these patients are given in Table 1. Both groups were evenly matched for age, sex, and COPD duration. Only one female was enrolled in group I. The mean ± SD age was 68.17 ± 6.05 and 70 ± 3.71 years, in groups I and II (P= 0.607) (Table 1). During the study period, six patients were lost the follow up, and two patients were hospitalized due to exacerbation with pneumonia after three months' Ipratropium MDI use. As a result, eight patients failed to complete the study. Spirometric measurements of the net change in FEV1 and FVC showed FVC=0.01 ± 0.68 L and FEV1= 0.03 ± 0.21 L in the Salmeterol group, and FVC= -0.10 ± 0.46L and FEV1= 0.01± 0.20 L in the Ipratropium group. The Salmeterol group yielded the same efficiency in net change of FEV1 and FVC as the Ipratropium group after 3 months' use, with no statistical difference (Table 2) (Figure 2).

In this study, the Salmeterol accuhaler, 50 mcg bid, and the Ipratropium MDI, 40 mcg qid, demonstrated clinical efficacy in increasing FEV1 and FVC (Figure 3). Patient device usage and compliance were observed at every visit. There was no significant difference in either group (accuhaler Vs MDI), and data with 95% confidence limits was acceptable (Table 3). However, the Ipratropium MDI was used incorrectly by patients when they visited the physician, and they said the Salmeterol accuhaler was easier to use than the Ipratropium MDI. No significant changes in pulse rate, or systolic and diastolic pressure, were found in the two groups (group I vs group II: pulse rate= 82.6 ± 12.2 vs 82.69 ± 14.73, P= 0.499; systolic BP= 128.86 ± 21.47 vs 130.69 ± 19.5, P= 0.78; diastolic BP= 76.22 ± 12.25 vs 76.67 ± 11.91, P= 0.54).

Discussion

Although patients with COPD do not respond to bronchodilators as dramatically as asthmatic patients do, some increase in the FEV1 and a reduction in dyspnea are nearly always achieved with the administration of bronchodilator agents.

At the present time, bronchodilator medications, including anticholinergics and long-acting β2-agonists, are central to symptom management in COPD [13].

Ipratropium is a quaternary ammonium compound with anticholinergic properties; it appears to inhibit vagally-mediated reflexes by

Table 2. Mean net change in primary efficacy after using Salmeterol or Ipratropium for 3 months

	Salmeterol					Ipratropium					p-value[a]
	N	mean	sd	median	p[b]	N	mean	sd	median	p[b]	
FVC (L)	24	0.01	0.68	0.08	0.936	23	-0.10	0.46	-0.08	0.320	0.601
FEV1(L/sec)	24	0.03	0.21	0.10	0.460	23	0.01	0.20	0.01	0.902	0.637

a. Between-treatment comparison test statistics based on analysis of covariance LSD
b. Within-treatment comparison test statistics based on Wilcoxon signed rank test
N: number
Sd: standard deviation
FVC: forced vital capacity
FEV1: forced expiratory volume in one second

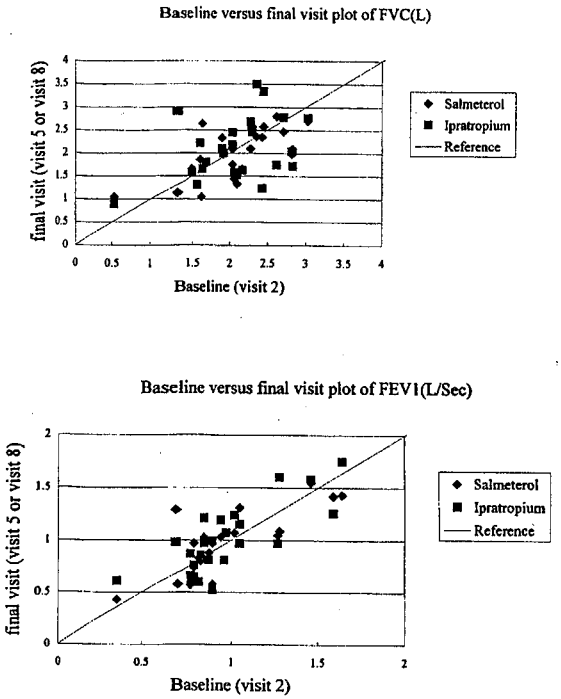

Fig. 3. Both the Salmeterol accuhaler 50 mcg bid and Ipratropium 40 mcg qid demonstrated clinical efficacy yin increasing FEV1 an FVC above baseline after 3 months' treatment.

antagonizing the action of acetylcholine. Ipratropium prevents the increase in the intracellular concentration of cyclic guanosine monophosphate caused by the interaction of acetylcholine with the muscarinic receptor on the bronchial smooth muscle, which then produces bronchodilation [14]. Salmeterol is a selective long-acting beta2-adrenoceptor agonist with a long side-chain that binds to the exo-site of the receptor. These pharmacological properties of Salmeterol offer more effective protection against histamine-induced bronchospasm and produce a longer duration to bronchodilation, lasting for least 12 hours, than recommended doses of conventional short-acting beta2-agonists or anticholinergic agents [15]. Combination treatment with Salmeterol plus Ipratropium has produced a significant increase in FVC and symptom relief in several reports [1,4], but few studies have compared Salmeterol with Ipratropium alone. Our study was designed to compare whether the response to the use of Salmeterol alone was better than that to Ipratropium alone or not, because Ipratropium MDI has an environmental pollution effect and must be decreased in use. In this study, the Salmeterol accuhaler, 50 mcg bid, and the Ipratropium MDI, 40 mcg qid, demonstrated the same clinical efficacy in increasing FEV1 and FVC. The response to Salmeterol appeared to be equal to that to Ipratropium; there was no statistically significant difference. One additional finding is of interest: Table 3 illustrates that the device usage (compliance) for Salmeterol and Ipratropium was the same, but in the clinical observation when the patient came back to visit the physician, the method of using the MDI was almost always incorrect. We must speed more time teaching the patient to use the MDI correctlt at every visit. So the patient must have a good technique and compliance with Ipratropium MDI treatment in order to achieve the same effect as with the Salmeterol accuhaler, with its easy application and lower use frequency.

Neither Salmeterol nor Ipratropium inhalation had any significant effect on pulse and blood pressure. Thus the two drugs were safe and free from appreciable cardiovascular effects.

Conclusion

The Salmeterol accuhaler was equal to the

Table 3. Compliance of device usage

	Salmeterol				Ipratropium				p-value[a]
	N	good	acceptable	not good	N	good	acceptable	not good	
The first month	33	63.6%	30.3%	6.1%	33	63.6%	30.3%	6.1%	1.000
The second month	27	63.0%	25.9%	11.1%	29	69.0%	24.1%	6.9%	0.561
The third month	27	74.1%	18.5%	7.4%	29	86.2%	10.3%	3.5%	0.272

a:Test statistics based on Mantel-Haenszel Chi-Square test
N: number

Ipratropium MDI in improving lung function, when used at the recommended doses over the 3-month periods; but the accuhaler was easier to use than the MDI. The safety profile of Salmeterol was similar to that of Ipratropium in this trial, and the twice-daily dosing schedule of Salmeterol should enhance compliance. These collective data support the use of Salmeterol as first-line therapy for the long-term treatment of airflow obstruction in patients with COPD.

References

1. van Noord JA, de Munck DR, Bantje TA, *et al.* Long-term treatment of chronic obstructive pulmonary disease with Salmeterol and the additive effect of Ipratropium. Eur Respir J 2000; 15: 878-85.
2. Siafakas NM, Vermeire P, Pride NB, *et al.* Optimal assessment and management of chronic obstructive pulmonary disease (COPD): ERS consensus statement. Eur Respir J 1995; 8: 1398-420.
3. Mahler DA, Donohue JF, Barbee RA, *et al.* Efficacy of Salmeterol xinafoate in the treatment of COPD. Chest 1999; 115: 957-65.
4. American Thoracic Society. Standards for the diagnosis and care of patients with chronic obstructive pulmonary disease. Am J Respir Crit Care Med 1995; 152: S77-120.
5. Ferguson GT, Cherniack RM. Management of chronic obstructive pulmonary disease. N Engl J Med 1993; 328: 1017-22.
6. Karpel JP. Bronchodilator responses to anticholinergic and beta-adrenergic agents in acute and stable COPD. Chest 1991; 99: 871-6.
7. Blosser SA, Maxwell SL, Reeves-Hoche MK, *et al.* Is an anticholinergic agent superior to a β_2-agonist in improving dyspnea and exercise limitation in COPD? Chest 1995; 108: 730-5.
8. Pino-Garcia JM, Garcia-Rio F, Gomez L, *et al.* Short-term effects of inhaled ß-adrenergic agonist on breathlessness and central inspiratory drive in patients with nonreversible COPD. Chest 1996; 110: 637-41.
9. Johnson M. The pharmacology of Salmeterol. [Review] [5 refs] Lung 1990; 168 Suppl: 115-9.
10. Cazzola M, Matera MG, Santangelo G, *et al.* Salmeterol and formoterol in partially reversible severe chronic obstructive pulmonary disease: a dose-response study. Respir Med 1995; 89: 357-62.
11. Cazzola M, Santangelo G, Piccolo A, *et al.* Effect of Salmeterol and formoterol in patients with chronic obstructive pulmonary disease. Pulm Pharmacol 1994; 7: 103-7.
12. Cazzola M, Matera MG, Di Pema F, *et al.* A comparison of bronchodilating effects of Salmeterol and oxitropium bromide in stable chronic obstructive pulmonary disease. Respir Med 1998; 92: 354-7.
13. Romain A, Pauwels A, Sonia Buist, *et al.* Global Strategy for the Diagnosis, Management, and Prevention of Chronic Obstructive Pulmonary Disease. NHLBI/WHO Global Initiative for Chronic Obstructive Lung Disease (GOLD) Workshop Summary. Am J Respir Crit Care Med 2001; 163: 1256-76.
14. Peter J Barnes. Airway Muscarinic Receptors, Sheldon L Spector, Anticholinergic Agents in the Upper and Lower Airways, First Edition, New York, Marcel Dekker, Inc, 1999: 31-55.
15. Lotvall J, Svedmyr N. Salmeterol. An inhaled beta 2-agonist with prolonged duration of action [Review] [47 refs]. Lung 1993; 171(5): 249-64.

比較 Salmeterol accuhaler 和 Ipratropium 在慢性阻塞性呼吸道疾病使用之效能及安全性

潘信宏　許正園　江自得

背景：支氣管擴張劑是目前處置慢性阻塞性呼吸道疾病症狀的主軸，這包括了副交感神經拮抗劑及長效乙二型交感神經刺激劑，但僅有少數文獻比較這兩者單獨使用之療效及安全性。

目的：本研究的目的是比較交叉使用 Salmeterol accuhaler 50 毫克一天兩次和 Ipratropium MDI 40 毫克一天四次三個月後兩者之療效及安全性。

方法：我們一共搜集了 35 位中度至重度的慢性阻塞性呼吸道疾病的病人，隨機地分成兩組然後分別接受 Salmeterol accuhaler 50 毫克一天兩次或 Ipratropium MDI 40 毫克一天四次，三個月後兩組交換藥物再使用三個月。完成後比較兩組之肺功能、收縮壓、舒張壓、心跳速率及器具使用等之差異。

結果：兩組病人使用了 Salmeterol accuhaler 50 毫克一天兩次或 Ipratropium MDI 40 毫克一天四次三個月後，FEV1 及 FVC 昇高之值變化不大。在各使用這兩種藥物三個月後，Salmeterol accuhaler 的這一組病人與 Ipratropium MDI 這一組病人其 FEV1 和 FVC 上昇之值相當，且沒有統計學上的意義。兩者藥物使用後對心跳速率、收縮壓、舒張壓均沒有明顯改變。

結論：比較使用三個月後肺功能的改善，Salmeterol accuhaler 與 Ipratropium MDI 兩者效果相當；但是器具之使用方面，accuhaler 則比 MDI 來得容易。 ***(胸腔醫學 2002; 17: 19-25)***

關鍵詞：Salmeterol，Ipratropium，慢性阻塞性呼吸道疾病

台中榮民總醫院　胸腔內科
索取抽印本請聯絡：許正園醫師，台中市中港路三段 160 號

Esophageal Schwannoma—Case Report and Review of the Literature

Hsao-Hsun Hsu, Yih-Leong Chang*, Yung-Chie Lee

This is a rare case report of a 34-year-old woman with a schwannoma of the esophagus. The patient was referred to our hospital with a 6-month history of dysphagia. The evaluation revealed a submucosal tumor of the esophagus, which was successfully resected through a right thoracotomy. During the pathologic examination, the tumor was disclosed in the muscular layers of the esophagus; there was no anatomic relationship between the tumor and the vagus nerve. Negative immunohistochemical staining for CD34 and CD117 proved the tumor had not originated in the smooth muscle cells. From the histological characteristics and positive immunohistochemical staining for S-100 protein, the diagnosis of esophageal schwannoma was made. ***(Thorac Med 2002; 17:26-30)***

Key words: esophageal schwannoma

Introduction

Benign tumors of the esophagus are rare, and most of them are leiomyomas. An esophageal schwannoma is extremely rare, and only 15 cases have been reported in the literature. To the best of our knowledge, it has never been reported in Taiwan. Herein, we describe a case of esophageal schwannoma with a literature review of the clinical and pathological features.

Case Report

A 34-year-old woman was admitted to our hospital in November 2000 with a 6-month history of dysphagia. About six months prior to admission, she had begun to suffer from occasional dysphagia when swallowing. Two months before this admission, an episode of dull pain over the sternum caused her to present at another hospital. She was diagnosed there with a submucosal tumor of the esophagus, and was referred to our institution for surgical treatment. She was a well-nourished woman without any loss in weight during this period. Physical examination revealed no abnormalities and the laboratory data were normal. The chest radiography demonstrated an abnormal shadow occupying the right central portion of the superior mediastinum. The chest computed tomography showed a 7 x 4 x 4 cm tumor of uniform density on the posterior aspect of the trachea, and adjacent to the esophagus (Figure 1A). The barium esophagogram revealed a remarkable segmental narrowing of the upper thoracic

Department of Surgery,* Department of Pathology, National Taiwan University Hospital
Address reprint requests to: Dr. Yung-Chie Lee, Department of Surgery, National Taiwan University Hospital, No.7, Chung Shan South Road, Taipei, Taiwan

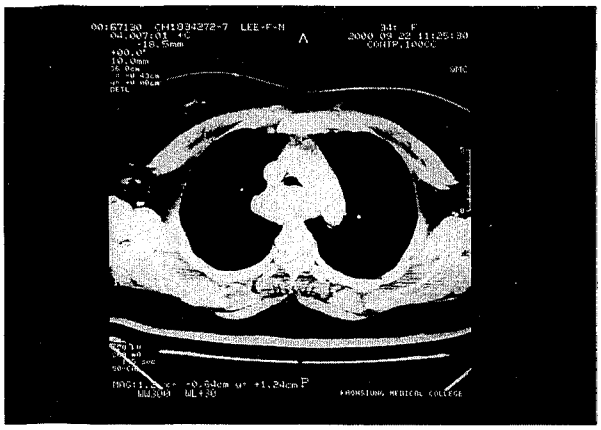

Fig 1A. The chest computed tomography showing a 7 × 4 × 4 cm tumor of uniform density on the posterior aspect of the trachea and adjacent to the esophagus.

esophagus, with smooth mucosa (Figure 1B). Esophagoscopy revealed a submucosal tumor with intact mucosa in the same position. On November 12, 2000, a right-sided posterolateral thoracotomy through the fourth rib bed was performed. An elastic and firm tumor was found in the muscular layers of the esophageal wall, with no anatomic relationship between the tumor and the trachea or vagus nerve trunk. The tumor was entirely resected, including the circumjacent muscle and the covering mucosa.

The well-demarcated tumor measured 7.5 x 4.2 x 4.0 cm in size, and had a rubbery consistency. It was yellowish-white, with a whorl-like appearance, and unencapsulated on sectioning (Figure 2). Microscopically, the tumor was mainly composed of compact ovoid and spindled cells with twisted nuclei, and indistinct cytoplasmic borders arranged in fascicles in the cellular (Antoni A) area. However, nuclear palisadling was not prominent (Figure 3). The other element (Antoni B), with tumor cells arranged within the loose and myxoid matrix, was occasionally present. There was no definite fibrous capsule, and occasional lymphoid cuffing was seen at the periphery of the tumor. The nuclei of the tumor cells displayed a remarkable uniformity in their chromatin distribution of shape and size, with an absence of mitotic activity. Furthermore, the tumor cells were strongly

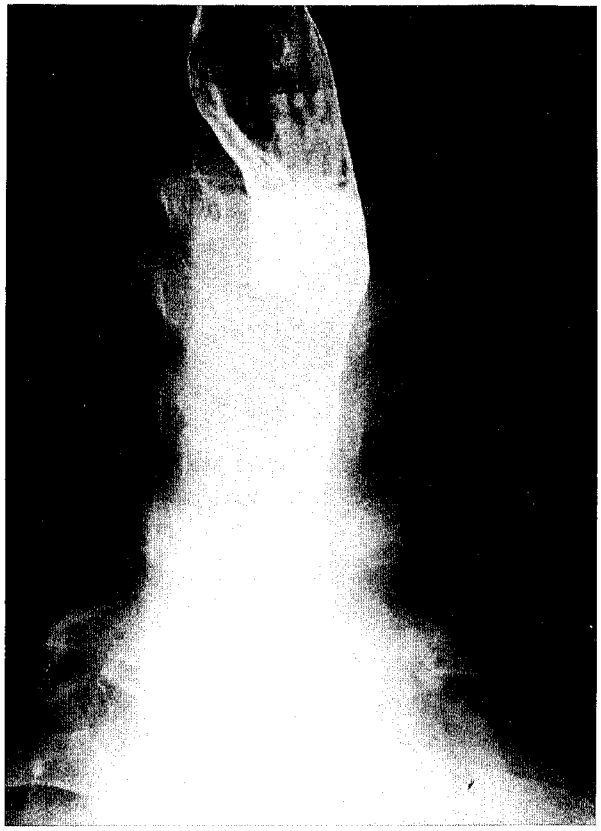

Fig 1B. The barium esophagogram showing a remarkable segmental narrowing of the upper thoracic esophagus with smooth mucosa.

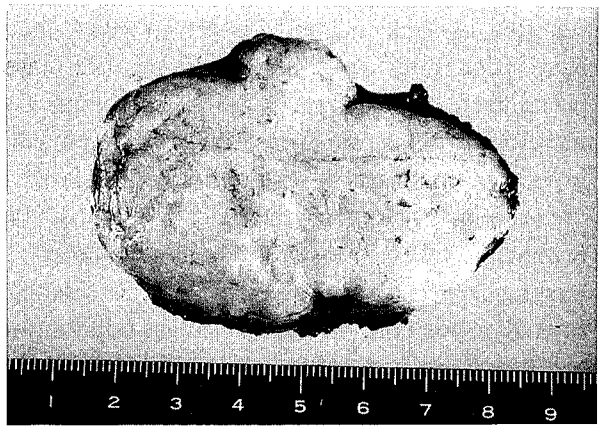

Fig 2. The cut surface of the gross specimen showing an unencapsulated, yellowish white tumor occupying the esophageal muscle layers.

immunoreactive to S-100 protein (Figure 4), but non-immunoreactive to CD34 and CD117. An esophageal schwannoma was diagnosed.

Postoperatively, the patient made an uneventful recovery, and was doing well 6

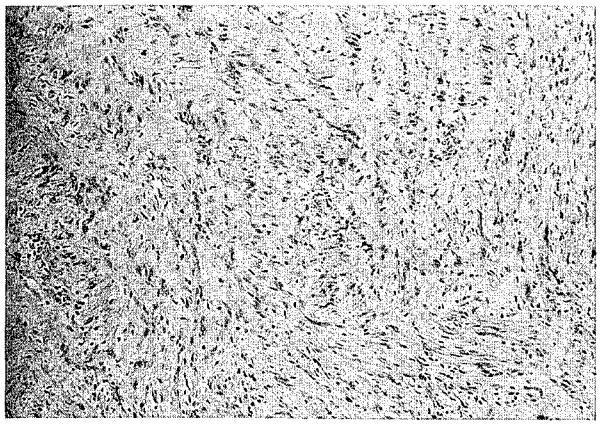

Fig 3. The tumor was composed of ovoid and spindled cell arranged in fascicles. (H&E, X 33 original magnification)

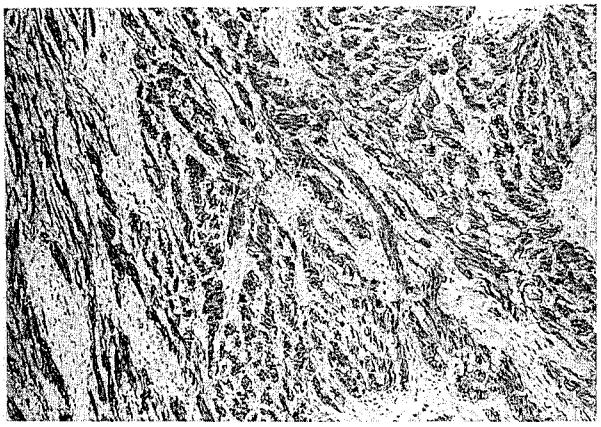

Fig 4. The tumor cells were stained strongly with the antibody t S-100 protein. (Avidin-Biotin complex method, X 33 origina magnification)

months after the operation, with no evidence of recurrence.

Discussion

An esophageal schwannoma is quite rare, and previous reports had suggested that the most common types of benign submucosal tumor of the esophagus are leiomyoma, cysts, or lipomas. Since an esophageal schwannoma was first reported by Chatelin and Fissore in 1967, there have been only 16 cases, including our case, presented in the literature [1-8]. Epidemiologically, the esophageal schwannoma occurs predominantly in women, and half of these tumors are situated at the cervical or upper thoracic portion of the esophagus. The most common symptom is dysphagia. The typical radiological findings include a posterior mediastinal mass adhering to the esophagus, as revealed on chest computed tomography, or a large, smooth, polypoid filling defect disclosed on the barium esophagogram. The differentiation of esophageal schwannoma from other submucosal tumors on preoperative examination is extremely difficult because there are no particular differences between them.

Neoplasms derived from fibroblasts, smooth muscles cells, and Schwann cells may have similar histological features [9]. Diamaru and colleagues [10] indicated that it is difficult to make a correct diagnosis of digestive schwannoma depending only on an ordinary histological examination. According to their statement, only 9 of 24 (37.5%) patients with schwannoma could be diagnosed correctly without an immunohistochemical analysis. Most of them tended to be diagnosed as smooth muscle tumors.

Negative immunohistochemical staining for CD34 and CD117 indicate that the tumor cells derived from neither fibroblasts nor smooth muscle cells. In soft tissues outside the central nervous system, positive immunohistochemical staining for S-100 protein is found normally only in Schwann cells [9]. The correct diagnosis of esophageal schwannoma can only be accepted if the immunohistochemical staining for S-100 protein is positive, and those for smooth muscle markers are all negative, suggesting that this tumor is a nerve sheath tumor. Interestingly, these tumors arising from the esophagus differ from typical schwannomas of the peripheral nerves. They lack the characteristic capsule, the sclerotic vessels, and the usual palisading growth pattern; they have a peculiar lymphoid cuff, a feature not associated with usual schwannomas [11].

Surgical resection is the only effective treatment. Generally, the prognosis of schwannoma is excellent if surgical resection is performed early. Although there has been only one reported of local recurrence after resection [3], Das Gupta et al. [12] thought that 49 of 303

(16.1%) patients with benign solitary schwannomas had malignant tumors apparently unrelated to the peripheral nerves. Therefore, we advocate the early removal of the tumor, and that follow-ups for a prolonged period postoperatively are necessary in all patients with esophageal schwannoma.

References

1. Chatelin CL, Fissore A. Schwanome degenere de l'esophage. Conffront Radio Anat Clin 1967;7: 114.
2. Brooks JS, Freeman M, Enterline HT. Malignant "Triton" tumors: natural history and immunohistochemistry of nine new cases with literature review. Cancer 1985; 55: 2543-9.
3. Eberlein TJ, Hannan R, Josa M, *et al.* Benign schwannoma of the esophagus presenting as a giant fibrovascular polyp. Ann Thorac Surg 1992; 53: 343-5.
4. Iwata H, Kataoka M, Yamakawa Y, *et al.* Esophageal schwannoma. Ann Thorac Surg 1993; 56: 376-7.
5. Arai T, Sugimura H, Suzuki M, *et al.* Benign schwannoma of the esophagus: report of two cases withimmunohistochemical and ultrastructual studies. Patol Int 1994; 44: 460-5.
6. Morita I, Mushiaki H, Shinozaki Y, et al. A case of the esophageal submucosal schwannoma with pathological malignant finding [in Japanese]. Geka 1996; 58: 506-10.
7. Ishida a, Masaki H, Tabuchi A, *et al.* A case of neuroschwannoma of the esophagus [in Japanese with English abstract]. J Jpn Soc Clin Surg 1997; 58: 2033-7.
8. Reijiro Saito, Michihiko Kitamura, Hiroyuki Suzuki, *et al.* Esophageal schwannoma. Ann Thorac Surg 2000; 69: 1949-51.
9. Stefansson K, Wollmann R, Jerkovic M. S-100 protein in soft tissue tumors derived from Schwann cells and melanocytes. Am J pathol 1982; 106: 261-8.
10. Daimaru Y, Kido H, Hashimoto H, *et al.* Benign schwannoma of the gastrointestinal tract: a clinopathologic and immunohistochemical study. Hum Pathol 1988; 19: 257-64.
11. Lewin KJ. and Appelman HD. Atlas of tumor pathology. Tumors of the esophagus and stomach. 1996: 442-3.
12. Das Gupta Tk, Brasfield RD, Strong EW, *et al.* Benign solitary schwannomas (neurilemomas). Cancer 1969; 24: 355-66.

食道神經鞘瘤——病例報告併文獻回顧

徐紹勛　張逸良*　李元麒

食道神經鞘瘤為一相當罕見之食道良性腫瘤。此種好發於女性之食道腫瘤在術前檢查中很難與其它發生於食道黏膜下之良性腫瘤區別。正確之診斷建立於術後病理標本玻片檢驗與特殊之螢光免疫染色。在施以完全切除手術後，其癒後相當良好。在此我們報告一個以外科手術成功切除食道神經鞘瘤之病例並回顧歷年來有關此種病例的文獻。 ***(胸腔醫學 2002; 17: 26-30)***

關鍵詞：食道神經鞘瘤

國立臺灣大學附設醫院　外科部　病理科*
索取抽印本請聯絡：李元麒醫師，台北市中山南路 7 號

Rapidly-Growth Giant Solitary Benign Fibrous Tumor of the Pleura in an Adult

Hsin-Yuan Fang, Alan Ronald Talbot*, Torng-Sen Lin, Kun-Chou Hsieh

A 61-year-old male presented with progressive shortness of breath lasting for three months. Chest radiographs and a computerized tomography scan showed a giant extra-pulmonary solid mass in the right thoracic cavity, with minimal pleural effusion, and the mass compressing the right lung. A lateral video-assisted mini-thoracotomy was performed, and a clearly-demarcated giant reddish solid mass measuring 17.0x14.5x7.2 cm, and weighing 1.02 kg was removed. The pathological diagnosis was benign solitary fibrous tumor. The histological examination showed a solitary fibrous tumor composed of bland-looking spindle cells that were haphazardly arranged and embedded in a densely collagenous matrix. After the operation, the patient recovered well, and is being followed up at the outpatient department. ***(Thorac Med 2002; 17: 31-34)***

Key words: benign solitary fibrous tumor, pleural tumor

Introduction

Solitary fibrous tumors (SFT) of the pleura are rare tumors originating in the mesenchymal tissue underlying the mesothelial layer of the pleura [1]. These tumors present an unpredictable clinical course probably related to their histological and morphological characteristics. We describe an adult male patient with a benign SFT in the right thoracic cavity who underwent the complete surgical removal of the tumor.

Case Report

A 61-year-old male presented with progressive shortness of breath lasting for three months. There was no fever, chest pain, or chest tightness, and only a decreased breathing sound at the right-side chest wall. Chest radiographs were done at the outpatient department, and showed a huge extra-pulmonary lesion in the right cavity with minimal pleural effusion (Figure 1). Chest computerized tomography (CT) showed a lower-density loculated extra-pulmonary mass, with the lung parenchyma compressed, and minimal pleural effusion at the right thoracic cavity (Figure 2). An old chest radiograph performed three years ago due to a blunt thoracic injury showed a negative finding. A lateral video-assisted mini-thoracotomy was performed and a clearly-demarcated, giant reddish solid mass, measuring 17.0x14.5x7.2 cm, and weighing 1.02 kg mass was removed with a tissue bag.

Divison of General Thoracic Surgery, Department of Surgery, Changhua Christian Hospital, Changhua, Taiwan, *Department of Critical Care Medicine, Changhua Christian Hospital, Changhua, Taiwan, and Department of Internal Medicine, Chung Shan Medical and Dental College, Taichung, Taiwan
Address reprint requests to: Dr. Talbot, Department of Critical Care Medicine, Changhua Christian Hospital, No.135 Nan Siau Street, Changhua, Taiwan

Fig. 1. Posterior-anterior and lateral chest radiographs show a huge extra-pulmonary lesion in the right lung field.

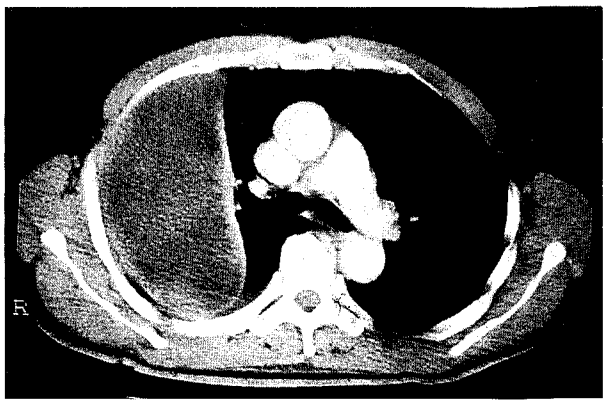

Fig. 2. Preoperative chest computerized tomography scan demonstrates an extra-pulmonary solid mass in the right thoracic cavity.

Minimal pleural effusion was found during the operation. This mass was free from the lung surface and attached to the parietal pleural with a 5x5 cm base stalk (Figure 3). The laboratory data of the pleural effusion revealed: white cell count, 198/cmm; red cell count, 4801/cmm; neutrophil/ lymphocyte, 1/99; protein, 4600 mg/dl; glucose, 112 mg/dl; lactate dehydrogenase, 283 iu/l; and pH, 7.7. The pathological diagnosis was a benign solitary fibrous tumor. The histological examination showed a solitary fibrous tumor composed of bland-looking spindle cells that were haphazardly arranged and embedded in a densely collagenous matrix. Myxohyaline degeneration of the tumor was prominent (Figure 4). The S-100 immunochemical stain was negative. After the operation, the patient recovered well, and is being followed up at the outpatient department.

Discussion

Primary tumors of the pleura can be divided into two major categories: diffuse and solitary. Diffuse pleural tumors are mesotheliomas. They are more common than solitary pleural tumors, arise from the mesothelial tissue, are associated with asbestos exposure, and almost always have a fatal course [1].

The most common symptoms of SFT are dyspnea (19%), coughing (14.3%), chest pain (28.5%), finger clubbing (14.3%), and hypoglycemia (14.3%) [1]. Hypoglycemia is related to a pathological incretion of insulin-like growth factor 2 by the tumor. This patient came to our hospital with progressive shortness of breath lasting for three months.

The most important diagnostic test for these tumors is the chest radiograph. Chest radiographs can reveal solitary, circumscribed, homogeneous lesions sometimes associated with pleural effusion, and rare calcifications within the tumor. On CT scanning, a sharply delineated, sometimes loculated mass with the same density as the musculature can be seen. Contrast enhancement is usually intense and homogeneous, as a result of the rich vascularization of the tumor. However, a CT scan also may show no enhanced areas, due to necrosis, myxoid degeneration, or hemorrhage within the tumor. Displacement rather than invasion of the adjacent structures is characteristic [2].

The differential diagnosis of SFT of the pleura includes solitary pleural metastasis, lipoma, pleural fibrosarcoma, intercostal nerve neurilemoma, organized inflammation, and peripheral bronchial carcinoma [3].

Since fibrous tumors of the pleura may rapidly enlarge and are potentially malignant, surgical resection is recommended in all cases. Preoperative transthoracic needle biopsy is not necessary, because it does not exclude malignant variants and does not influence the need for

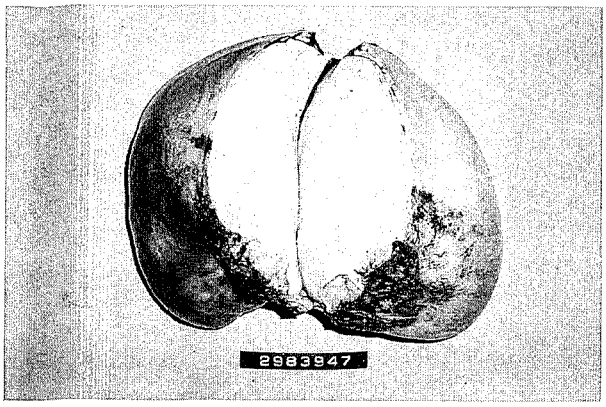

Fig. 3. The tumor measured 17.0x14.5x7.2 cm in size, and had a sticky-white surface when cut.

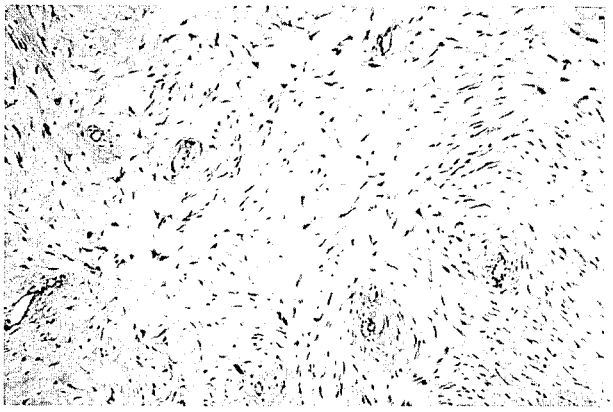

Fig. 4. Micrography shows a solitary fibrous tumor composed of bland-looking spindle cells that were haphazardly arranged and embedded in a densely collagenous matrix. Myxohyaline degeneration of the tumor is prominent (hematoxylin and eosin x 100).

surgical resection. Care should be taken to remove the whole mass. Hence, although the tumor may be well-circumscribed, a large resection of the lung parenchyma and surrounding pleura is encouraged, in particular with tumors presenting a broad base of attachment to the pleural surface [4].

Although histologically benign, solitary fibrous tumors of the pleura may enlarge rapidly and occasionally transform into malignant variants after several years. Therefore, complete surgical resection and long-term follow-up is recommended for all patients [2]. This patient's tumor had enlarged rapidly, since the chest radiograph was normal three years ago. Grossly, the tumor was reddish and elastic, with some hemorrhage. The histological examination showed no malignant change.

The prognosis depends, first, on the resectability of the tumor, second, on it's size, and then, in decreasing order of importance, on the mitotic count, polymorphism, and necrosis within the tumor [5].

The surgical treatment of choice is local removal by video-assisted thoracic surgery (VATS), with an intraoperative assessment of the free surgical margins. In parietal-pleura-based lesions, a minimal extrapleural resection to assess the margins is mandatory [6]. In large size lesions, a mini-thoracotomy with video-assisted resection is technically feasible, the surgical specimen is extracted with a tissue bag.

Postoperative adjuvant therapy with radiotherapy, chemotherapy, or both has been sporadically used, but its benefit remains unproved. Recurrence after complete resection is possible in benign and malignant variants, therefore, long-term annual follow-up with chest radiographs is highly recommended [4].

References

1. Rena O, Filosso PL, Papalia E, *et al.* A. Solitary fibrous tumour of the pleura: surgical treatment. Eur J Cardiothorac Surg 2001; 19: 185-89.
2. Perrot M, Kurt AM, Robert JH, *et al.* Clinical behavior of solitary fibrous tumors of the pleura. Ann Thorac Surg 1999; 67: 1456-9.
3. Desser TS, Stark P. Pictorial essay: solitary fibrous tumor of the pleura. J Thorac Imaging 1998; 13: 27-35.
4. Perrot MD, Kurt AM, Robert JH, *et al.* Clinical behavior of solitary fibrous tumors of the pleura. Ann Thorac Surg 1999; 67: 1456-9.
6. Sandvliet RH, Heysteeg M, and Paul MA. A large thoracic mass in a 57-year-old patient. Chest 2000; 117: 897-900.
7. Cardillo G, Facciolo F, Cavazzana AO, *et al.* Localized (solitary) fibrous tumors of the pleura: an analysis of 55 patients. Ann Thorac Surg 2000; 70: 1808-12.

巨大良性的胸膜纖維腫瘤—病例報告

方信元 陶阿倫* 林同森 謝坤洲

61 歲男性病人因為漸進性呼吸喘已有三個多月。胸部 X 光照片和電腦斷層攝影掃描顯示右邊的胸腔內有巨大的肺外病兆合併胸水，病人三年以前因外傷而照的胸部 X 光則無病兆發現。病人接受影像輔助迷你開胸將腫瘤完全取出，腫瘤與胸壁有 5x5 公分的沾黏，與肺部則沒有相連。腫瘤大小 17.0x14.5x7.2 公分且重 1.02 公斤，腫瘤表面平滑成粉紅色，切開時呈現黃色與少數點狀出血。 病理的診斷是良性的胸膜纖維腫瘤。病人手術後順利出院，目前在門診追蹤。 ***(胸腔醫學 2002; 17: 31-34)***

關鍵詞：良性胸膜纖維腫瘤，肋膜腫瘤

彰化基督教醫院 外科部 胸腔外科 重症醫學科* 中山醫學院 醫學系*
索取抽印本請聯絡：陶阿倫醫師，彰化南校街 135 號

Relapsing Polychondritis with Acute Respiratory Failure —A Case Report

Chih-Ming Lin, Ying-Huang Tsai, Chung-Chi Huang, Kuo-Chin Kao, Chin-Kuo Lin, Thomas C-Y Tsao

Relapsing polychondritis (RP) is a rare disease characterized by recurrent inflammation and the destruction of the cartilaginous structures. Airway manifestations are ultimately present in about 50% of patients with RP. Airway involvement, especially the large airway, is a dreaded complication of RP. We report a case of acute respiratory failure due to tracheobronchomalacia secondary to RP, which was treated with steroids, a tracheostomy, and continuous positive airway pressure (CPAP). ***(Thorac Med 2002; 17: 35-39)***

Key words: Relapsing polychondritis, tracheobronchomalacia, tracheostomy, continuous positive airway pressure

Introduction

Relapsing polychondritis is a rare disease of unknown etiology characterized by episodic, painful, and destructive cartilaginous inflammation. The disease, commonest among Caucasians, affects men and women equally, with a peak incidence between 40 and 60 years of age. Considered an auto-immune process, autoantibodies directed against the cartilage and type II collagen have been found. Diagnosis is made on the basis of clinical presentations, but can be confirmed at biopsy [1]. The condition is usually multifocal and affects the cartilage of the ear in 88%, the nose in 82%, and the upper respiratory tract in 56-70% of patients. Additionally, patients frequently suffer non-erosive arthropathy (80%), ocular inflammation, and vestibulocochlear dysfunction that may occur as part of a connective tissue disease. The course of RP may be relatively benign and indolent, or it may be rapidly fatal, even after pharmacologic treatment, tracheostomy, and tracheobronchial stent emplacement [2-4]. Death is directly attributable to RP in about half of the fatal cases. Survival rates for 5 and 10 years are 74% and 55%, respectively [2]. Reported deaths from respiratory tract involvement vary from 10% to 59% of total deaths [2,5].

Case Report

This 45-year-old woman had been quite well before. She began to suffer a nonproductive cough and dyspnea in May 2000, and several diagnoses were made by local hospitals, including acute bronchitis, bronchial asthma, and hyperventilation syndrome. She was admitted to

Divison of Pulmonary and Criticl Care Medicine, Chang Gung Memorial Hospital, Taipei, Taiwan
Address reprint requests to: Dr. Chung-Chi Huang, Chang Gung Memorial Hospital 5 Fu-Shin Street, Kweishan, Taoyuan, Taiwan

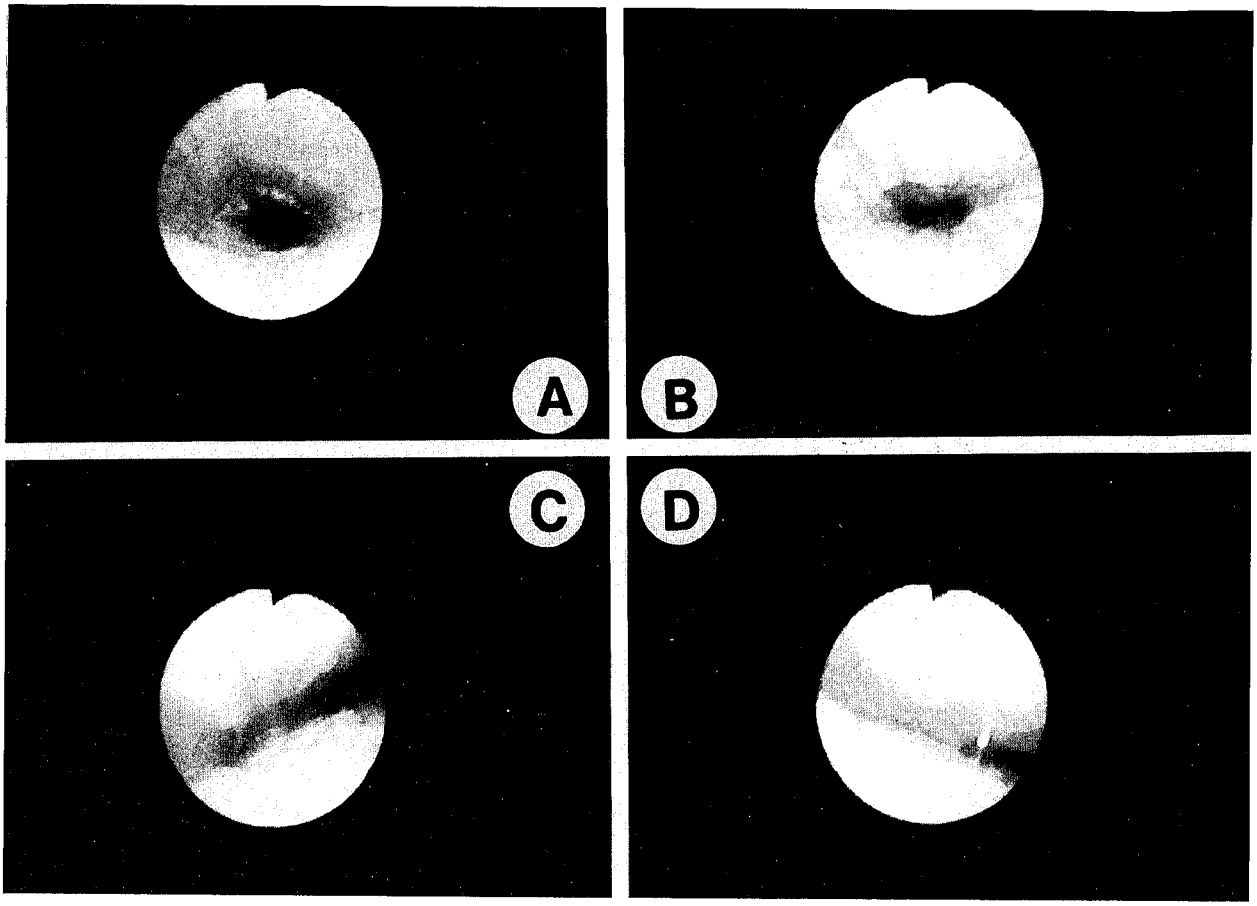

Fig. 1. The bronchoscope shows: A). a patent trachea during the inspiratory phase; B). a collapsed trachea during the expiratory phase; C). patent right and left main bronchi during the inspiratory phase; D). collapsed right and left main bronchi during the expiratory phase

Chang Gung Memorial Hospital once in July 2000, due to the above symptoms. Physical examination, chest radiography, and biochemistry data were all normal at that admission. Pulmonary function tests revealed mild airway obstruction without response to a bronchodilator, and a negative provocational test. The clinical manifestations improved with treatment by a bronchodilator and inhaled steroids.

Generalized arthralgia, tinnitus, blurred vision, painful swelling of the helices of both ears, and erythematous skin changes developed one month after discharge. The nasal bridge depressed later forming a saddle nose. Due to the exacerbated dyspnea and progressive inspiratory stridor, as well as the arterial blood gas showing respiratory alkalosis (pH: 7.505, PCO_2:28.4 mmHg, PO_2: 93.3mmHg, HCO_3^-: 21.9 mmol/l, Osat: 97.8%) in room air, she was admitted again in Feb 2001. An emergency bronchoscopy revealed a limited opening of the vocal cords, hence, a tracheostomy was performed to relieve the upper airway obstruction. She was transferred to the medical intensive care unit for mechanical ventilation support. Autoantibodies, including antinuclear antibody (ANA), rheumatoid factor (RF), and anti-neutrophil cytoplasmic antibody (ANCA), the titers of which were all negative, were checked to exclude autoimmune disease. Relapsing polychondritis was diagnosed based on the chondritis involving the larynx, trachea, nasal cartilage, and both auricles, as well as the audiovestibular damage (tinnitus and vertigo), ocular inflammation (blurred vision), and non-erosive seronegative inflammatory polyarthritis. A second bronchoscope showed the expiratory

collapse of the lower trachea and both main bronchi (Figure 1). Steroids were started to control the inflammation, and the patient's clinical condition improved gradually. Mechanical ventilation was weaned, and she was put on spontaneous breathing with the support of BiPAP (S/T-D30, RESPIRONICS INC., Pennsylvania, USA) to prevent the expiratory collapse of the large airway. With an expiratory collapse, the suction tube could be passed into the lower bronchi to remove secretions only during the inspiratory phase. Because the tracheal stent was not available in our hospital, she was discharged with the aid of CPAP (S/T-D30, RESPIRONICS INC., Pennsylvania, USA) with FiO_2 30% use, and arterial blood gas (pH:7.409, PCO_2: 43.2 mmHg, PO_2: 162.3mmHg, HCO_3^-: 27.3 mmol/l, Osat: 99.1%) within acceptable range.

Discussion

The diagnostic criteria for RP were first described by McAdam et al in 1976. They include the presence of three or more of the following clinical features: 1), chondritis of the larynx, trachea, or bronchi; 2), chondritis of the nasal cartilages; 3), chondritis of both auricles; 4), audiovestibular damage (sensorineural hearing loss, tinnitis, and vertigo); 5), ocular inflammation; and 6), non-erosive seronegative inflammatory polyarthritis [5]. The RP diagnostic criteria were revised by Damiani and Levine in 1979 [1] to be: 1), the presence of any one of the given combinations of three or more McAdam's signs (histologic confirmation not necessary); 2), one or more of McAdam's signs with positive histologic confirmation by biopsy of the cartilage; and 3), involvement of two or more separate anatomic locations with response to steroids and/or dapsone. In addition, the criteria must exclude other autoimmune or rheumatic conditions, such as systemic lupus erythematosus, vasculitis, and rheumatic arthritis, because their immunological mechanisms play a major role in the pathogenesis of RP [6]. Our patient fulfilled McAdam's criteria by the presentations of auricular chondritis, saddle nose due to chondritis of the nasal cartilage, multiple arthritis, tinnitus, blurred vision, and respiratory tract complications.

The etiology of RP is unclear. Autoimmune mechanisms are considered to be most likely. Due to the recurrent and potentially progressive course, early diagnosis and treatment is necessary to avoid the involvement of the respiratory tract, which is a dreaded complication and typically occurs later in the course of RP [7]. Up to 50% of patients will die of respiratory tract complications. Airway manifestations ultimately occur in about 50% of patients with RP, although they may not be the presenting features [2,5]. The airway obstruction, usually diffuse and involving the upper airways, may be asymptomatic in the earlier stages, and detected only by pulmonary function testing [2-3]. Many RP patients have been treated as bronchial asthma [8] initially, due to mild airway obstructive symptoms and the effectiveness of steroids, and finally diagnosed as RP after more criteria were noted. Our patient was also suspected of having bronchial asthma due to the clinical presentations and the pulmonary function change, as well as the clinical response to bronchodilator therapy. When the large airway is involved, the symptoms/signs become more apparent. The dosage of steroids for bronchial asthma may be effective for RP initially, and become ineffective when RP progresses.

RP with chondritis involving the larynx may induce large airway obstruction and stridor. Emergency airway management, such as a tracheostomy to keep the airway patent, should be done immediately. However, the larynx may not be the sole involved area. The symptoms develop when the polychondritis involves the glottis, subglottic area, or upper trachea. Tracheal collapse may occur suddenly and cause dyspnea, respiratory arrest, asphyxia, and rapid death [4]. The placement of endobronchial stents at the main points of airway obstruction can help to allay the need for tracheostomy and mechanical ventilation, and may lead to improved patient functionality and

survival [9]. However, stent implantation, which is common in the US, is not popular in Taiwan. CPAP has been reported in the treatment of patients with variable intrathoracic obstruction. Ferguson and Benoist described three patients with tracheobronchomalacia in whom CPAP therapy improved airflow limitation [10]. We use BiPAP, in which the PEEP level was set at 16/8 cm H2O, then CPAP, in which the PEEP level was set at 5 to 10 cm H2O, to keep patient airways patent. If a stent is not available, CPAP is an effective alternative. However, CPAP with a PEEP greater than 12.5 cm H2O may induce sputum retention. A PEEP level kept below 10 to 12.5 cm H2O has been suggested [7].

Unexplained dyspnea, stridor, hearing deficit, ocular involvement, recurrent ear chondritis, and nasal cartilage inflammation with deformity are the clinical manifestations of RP. Physicians should have a high index of suspicion in the presence of these presentations for the early diagnosis and treatment of this disease. No single medical or surgical treatment is uniformly effective in curing the disease, in relieving the symptoms, or in preventing the progression of airway manifestations. A multidisciplinary team, including pulmonologists, otolaryngologists, rheumatologists, and thoracic surgeons, is required for the efficient management of this disease [9].

References

1. Damiani JM, Levine HL. Relapsing polychondritis. Laryngoscope 1979; 89: 929-46.
2. Michet CJ, McKenna CH, Luthra HS, *et al.* Relapsing polychondritis: survival and predictive role of early disease manifestations. Ann Intern Med 1986; 104: 74-8.
3. Eng J, Sabanathan S. Airway complications in relapsing polychondritis. Ann Thorac Surg 1991; 51: 686-92.
4. Dunne JA, Sabanathan S. Use of metallic stents in relapsing polychondritis. Chest 1994; 105: 864-7.
5. McAdam LP, O'Hanlan MA, Bluestone R, *et al.* Relapsing polychondritis. Medicine 1976; 55: 193-215.
6. Carlos OR, Maria TGI, Francisco JBR, *et al.* When is a biopsy justify in a case of relapsing polychondritis? The Journal of Laryngology and Otology 1999; 113: 663-5.
7. Shaf K, Scott B, John TG. Treatment of diffuse tracheomalacia secondary to relapsing polychondritis with continous positive airway pressure. Chest 1997; 112: 1701-3.
8. Bipin DS, Asok D, Atul CM. Management of airway manifestations of relapsing polychondritis. Chest 1999; 116: 1669-75.
9. John LF, Stephen DK, Norman WR. Endobronchial stenting for severe airway obstruction in relapsing polychondritis. Chest 1999; 116: 825-7.
10. Ferguson GT, Benoist J. Nasal continuous positive airway pressure in the treatment of tracheobronchomalacia. Am Rev Respir Dis 1993; 147: 457-61.

復發性多軟骨合併急性呼吸衰竭—病例報告

林志明　蔡熒煌　黃崇旂　高國晉　林進國　曹昌堯

復發性多軟骨炎是一種少見的疾病，它常會反覆地軟骨發炎並致使軟骨破壞。大約有百分之五十的病人會有呼吸道表徵，一旦影響到大型呼吸道常會有危及生命的併發症。我們報導一位女性病患因復發性多軟骨炎導致氣管支氣管軟化，而使用類固醇、氣管切開術和持續呼吸道正壓治療。*(胸腔醫學 2002; 17: 35-39)*

關鍵詞：復發性多軟骨炎，氣管支氣管軟化，氣管造口術，持續呼吸道正壓

林口長庚紀念醫院　胸腔一科
索取抽印本請聯絡：黃崇旂醫師，桃園縣龜山鄉復興街 5 號

Bronchobiliary Fistula and Bile Pneumonitis after Transcatheter Arterial Chemoembolization and Hepatic Surgery for Hepatocellular Carcinoma—Report of A Case

Jann-Yuan Wang, Li-Na Lee*, Yih-Leong Chang**

Biloma and bronchobiliary fistula (BBF) are rare complications of transcatheter arterial chemoembolization (TACE) or hepatic surgery. A 77-year-old man, who had undergone TACE and hepatic surgery for hepatocellular carcinoma twice, was admitted due to biliptysis and dyspnea. A BBF was suspected and then resected. The patient died of respiratory failure two months later, because of recurrent biliptysis and bile pneumonitis. We herein show the radiologic findings of bile pneumonitis at the initial and late stages, and review the causes and clinical manifestations of BBF and bile pneumonitis. ***(Thorac Med 2002; 17: 40-44)***

Key words: bronchobiliary fistula, biloma, bile pneumonitis, transcatheter arterial chemoembolization, hepatic surgery

Introduction

Hepatic surgery and transcatheter arterial chemoembolization (TACE) are established treatments for hepatocellular carcinoma and some metastatic hepatic tumors. The complications of these treatments, such as hepatic biloma, abscess, and bronchobiliary fistula, are sometimes life-threatening [1-3]. Herein, we describe a case of hepatic biloma and bronchobiliary fistula (BBF) complicated with bile pneumonitis and respiratory failure, after TACE and hepatic surgery.

Case Report

A 77-year-old man, a chronic B-hepatitis patient with liver cirrhosis, was diagnosed with hepatocellular carcinoma in 1996. Due to the presence of multiple intrahepatic tumors, he received TACE in Jun. 1996, followed by an intra-tumor alcohol injection. Because of recurrence, he underwent a multiple segmental resection of the right hepatic lobe in Nov. 1997, and another course of TACE in Dec. 1999, followed by another segmental hepatic resection. In Aug. 2000, a cough, with much dark-yellow sputum, as well as dyspnea, developed. The

Department of Internal Medicine, *Laboratory Medicine, **Pathology, National Taiwan University Hospital Taipei, Taiwan
Address reprint requests to: Dr. Li-Na Lee, Department of Laboratory Medicine, National Taiwan University Hospital No., 7, Chung-Shan South Road, Taipei, Taiwan

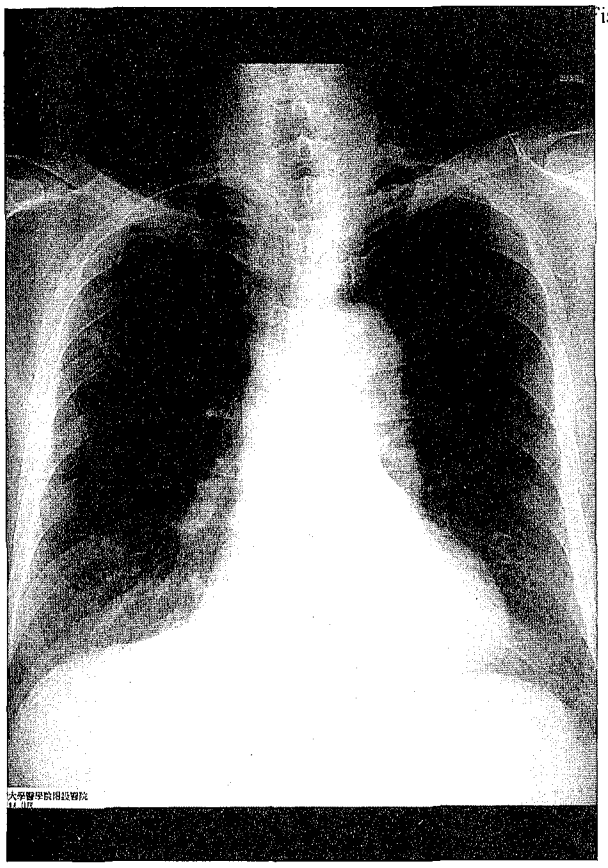

Fig. 1. Standing chest radiography at the beginning of this admission showed a well defined pulmonary nodule about 1 cm in diameter at the upper right lobe, as well as reticular-linear infiltrates at the right basal lung, suggesting chronic interstitial disease.

symptoms usually became worse when lying supine. The presence of a large amount of bilirubin in the sputum was confirmed, using dipsticks. Laboratory tests revealed increased alkaline phosphatase (367 U/L) and γ-glutamyltranspeptidase (337 U/L) without hyperbilirubinemia and leucocytosis. The chest radiography (Figure 1) and computed tomography (CT) revealed prominent reticular infiltrates in the right posterior basal lung field, suggesting chronic interstitial lung disease. Magnetic resonance imaging (MRI) showed a fluid accumulation (a biloma) in the lateral segment of the left hepatic lobe, with mild dilatation of the intrahepatic bile ducts. The leakage of bile into the lower lobe of the right lung suggested the presence of a fistula from the bile ducts (Figure 2). Thus, a clinical diagnosis of BBF and bile pneumonitis was made. During the operation in Sep. 2000, a 0.5 cm fistula was found passing from the surface of the liver into the lower lobe of the right lung, which was severely inflamed, consolidated, and stained with bile. A fistulectomy and wedge resection of the lower lobe of the right lung were performed (Figure 3). The biliptysis subsided temporarily, but recurred one month later with fever, jaundice, and dyspnea. Parenteral antibiotics and percutaneous drainage of the biloma failed to improve his symptoms. A chest radiography and high-resolution CT (Figure 4) performed on Nov. 6, 2000, revealed multiple patches of alveolar infiltrates and a honeycombing appearance over the bilateral lower lung fields, suggesting bile pneumonitis and fibrosis. He died of septic shock and respiratory failure on Nov. 24, 2000.

Discussion

The most common cause of BBF is bile duct obstruction, usually secondary to postoperative bile duct stenosis, with the onset ranging from 3 weeks to 18 months [2-4]. Thoracoabdominal trauma, liver abscesses, and congenital defects can also result in the development of BBF [5-8]. However, TACE complicated with biloma and BBF has never been described.

In 2,300 TACE procedures, Sakamoto [1] reported that the complication rate was 4.4% (102 cases), including intrahepatic biloma in 20 patients. The cause of biloma is generally considered to be ischemic injury to the intrahepatic bile duct following embolization of

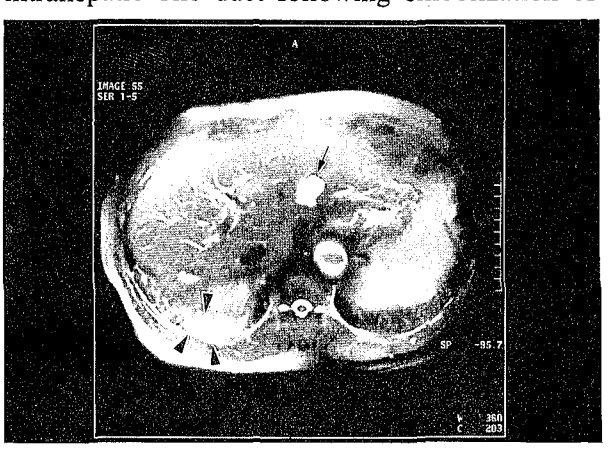

Fig. 2. Magnetic resonance imaging revealed a large cyst (arrow) i the lateral segment of the left hepatic lobe, and the presence of bil in the lower lobe of the right lung (arrowhead).

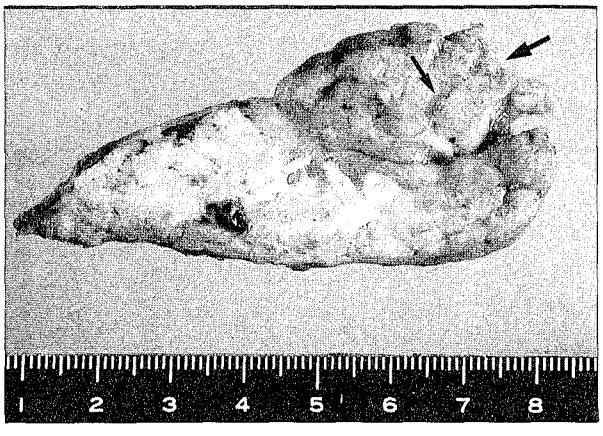

Fig. 3. Grossly, the wedge-resected lower right lung was consolidated with bile staining. A small bronchial fistula tract (arrows) was present.

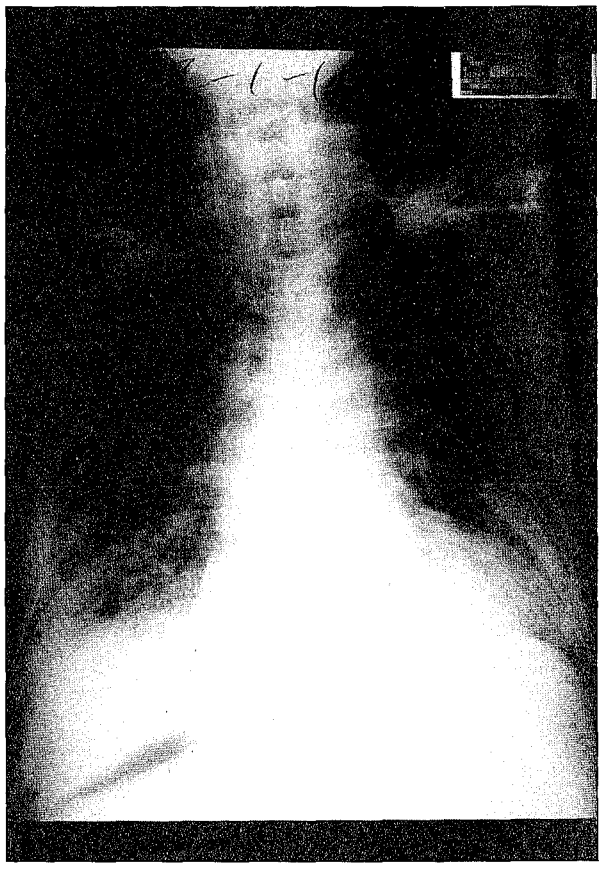

Fig. 4. Chest radiograph performed 18 days before death showed multiple patchy haziness in the bilateral lung fields, and a honeycombing change in the bilateral lower lobes.

the peribiliary plexa, which derive blood from the hepatic artery and nourish the bile duct. The necrosis of the proximal bile duct results in bile flow obstruction and distal bile accumulation [9]. It is likely that when the accumulation of bile is located near the surface of the liver or becomes distended in the subphrenic space, the soft diaphragm and lung yield, with the result that bile perforates into the negative-pressured pleural cavity or bronchial tree [5, 10], and causes bile pleuritis [11] or bile pneumonitis. In our case, it is difficult to decide whether hepatic surgery or TACE caused the BBF. However, we believe that TACE is at least a contributing factor, because several image studies demonstrated a biloma over the lateral segment of the left hepatic lobe, an area the previous hepatic surgeries had never approached.

The most common manifestation of BBF is biliptysis (expectorating bile), associated with a severe irritating cough. The diagnosis should be suspected by the presence of bile pigments in the sputum, a pathognomonic finding of BBF. The chest radiograph or CT often fails to show the fistula itself, but may show changes in bile pneumonitis, including alveolar or interstitial infiltrates, bronchiectasis, or pulmonary fibrosis, especially in the lower right lobe [12-13]. The presence of a fistula can be confirmed by invasive procedures such as percutaneous transhepatic cholangiography, endoscopic retrograde cholangiopancreatography, or a nuclear scan of the biliary tree [6, 10]. In our patient, an MRI, a non-invasive study, demonstrated a biloma with a dilated intrahepatic bile duct, as well as a suspicious BBF in the lower right lobe of the lung (piercing through the right hemi-diaphragm). Thus, an MRI may be included in the diagnostic studies of BBF.

The course of BBF can be chronic and intermittent [6], or as in our patient, progress from acute bronchiolitis and interstitial pneumonitis to respiratory failure in only three months, due to recurrent biliptysis and bile aspiration. The chest radiographs and CT of our patient showed the initial manifestation of local interstitial disease, which progressed to multiple patches of bile pneumonitis and honeycombing

change in the terminal stage. To our knowledge, this is the first case showing the serial radiologic manifestations of bile pneumonitis.

Using a porcine model, Porembka *et al* [14] compared the effects of intratracheally-administered saline, gastric contents, and bile, and discovered that bile aspiration consistently had a more severe impact on pulmonary function and pathologic alterations, leading to alveolar hemorrhage and bronchial denudation, with a higher alveolar-arterial pressure gradient of oxygen and a compliance lower than gastric acid aspiration. Though not well understood, the pathogenesis of bile-induced pulmonary injury is likely to be a bile-induced calcium accumulation in type II pneumocytes, and a subsequently calcium-dependent cytotoxicity [15].

In conclusion, we have described a case of bile pneumonitis with respiratory failure due to biloma and BBF after TACE treatment for hepatocellular carcinoma. Biloma and BBF are rare, but their presence should be considered in patients with biliptysis and histories of hepatic surgery or TACE treatment.

References

1. Sakamoto I, Aso N, Nagaoki K, *et al.* Complications associated with transcatheter arterial embolization for hepatic tumors. Radiographics 1998; 18: 605-19.
2. Rose DM, Rose AT, Chapman WC, *et al.* Management of bronchobiliary fistula as a late complication of hepatic resection. Am Surg 1998; 64: 873-6.
3. Oettl C, Schima W, Metz-Schimerl S, *et al.* Bronchobiliary fistula after hemihepatectomy: cholangiopancreaticography, computed tomography and magnetic resonance cholangiography findings. Eur J Radiol 1999; 32: 211-5.
4. Koch KA, Crump JM, Monteiro CB. A case of biliptysis. J Clin Gastroenterol 1995; 20: 49-53.
5. Boyd DP. Bronchobiliary and bronchopleural fistulas. Ann Thorac Surg 1977; 24: 481-7.
6. Moreira VF, Arocena C, Cruz F, *et al.* Bronchobiliary fistula secondary to biliary lithiasis - treatment by endoscopic sphincterotomy. Digest Dis & Sci 1994; 39: 1994-9.
7. Tekant GA, Joseph VT, Cheah SL. Congenital tracheobiliary fistula. J Pediatr Surg 1994; 29: 594-5.
8. Egrari S, Krishnamoorthy M, Yee CA, *et al.* Congenital bronchobiliary fistula: diagnosis and postoperative surveillance with HIDA scan. J Pediatr Surg 1996; 31: 785-6.
9. Kan Z, Ivancev K, Lunderquist A. Peribiliary plexa – important pathways for shunting of iodized oil and silicon rubber solution from the hepatic artery to the portal vein. Invest Radiol 1994; 29: 671-6.
10. Khandelwal M, Inverso N, Conter R, *et al.* Endoscopic management of a bronchobiliary fistula. J Clin Gastroenterol 1996; 23: 125-7.
11. Ichikawa T, Yamada T, Takagi H, *et al.* Transcatheter arterial embolization-induced bilious pleuritis in a patient with hepatocellular carcinoma. J Gastroenterol 1997; 32: 405-9.
12. Yilmaz U, Sahin B, Hilmioglu F, *et al.* Endoscopic treatment of bronchobiliary fistula: report on 11 cases. Hepatogastroenterology 1996; 43: 293-200.
13. Warren KW, Christophi C, Armendariz R, *et al.* Surgical treatment of bronchobiliary fistulas. Surg Gynecol Obstet 1983; 157: 351-6.
14. Porembka DT, Sehlhorst S, Orlowski JP, *et al.* The pathophysiologic changes following bile aspiration in a porcine lung model. Chest 1993; 104: 919-24.
15. Oelberg DG, Downey SA, Flynn MM. Bile salt-induced intracellular calcium accumulation in type II pneumocytes. Lung 1990; 168: 297-308.

肝癌患者經肝切除手術及動脈導管化學栓塞後併發膽道支氣管瘻管及膽汁性肺炎—病例報告

王振源　李麗娜*　張逸良**

局部膽汁鬱積和膽道支氣管瘻管是肝切除手術及動脈導管化學栓塞後罕見之併發症。一位因肝癌而曾經接受過兩次局部肝切除手術和動脈導管化學栓塞的七十七歲男性病人，因為氣促以及咳嗽中帶有膽汁而住院接受治療。檢查結果高度懷疑有膽道支氣管瘻管，隨即安排手術切除。但兩個月後，病人仍因為上述症狀復發及膽汁性肺炎導致呼吸衰竭而死亡。文章中將討論膽汁性肺炎初期和末期之影像學檢查之變化，並且探討膽道支氣管瘻管及膽汁性肺炎發生之原因以及臨床表現。 ***(胸腔醫學 2002; 17: 40-44)***

關鍵詞：膽道支氣管瘻管，局部膽汁鬱積，膽汁性肺炎，動脈導管化學栓塞，肝切除手術

國立台灣大學醫學院附設醫院　內科　實驗診斷科*　病理科**
索取抽印本請聯絡：李麗娜醫師，台北市中山南路七號

Late Management of Spontaneous Esophageal Perforation Associated with Mediastinal Abscess —A Survival Case Report

Shi-Chi Lin, Chih-Yu Hsu

The early diagnosis and prompt aggressive management of Boerhaave's syndrome (spontaneous esophageal perforation) is a continuing challenge. The longer the diagnosis and treatment are delayed, the greater the mortality. We herein report the case of a 51-year-old man who was successfully treated with surgical intervention for a delayed esophageal perforation with mediastinal abscess.. ***(Thorac Med 2002; 17: 45-49)***

Key words: Boerhaave's syndrome, esophageal perforation, mediastinal abscess

Introduction

The diagnosis of intrathoracic esophageal perforation is frequently delayed. A long interval between the perforation and intervention carries a high morbidity and mortality. Recent studies have reported that the delayed management of esophageal perforation is associated with mortality rates as high as 10% to 50%[1-3]. We report a case complicated by bilateral empyema and mediastinal abscess, referred to us 3 weeks after combined treatment with parenteral antibiotics and chest tube insertion, which was managed successfully using a thoracotomy.

Case Report

A 51-year-old previously healthy male was admitted to a local hospital with an acute onset of fever and dyspnea. The patient had also had an episode of vomiting after eating hot noodles the day before admission to the local hospital. During the preceding 3 weeks, the patient had been given parenteral antibiotics (Imipenem and Ceftazidime) and multiple insertions of small bore chest tubes (pig-tail), with a primary diagnosis of left side empyema of unclear etiology. Unfortunately, his condition deteriorated and he was transferred to our hospital.

On admission, he looked ill. His temperature was 35.9°C, pulse rate was 114/min, blood pressure was 94/76 mm Hg, and respiratory rate was 22/min. Decreased breathing sounds with crackles were noted in the base of the left lung. The heart sounds were normal, without a murmur or Hamman's crunch. Otherwise, the physical examination was normal.

The laboratory examination showed a hemoglobin level of 10.7g/dl, and a white blood cell count of 17060/mm^3 with 86% neutrophils. The arterial blood gas analysis in room air revealed pH = 7.494, $PaCO_2$ = 33.1 mm Hg, HCO_3 = 25.4 mEq/dl, and PaO_2 = 90.4mm Hg.

Division of Chest Medicine, Department of Internal Medicine, Cathay General Hospital, Taipei, Taiwan
Address reprint requests to: Dr. Shi-Chi Lin, Number 280, Section 4, Len-Ai Road, Taipei, Taiwan

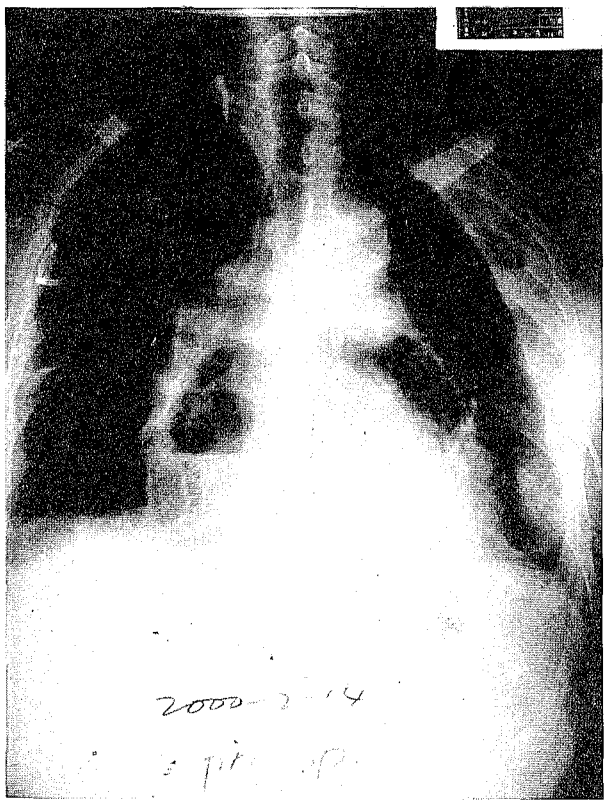

Fig. 1. Chest roentgenogram in AP view shows a homogenous infiltration with a large air-fluid level in the mediastinum, multiple insertions of small bore chest tubes, and a central venous catheter

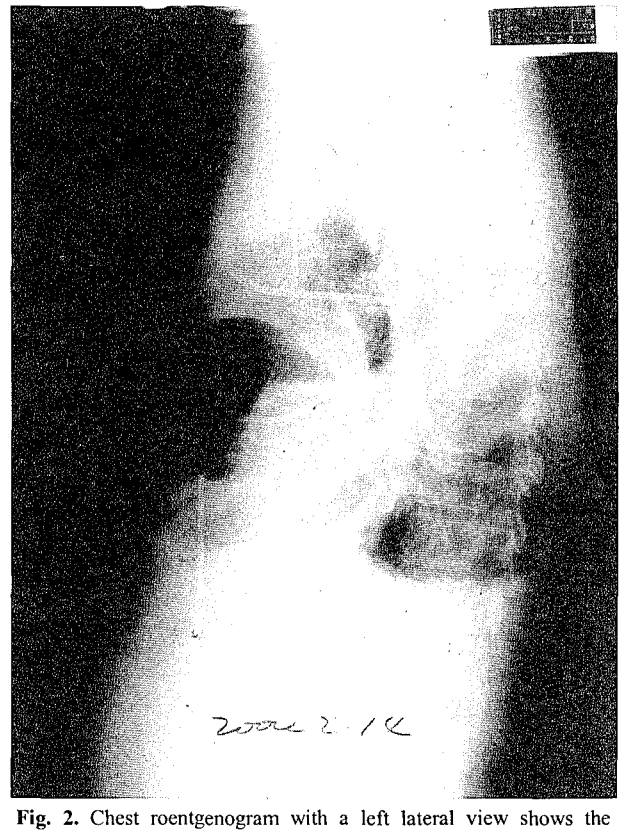

Fig. 2. Chest roentgenogram with a left lateral view shows the homogenous infiltration with the air-fluid level in the anterior mediastinum

Serum biochemistry showed albumin 3.0 g/dl and total protein 5.1 g/dl. The liver and kidney function tests, and serum electrolytes were all within the normal range. The chest radiography on admission showed a homogeneous infiltration with a large air-fluid level in the mediastinum (Figure 1 and Figure 2).

There was no pleural fluid draining from the chest tubes. Intravenous antibiotics (penicillin and gentamicin) were started, and a minithoracotomy with drainage and biopsy was performed 2 day later; food particles and pus were evacuated. There was a transmural erosion of the esophageal wall at about 5 cm below the carina, and there was no evidence of tumor macroscopically or microscopically. The pus of the mediastinal abscess yielded Pseudomonas aeruginosa, and then a yeast-like organism.

An esophagography with a water-soluble contrast agent demonstrated leakage from the distal esophagus (Figure 3). Four days later, he underwent laparotomy with a feeding jejunostomy. The patient improved gradually, and reached complete recovery after 2 months in the hospital.

Based on the above findings, we diagnosed bilateral empyema and a mediastinal abscess caused by an esophageal perforation occurring spontaneously in association with emesis.

Discussion

Boerhaave's syndrome (spontaneous esophageal perforation) is an uncommon clinical entity that frequently presents with an antecedent history of marked vomiting followed by chest or abdominal pain. Mediastinitis due to spontaneous esophageal perforation is associated with a high mortality. The uniformly high mortality of the untreated disease occurs because of a leak in the serosal covering of the esophagus allowing

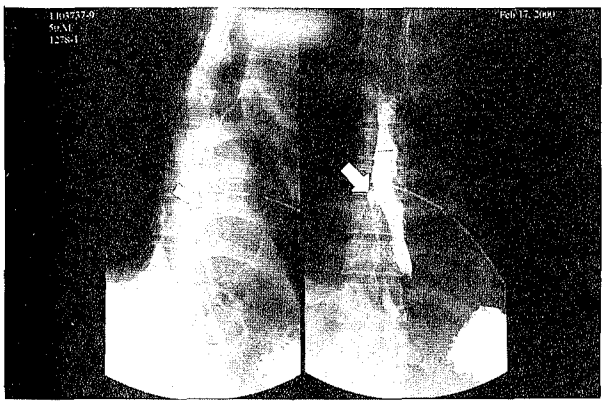

Fig. 3. Esophagography shows leakage of contrast medium from the right lateral aspect of the lower esophagus

gastrointestinal contents to spill directly into the mediastinum. Some studies confirm that an abrupt rise in esophageal intra-luminal pressure will usually cause a longitudinal tear in the distal esophagus. The preponderance of esophageal perforations occur on the left posterolateral wall of the distal esophagus. The causes of esophageal perforation are shown in the box.

Causes of esophageal perforations
• iatrogenic etiology, postoperatively or due to instrumentation
• swallowed foreign bodies or corrosive ingestion
• external trauma
• spontaneous perforation
• progressive disease: peptic ulcer, tumors

It appears that 50-75% of the perforations occur in a normal esophagus without preexisting esophageal disease [5], as in our patient.

In the beginning, vomiting followed by severe chest pain is the typical presentation. Esophageal motility disturbance and reflux esophagitis are present in most patients with a spontaneous esophageal rupture. Patients can also present with dysphagia, tachycardia, and fever, all of which were present in this patient. Subcutaneous air in the neck is uncommon in cases of a lower esophageal perforation. Untreated esophageal perforation can result in a chemical injury and superinfection to the adjacent area. This leads to the development of severe empyema and mediastinal abscess. Presenting symptoms and signs include pleuritic chest pain, dyspnea, cough, and fever. The mediastinal air that surrounds the heart may give rise to a systolic crunching sound known as Hamman's crunch. In addition, swallowed salivary enzyme may cause elevated pleural fluid amylase levels, which are highly suggestive of an esophageal rupture.

Pneumomediastinum is the abnormality seen most often on plain film. The second most common finding is a density in the left cardiophrenic angle which results in the loss of contour of the descending aorta. Further leakage of gas and fluid, combined with inflammation and edema, cause mediastinal widening. If the perforation extends to the adjacent pleura, an effusion with or without hydropneumothorax will develop. This occurs on the left side in nearly 75% of the cases [6-7]. Some cases of mediastinal abscess due to an esophageal perforation have also been reported. Contrast esophagograms are useful in the diagnosis of esophageal perforation. It is recommended that water-soluble iodinated compounds be used initially. Alternatively, barium studies might be more sensitive. A computerized tomographic evaluation has also been used as an adjunct to clarify ambiguous clinical presentations in patients with a negative chest radiograph.

The major prognostic factor of esophageal perforation is the interval between perforation and treatment. Various series have identified the first 24 hours as the interval acceptable for successful primary repair. The mortality rate is higher for patients treated after 24 hours (14%) compared to patients treated within 24 hours (5%) [3].

Mediastinal abscess due to esophageal perforation is associated with high mortality. Therefore, both a correct diagnosis and swift surgical treatment are usually essental. However, some clinical cases of esophageal perforation with a favorable clinical course under conservative

therapy have been reported [8]. The reasons for the improvement and favorable outcome in our case were the effectiveness of antibiotic treatment, intercostal drainage, and intravenous fluid.

References

1. Jone WG, Ginsberg RJ. Esophageal perforation: a continuing challenge. Ann Thorac Surg 1992; 53: 534-43.
2. Wite RK, Morris DM. Diagnosis and management of esophageal perforations. Am J Surg 1992;58: 112-9.
3. Laurie B. Reeder, MD, Vincent J. Defilippi, MD. Current results of therapy for esophageal perforation. Am J Surg 1995;169: 615-7.
4. S Mahmoud, R Prudham, G Sidra. Oesophageal perforation. Postgraduate Med J 1998; 74: 418-9.
5. A. Solomonov, L.A. Best. Pleural empyema: an unusual presentation of esophageal perforation. Respiration 1999; 66: 366-8.
6. Frederick Levy, MD, Wiliam K. Spontaneous esophageal perforation presenting with right-sided pleural effusion. J Emerg Med 1995; 13: 321-5.
7. Gray G. Ghahremani. Radiologic evaluation of suspected gastrointestinal perforations. Radiologic Clinics of North America 1993; 89; 367-70.
8. Tadahiro Nozoe, Masayuki Kitamura. Successful conservative treatment for esophageal perforation by a fish bone associated with mediastinitis. Hepato-Gastroenterology 1998; 45: 2190-2.

自發性食道破裂併縱膈腔膿瘍

林思齊　徐志育

自發性食道破裂是一種較少見的疾病，不易早期診斷，常發生在嘔吐後併有胸痛或腹痛，臨床症狀包括發燒，氣胸，縱膈腔氣腫，皮下氣腫，膿胸，或縱膈腔膿瘍。自發性食道破裂若是無法在 24 小時內診斷併外科治療，死亡率會驟增。大部分的病患可由病史加上 X 光攝影檢查而作出診斷，若不及時治療將導致局部化學性傷害併感染最後導致敗血症，診斷與治療時間久，年紀大，或是自發性的食道破裂預後較差。這裏將提出一個 51 歲的中年男性因發燒及呼吸困難而住進當地的醫院使用抗生素治療，住院後出現膿胸並置放胸管作引流，轉到本院後胸部 X 光發現有一個巨大的中膈腔膿瘍，仔細詢問病史發現病患在住院的前一天吃麵後曾發生劇烈嘔吐，在經過 26 天後才診斷是自發性食道破裂併縱膈腔膿瘍，病患接受開胸手術併十二指腸灌食，經過二個月後病癒出院。 ***(胸腔醫學 2002; 17: 45-49)***

關鍵詞：Boerhavve's syndrome，自發性食道破裂，縱隔腔膿瘍

國泰醫院　胸腔內科
索取抽印本請聯絡：林思齊醫師，台北市仁愛路四段 280 號

Bilateral Hydropneumothorax Secondary to Multiple Rapidly-Growing Cystic Metastases in Angiosarcoma of the Scalp

Chau-Ming Tsai, Tung-Ying Chao, Yung-Fa Lai

Angiosarcoma of the scalp is a rare tumor of vascular origin, with a poor prognosis. We report a 72-year-old male patient with bilateral hydropneumothorax secondary to multiple rapidly-growing cystic metastases in angiosarcoma of the scalp. The chest X-ray and computerized tomography (CT) showed multiple rapid onset and growing cystic metastasis during a one-month period, with some central breakdown of nodule lesions. These findings suggest tumor central necrosis rapidly forming large thin-walled cysts that induce a bronchopleural fistula and are complicated with hydropneumothorax. ***(Thorac Med 2002; 17: 50-55)***

Key words: angiosarcoma of the scalp, cystic metastases, bilateral hydropneumothorax

Introduction

Angiosarcoma of the scalp is a rare tumor of vascular origin that affects the elderly, and its prognosis is reported to be very poor[1-8]. The risk factors are radiation therapy, arsenic oxide, and vinyl chloride exposure[1,9-10]. Cystic pulmonary lesions caused by the metastasis of soft tissue sarcoma are rare[2-3,6,11-12]. We report a very rare case with multiple rapidly-growing cystic metastases in angiosarcoma of the scalp, complicated by bilateral hydropneumothorax.

Case Report

In September 1998, a 72-year-old male presented with bruise-like macules on the post parietal area, which had been present for a few months. On clinical examination, he was generally fit and apyrexial. The chest X-ray showed no abnormalities. (Figure 1) A wide surgical excision was performed, and the pathology showed angiosarcoma with deep margin involvement. Postoperatively, he underwent radiation therapy. In March 1999, an erythematous tumor reappeared near the operative scar and was excised again. At the same time, the chest X-ray and computerized tomography (CT) showed right lung basal and upper left lobe nodule lesions with an air-fluid level. (Figures 2, 3A, 3B) The patient had no symptoms at that time. One month later, the patient was hospitalized in our department because of severe dyspnea and right neck lymphoadenopathy. His body temperature was 36.7℃, blood pressure 130/70 mm Hg, heart rate 96 beats per min, and

Department of Thoracic Medicine, Kaohsiung Chang Gung Memorial Hospital
Address reprint requests to: Dr. Chau-Ming Tsai, 123 Ta-Pei Road, Niao Sung Hsiang, Kaohsiung Hsien, Taiwan

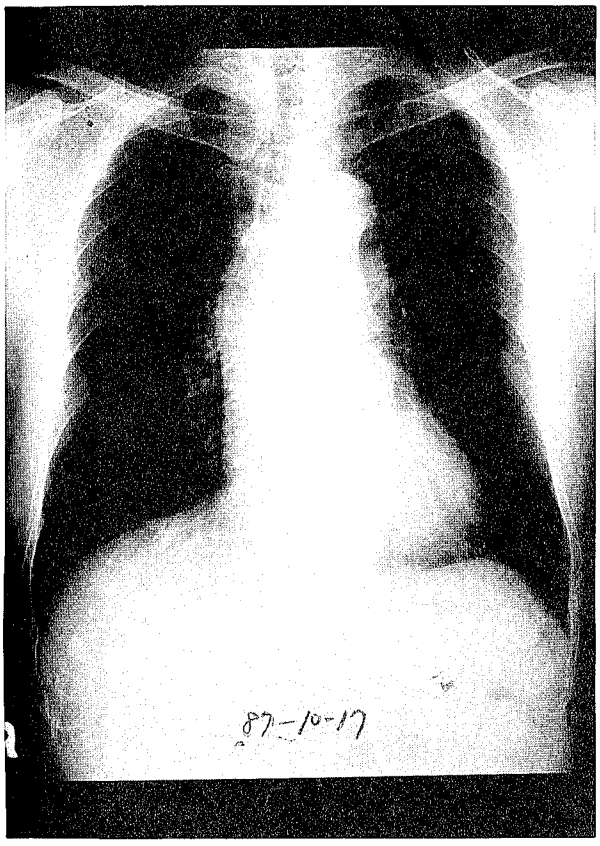

Fig. 1. Chest X-ray shows no abnormalities at the time of angiosarcoma of the scalp onset

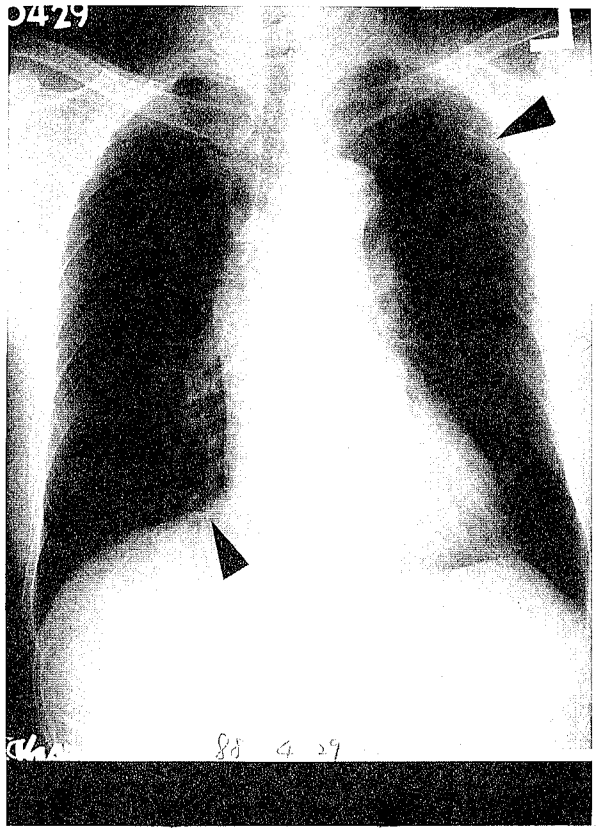

Fig. 2. Chest X-ray shows two small nodules when the tumor local recurred (arrow)

respiration rate was 25 per min. His heart sound was regular and clear, but the breathing sounds had decreased bilaterally. The follow-up image study showed multiple cystic lung lesions with bilateral hydropneumothorax. (Figures 4 and 5) A biopsy from the right neck mass was performed, and its pathology showed metastasized angiosarcoma. In the pleural effusion study, only a single malignant cell was found. The effusion CEA (carcinoembryonic antigen) was in the normal range. Tuberculosis and bacterial cultures showed no growth. The full blood and differential count were within normal ranges. Thoracic drainage and continuous aspiration were performed after admission, and a pleural adhesion with OK-432 (group A Streptococcus pyrogenes of human origin) was carried out, but a sporadic air leak was noted. He died of respiratory failure and secondary ventilatory-associated pneumonia on August 26, 1999.

Discussion

Angiosarcoma is an extremely rare tumor of vascular origin. Only 48 patients had been reported from 1926 to 1980 [4,8]. It almost exclusively affects the elderly [1-2,4-5]. The tumor behaves aggressively with a local persistence, and spreads into soft tissues with distant metastases in a high proportion of patients. The prognosis is very poor. In the series by Haustein et al, one half of the patients died within 15 months of diagnosis. Only 12% of the patients survived more than 5 years [1].

In our report, the patient's diffuse cystic pulmonary metastasis was multiple nodule lesions with rapid central breakdown forming thin-walled lesions. The most common causes of bilateral multiple pulmonary cystic lesions include eosinophilic granuloma (Histiocytosis X), lym-

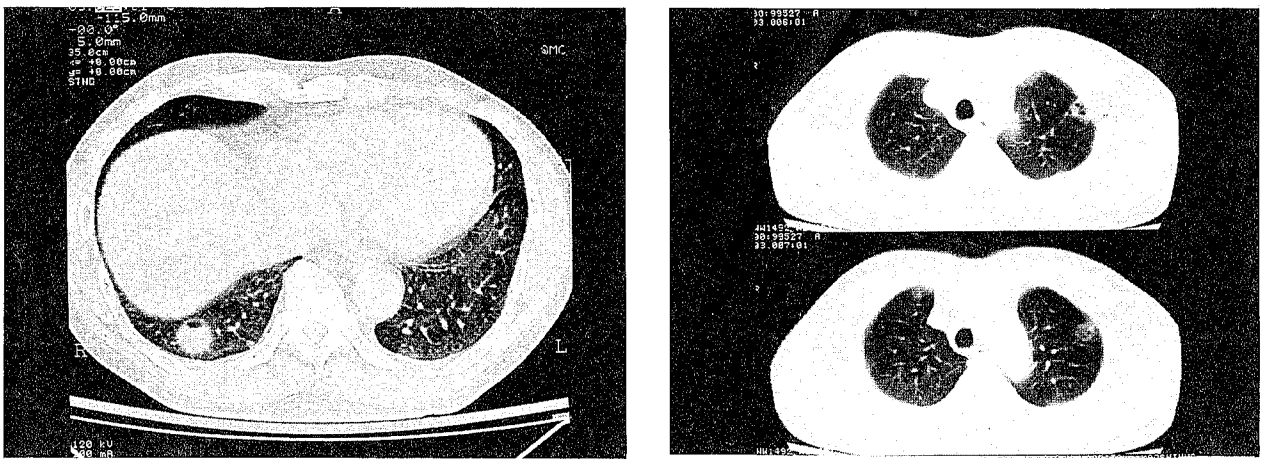

(A) (B)

Fig. 3A and 3B. An air-fluid level was found at the lower right lobe nodule (A). The nodule lesion on the upper left lobe existed at the same time as the tumor recurrence (B)

phangiomyomatosis, tuberous sclerosis, and infections [13-14]. Eosinophilic granuloma and lymphangiomyomatosis were not likely because of the gender, age, and chest CT findings of our patient. Tuberous sclerosis was not favored because there was no family history or neurologic symptom. There was also no infection sign or symptom during the cystic lesions formation. The full blood and differential count were within normal ranges. The pleural effusion study showed no evidence of infection, either. So, the infection was not likely. Berry and co-workers have reported that the cytology of pleural effusion from angiosarcoma of the scalp could only present a single malignant cell [15]. This could not confirm the lung metastasis of angiosarcoma, but could hint at the diagnosis. Our patient presented a similar finding. On the other hand, the pathology of the right neck mass biopsy

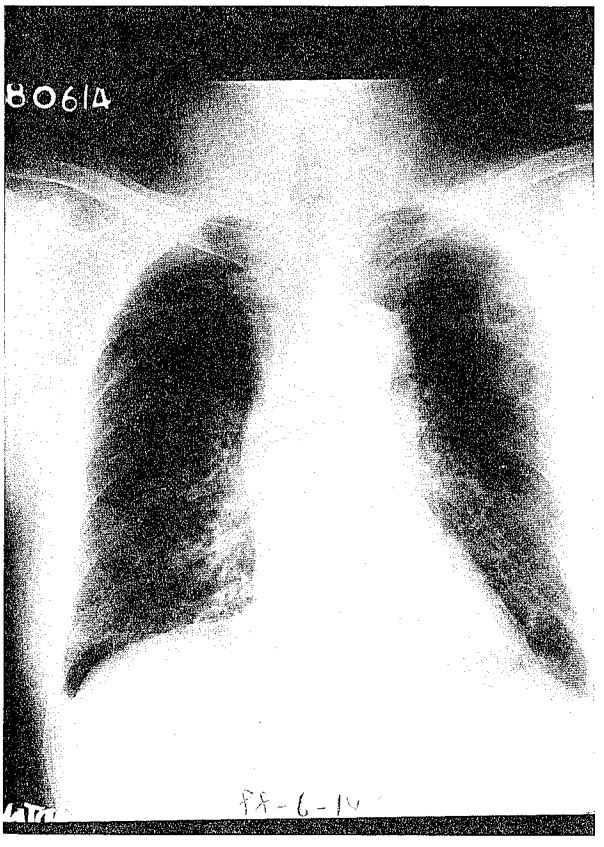

Fig. 4

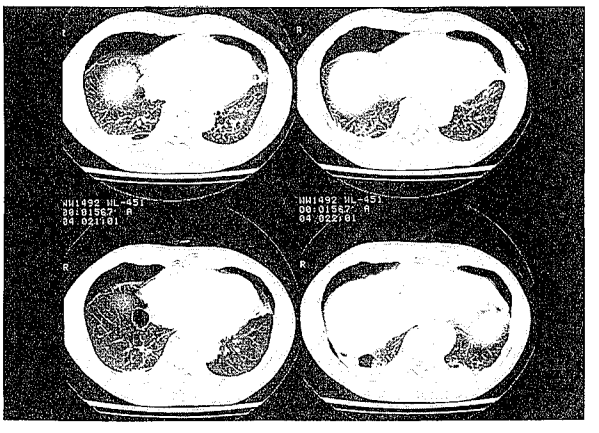

Fig. 5

Fig. 4 and 5. The chest X-ray and CT show multiple cystic lung lesions with bilateral hydropneumothorax, one month later

showed metastatic angiosarcoma. So we concluded that the multiple rapidly-growing cystic lesions in our patient were due to metastases of the angiosarcoma of the scalp.

Angiosarcoma of the scalp is a special tumor with pulmonary cavitation metastasis. Two different series have been reported. In Asia, cavitation with pneumothorax in angiosarcoma of the scalp was found in 11% of the patients, as described by Kitagawa et al (1987). In America and Europe, this relatively high incidence was not found in the series of patients studied by Holden et al, nor in the other large series by Enzinger and Weiss (1983). This difference may be due to a racial factor [2,7,16-17]. Our report supports this hypothesis.

Three possible mechanisms for the development of malignant cysts have been described [6]: (1) the excavation of a nodular tumor through the discharge of the necrotic material inside; (2) the infiltration of malignant cells into the walls of a preexisting benign pulmonary bulla; and (3) the infiltration of malignant cells into the walls of air sacs formed by the cystic distension of small airways or the tumor structure through the ball-valve effect of the tumor. The second mechanism was ruled out, because no cystic lesion had been found on the chest CT before. The third mechanism was ruled out because some nodule lesions were found. The first mechanism was suspected, because some nodule lesions were found with a central breakdown. However, the phenomenon of a large majority of metastatic cavities with rapid progression and thin walls can hardly be explained as only ischemic central necrosis. Zorini suggested that the digestion of the neoplastic and surrounding tissues by tumor-produced proteolytic or lipolytic enzymes, might result in cavitation [11,18]. This mechanism can explain the rapid cyst formation and the bronchopleural fistula with the bilateral hydropneumothorax [3].

The OK-432 was carried out for pleural adhesion in our patient, but the air leakage was persistent. The patient died of respiratory failure. The poor OK-432 response may be due to the persistent air leakage. This condition had been reported previously [3]. We suggest that the early management of the respiratory complication be considered before a large amount of air leakage occurs.

References

1. Uwe-F. Haustein. Angiosarcoma of the Face and scalp. Int J Dermatol 1991; 30: 851.
2. P.A. Lawton, S. Knowles, S. J. Karp, *et al.* Bilaterial pneumothorax as a presenting feature of metastatic angiosarcoma of the scalp. Br J Radiol 1990; 63: 132.
3. Masahiro Nomura, Yutaka Nakaya, Ken Saito, *et al.* Hemopneumothorax Secondary to Multiple Cavitary Metastasis in Angiosarcoma of the scalp. Respiration 1994; 61: 109.
4. Liu AC,Kapp DS, EgbertB, Waters L, Rosen JM. Angiosarcoma of the face and scalp. Ann Plast Surg 1990; 24: 68.
5. Judith M. Aronchick, Harold I. Palevsky, and Wallace T. Millwe T. Miller: Cavitary Pulmonary Metastasis in angiosarcoma, Diagnosis by transthoracic Needle aspiration. Am Rev Respir Dis 1989; 139: 252.
6. Hasegawa, Seiki; Inui, Kenji; Kamakari, Kunihiko; *et al.* Pulmonary Cysts as the Sole Metastatic Manifestation of Soft Tissue Sarcoma, Case Report and Consideration of the Pathogenesis. Chest 1999; 116: 263.
7. Holden C, Spittle M, Jones E. Angiosarcoma of the face and scalp, prognosis and treatment. Cancer 1987; 59: 1046.
8. Knight T, Robinson H,Sina B. Angiosarcoma of the scalp. Arch Dermatol 1966; 226: 318.
9. Ward CM, Buchanan R. Haemangiosarcoma following irradiation of a haemaangioma of the face. J Maxillofac Surg 1977; 5: 164.
10. Otis CN, Peschel R, McKhann, *et al.* The rapid onset of cutaneous angiosarcoma after radiotherapy for breast carcinoma. Cancer 1986; 57: 2130.
11. Kenji Baba, Tsutomu Hattori, Isao Koishikawa, *et al.* Cavitary Pulmonary Metastases of Gallbladder cancer. Respiration 1998; 65: 219.
12. Traweek T, Rotter AJ, Swartz W, et al. Cystic pulmonary

metastatic sarcoma. Cancer 1990; 65: 1805.

13. Stern, E. J. Cystic lung disease associated with eosinophilic granuloma and tuberous slerosis, Air trpping at dynamic ultrafast hight resolution CT. Radiology 1992; 182: 325.
14. Shan C. Chu, Hoji Horiba, Jiro Usuki *et al.* Comprehensive Evaluation of 35 patients with lymphangioleiomyomatosis. Chest 1999; 115: 1041.
15. Gerald J. Berry, Carol J. Anderson, William C. Pitts, *et al.* Cytology of Angiosarcoma in Effusions. Acta Cytologica 1991; 35: 538.
16. Kitagawa, M., Tanaka, T., Matsubara, O. *et al,* Angiosarcoma of the scalp:report of two case with fatal pulmonary complications and a review of Japaneses autopsy registry data, Virchows Archuv 1987, 412: 83.
17. Enzinger,F.M. & Weiss, S.W. Soft tissue tumors (Mosby , St.Louis, USA) 1983; p422-62.
18. Zorini AO: Primary carcinomatous cavities of the lung. Possible role of neoplastic cell autophagism. Dis Chest 1967; 52: 329.

頭皮之血管肉瘤快速多發囊性肺轉移導致雙側性水氣胸病例報告

蔡昭民　趙東瀛　賴永發

頭皮之血管肉瘤是一種很少見的血管性肉瘤,其預後非常的差。我們報告一位 72 歲男性病人,因頭皮之血管肉瘤快速多發囊性肺轉移，導致雙側性水氣胸。在胸部之影像檢查上，可以發現許多的囊狀肺轉移。同時合併存在許多中心已腐化之小腫瘤結節。這個發現支持腫瘤快速中心腐化形成許多的囊狀薄壁結構，這些結構導致氣管肋膜相交通，以至於雙側的水氣胸。 ***(胸腔醫學 2002; 17: 50-55)***

關鍵詞：頭皮之血管肉瘤，囊性肺轉移，雙側性水氣胸

高雄長庚紀念醫院　胸腔內科
索取抽印本請聯絡：蔡昭民醫師，高雄縣鳥松鄉大埤路 123 號

Single Lung Cyst Caused by Metastatic Bladder Cancer —A Case Report

Jin-Duo Wang, Chih-Bin Lin, Min-Shin Kuo*, Jen-Jyh Lee

The lungs are one of the most common sites of metastases from transitional cell carcinoma of the urinary bladder, with the typical radiological manifestations of multiple nodules and variable sizes. It is unusual for the metastatic nodules to be cavitary. Lung cysts caused by metastatic tumors are far more rare. We present a 50-year-old male who had undergone a radical cystectomy due to bladder cancer 7 years previous. He had suffered from productive cough and lower right chest pain for 10 days prior to admission. The chest radiography showed a solitary thin wall cyst in the right middle lobe. A lobectomy was done, and the pathology showed lung metastasis from transitional cell carcinoma of the urinary bladder. Although a single lung cyst caused by metastatic cancer is extremely rare, we emphasize that in the long list of differential diagnoses of single lung cyst, the clinician should consider the possibility of a secondary neoplasm with lung metastasis. ***(Thorac Med 2002; 17: 56-60)***

Key words: lung cyst, transitional cell carcinoma, lung metastasis

Introduction

Lung cysts are not uncommon, and most are acquired. The term "cyst" is used to describe any thin-walled gas- or fluid-containing space in the organ. The differential diagnoses of cystic lung lesions [1] are usually divided into congenital (e.g., bronchogenic cysts, cystic adenomatoid malformations, pulmonary sequestration) or acquired cystic diseases (e.g., bullous emphysema, traumatic lung cysts, post-infectious pneumatoceles, pulmonary hadatid cysts). Cysts are rarely caused by metastatic tumors. We herein report a case of a lung cyst caused by metastasis from transitional cell carcinoma (TCC) of the urinary bladder.

Case Report

A 50-year-old male was diagnosed with TCC of the urinary bladder, and had received a radical cystectomy 7 years ago. The pathological staging was Grade Ⅱ , stage B1. The chest radiography was normal at that time (Figure 1). After surgery, he was regularly followed up in the urologic clinic. He had smoked ten cigarettes per

Division of Chest Medicine, Department of Internal Medicine, Buddhist Tzu Chi General Hospital, Hualien, Taiwan
*Department of Pathology, Buddhist Tzu Chi General Hospital, Hualien, Taiwan
Address reprint requests to: Dr. Jen-Jhy Lee, Division of chest medicine, Department of Interal Medicine, Buddhist Tzu Chi General Hospital, No707, Section 3, Chung Yan Rd, Hualien, Taiwan

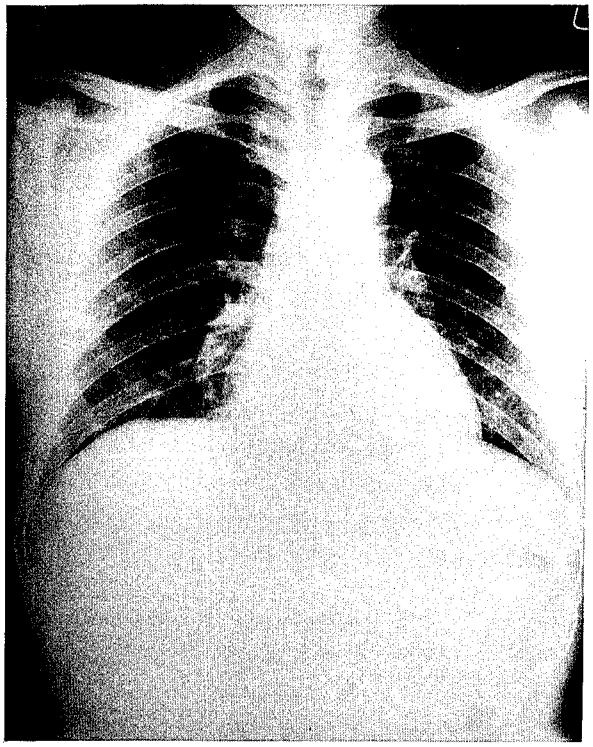

Fig. 1. The chest radiography taken 7 years ago was normal.

day since he was young. Otherwise, no systemic disease was revealed. He presented to the chest clinic with the chief complaints of lower right chest pain and a productive cough lasting for 10 days prior to admission. No body weight loss or fever was noted. The chest posteroanterior and lateral views revealed a 4×3.5×4.5 cm^3 thin-walled cystic lesion in the right middle lobe (Figure 2). Computed tomography (CT) showed a thin-walled cystic lesion with mildly irregular lining in the same region (Figure 3). The sputum cytology was negative, and the bronchoscopic examination was negative for a central lesion. Bronchial brushing cytology showed a few degenerative bronchial epithelial cells, and a transbronchial lung biopsy revealed only minimal fibrosis. So, he was referred to the chest surgeon for a right middle lobe lobectomy. The pathology report showed one cystic lesion, measuring 4.2×3.2×2.4 cm^3 in size. Microscopically, it revealed metastatic transitional cell carcinoma with a papillary pattern (Figure 4). The diagnosis of bladder cancer with lung metastasis was then made.

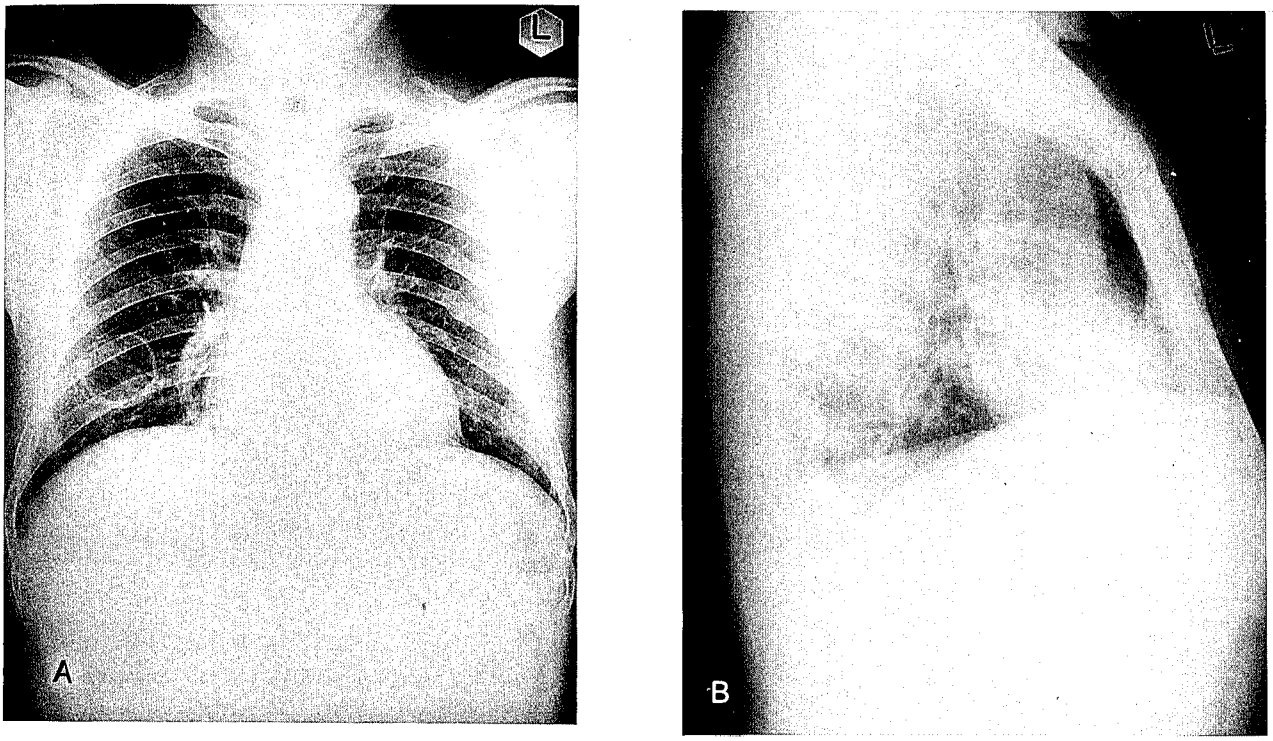

Fig. 2. Chest posteroanterior (A) and lateral (B) films showed a 4×3.5×4.5 cm^3 thin-walled cystic lesion in the right middle lobe.

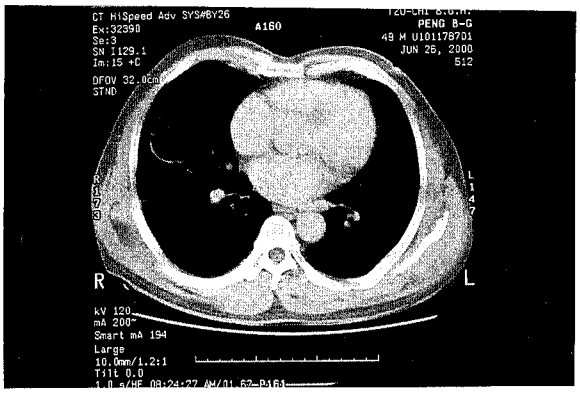

Fig. 3. The CT scan demonstrates a thin-walled cystic lesion with irregular lining in the right middle lobe.

Discussion

The lungs are one of the most common metastatic sites for a variety of malignancies. The pulmonary arteries are the most common route by which a tumor spreads to the lungs. The most common manifestation of metastatic disease to the lungs consists of solitary or multiple nodules within the lung parenchyma [2-3].

The cavitation of a nodular metastasis is not as common as in those with primary lung carcinoma [4,5-6]. For example, in one report, cavitation was identified in 4% of metastatic deposits and in 9% of primary neoplasms [6]. Up to two thirds of cavitary metastases are squamous cell carcinomas originating from the larynx, pharynx, esophagus, or uterine cervix, and the other one third may be adenocarcinomas arising most commonly from the colon or rectum [4,5-6].

Lung metastasis from transitional cell carcinoma is not uncommon [7]. But, a cystic form of lung metastasis is rare. To our knowledge, only one case has been reported in the English literature since 1966 [8]. In that report, by Margolis and Liss, the cysts caused by TCC lung metastasis were multiple; there was no detailed description of the cystic wall. In our case, the CT scan demonstrated an irregular lining in this thin-walled cystic lesion. We thus suggest that the irregular lining might heighten the possibility of malignancy.

Single lung cyst can be of many differential diagnoses (e.g., bronchogenic cysts, post-traumatic lung cysts and post-infectious pneumatoceles). Some studies have demonstrated that bronchial carcinoma might arise from a preexisting bronchogenic cyst [9,10-11]. However, in our case, the chest radiography taken 7 years ago was normal, and there was no history of chest contusion or pulmonary infection. Since he had has TCC 7 years ago, a single lung cyst caused by TCC metastasis should be considered.

In summary, we emphasize that, with a history of malignancy, clinicians should be aware that a single lung cyst might be caused by metastatic lung cancer.

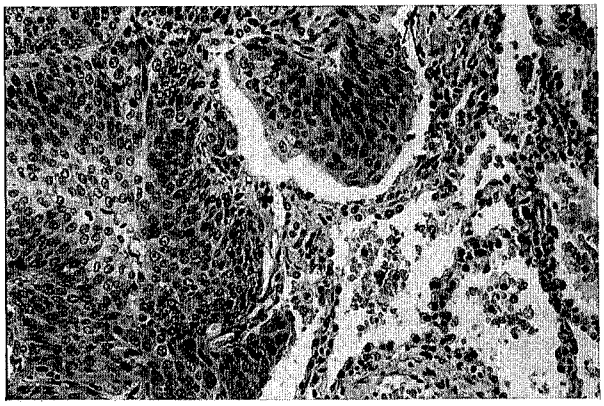

(A)

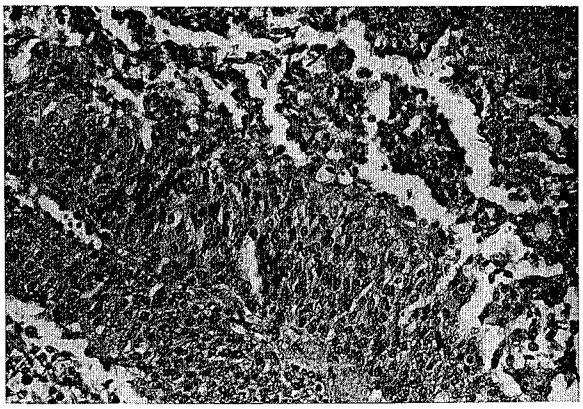

(B)

Fig. 4. Microscopic examination of the resected lung cyst (A) reveals papillary transitional cell carcinoma. The malignant cells were of moderately poor differentiation, and contained large staining nuclei. The histologic pattern was the same as that of the primary bladder cancer (B).

References

1. Shamji FM, Sachs HJ, Perkins DG. Cystic disease of the lungs. Surgical Clinics of North America 1988; 68(3): 581-620.
2. Woodard PK, Dehdashti F, Putman CE. Radiologic diagnosis of extrathoracic metastases to the lung. Oncology (Huntington). 1998; 12(3): 431-8.
3. Fraser RS and Pare PD. Secondary Neoplasms. In: Diagnosis of diseases of the chest, 4th edition, Philadelphia: W.B. Saunders company, 1999: 1381-99.
4. LeMay M, and Piro AJ. Cavitary pulmonary metastases. Ann Intern Med 1965; 62: 59-66.
5. Chanduri MR. Cavitary pulmonary metastases. Thorax 1970; 25: 375-81.
6. Dodd GD, and Boyle JJ. Excavating pulmonary metastases. Am J Roentgenol 1961; 85: 277-93.
7. Babaian RJ, Johnson DE, Llamas L, *et al.* Metastases from transitional cell carcinoma of urinary bladder. Urology 1980; 16(2): 142-4.
8. Margolis RM, and Liss HP. Unusual etiology of cystic lesions in the lung. Chest 1986; 89(6): 857-8.
9. Peabody JW, Katz S, Davis EW. Bronchial carcinoma arising in a lung cyst. Am J Roentgenol 1957; 77: 1048-50.
10. Svennevig JL, Bugge-Asperheim B, Boye NP. Carcinoma arising in a lung cyst. Scand J Thor Cardivasc Surg 1979; 13(2): 153-5.
11. Miralles Lozano F, Gonzalez-Martinez B, Luna More S, *et al.* Carcinoma arising in a calcified bronchogenic cyst. Respiration 1981; 42(2): 135-7.

膀胱癌併發單一肺囊泡轉移——一病例報告

王金鐸　林智斌　郭明勳*　李仁智

膀胱癌易併發肺及骨骼轉移，癌症併發肺轉移多形成大小不一之腫塊為主，而以空洞表現者已經少見，而以囊泡表現者更是少見。本病例為一 50 歲男性患者因咳痰及右下胸痛至本院胸腔科檢查，病人 7 年前被診斷為膀胱癌，接受膀胱切除手術，胸部X光攝影顯示右中葉單一囊泡病變，經開刀證實為膀胱癌肺轉移，雖然癌症併發肺單一囊泡病變極為少見，但臨床X光判讀對單一囊泡病變仍應將癌症併發肺轉移，列入鑒別診斷之一。*(胸腔醫學 2002; 17: 56-60)*

關鍵詞：肺囊泡，膀胱癌，肺轉移

佛教慈濟綜合醫院　胸腔內科　病理科*
索取抽印本請聯絡：李仁智醫師，花蓮市中央路三段 707 號

Pulmonary Lymphangioleiomyomatosis —A Case Report

Kwo-Huei Shin, Ming-Chienh Lin*, Shinn-Liang Lai, Guang-Ming Shiao

Pulmonary lymphangioleiomyomatosis (LAM) is a rare disease of unknown cause that occurs mainly in women of reproductive age. It has seldom been reported among the Chinese population. Herein, we report a young female presenting with a left ovarian cyst, chylous ascites,a left iliac lymphadenopathy, right chylothorax, and diffuse reticular interstitial pulmonary lesions. A high resolution computerized tomography (HRCT) and left iliac lymph node biopsy confirmed the diagnosis of LAM. She then was treated with total parenteral hyperalimentation, diet therapy with medium chain triglycerides (MCT), chest tube drainage with chemical pleurodesis, and hormone therapy with Tamoxifen 20mg and Medroxyprogesterone 15mg daily. Her lung condition gradually improved. The chest tube was successfully removed, and both the radiographic findings and pulmonary function had improved, too. It is therefore concluded that for Chinese women of child-bearing age, LAM should be included in the differential diagnosis of pneumochylothorax. ***(Thorac Med 2002; 17: 61-67)***

Key words: pulmonary lymphangioleiomyomatosis, chylothorax.

Introduction

Pulmonary lymphangioleiomyomatosis (LAM) is a rare pulmonary disease with unknown etiology that afflicts young women of child-bearing age [1-3]. LAM has rarely been reported in the Chinese population [4-5], and is characterized by a peribronchial, perivascular, and perilymphatic proliferation of atypical pulmonary interstitial smooth muscle cells, and also by cyst formation. Clinical findings include progressive dyspnea, hemoptysis, pneumothorax, and chylous pleural effusion, and the disease runs a variable course culminating usually in respiratory failure [1]. Lymph nodes in the abdomen and pelvis may be involved, too. The clinical diagnosis is usually based on the presence of variable-sized thin-walled cysts throughout the whole lung as demonstrated by HRCT and positive human melanosome black (HMB-45) stain in the pathologic specimen.

Case Report

A 29-year-old woman visited a medical center in May, 2000. She complained of low abdominal discomfort lasting for one month, and

Chest Department, Taipei Veterans General Hospital
*Department of Pathology, National Taiwan University Hospital
Address reprint requests to: Dr. Kwo-Huei Shin, Chest Department, Taipei Veterans General Hospital, No.201, Sec.2, Shih-Pai Road, Taipei, Taiwan

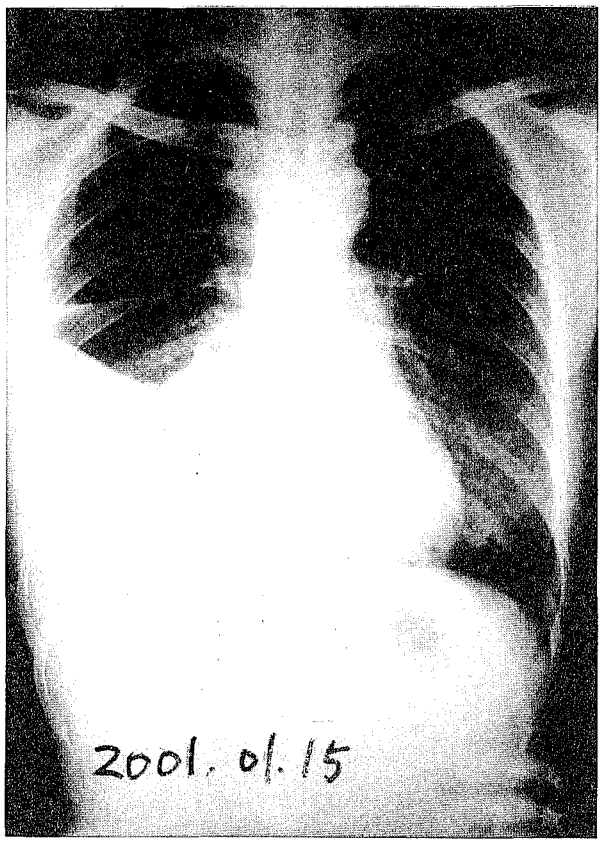

Fig. 1. Chest radiograph only shows interstitil infiltration in the bilateral lower lung fields, right pleural effusion, and hazziness in the lower right lung.

occasional chest tightness for about 2-3 years. Chest radiography (CXR) revealed a prominent mediastinal shadow on the right side of the mediastinum, but a chest computerized tomography (CT) showed no mediastinal lymphadenopathy in the axillary and hilar area, no pleural effusion, and no lung lesion. The hospital abdominal sonography showed a left ovarian tumor and left enlarged cysts. The abdominal CT revealed a low-density, with homogenous-appearing mass at the left pelvic side wall. The mass seemed to be engulfing the vessels, and showed a more mass- like effect on the adjacent structures than encasement. There was extensive lymphadenopathy of a acceptable size in the left iliac area. An open abdomen biopsy revealed a left retroperitoneal abscess and left paratubal cyst. Drainage of the retroperitoneal abscess and a left tubal cystectomy were then performed. No bacteria was cultured from the abscess. Pathology showed a cystic lesion on the left tubal tissue only. One week later, the patient complained of abdominal distention. An abdominal sonography showed ascites, about 200cc. Milky ascites 20cc was aspirated and a laboratory exam showed triglycerides (TG) 1606 mg/dL and cholesterol 100 mg/dL. The cytology was negative and the cell count showed lymphocytes dominant. Chylous ascites was suspected. In the following months, abdominal distention occasionally bothered her, but no more accumulated ascites could be found by sonography. The residual ascites could not be easily aspirated.

At the end of December 2000, the patient visited the hospital on account of progressive dyspnea. Massive ascites, right pleural effusion and relative lymphadenopathy in the peritoneum were revealed by abdominal CT. The chest sonography showed a right pleural effusion. Thoracocentesis found milk-like effusion with lymphocytes predominant, and the laboratory exam showed protein 5.4 gm/L, TG 651 mg/dL, cholesterol 160 mg/dL, and glucose 85 mg/dL. As a result, chylothorax was suspected. In January 2001, she was readmitted when the CXR disclosed right pleural effusion, hazziness in the lower right lung, and interstitial shadows in both lower lung fields (Figure 1). As sono-guided drainage of the pleural effusion was performed. Laparotomy was then undertaken, and revealed a lot of milky ascites. The iliac node biopsy demonstrated an abnormal muscle cell infiltration. The smooth muscle actin and HMB-45 stain showed a positive result (Figure 2 and Figure 3), which was compatible to lymphangioleiomyomatosis. Unfortunately, the patient had suffered from dyspnea since the laparotomy. One week later, the CXR showed chylopneumothorax (Figure 4). An HRCT of the chest revealed a massive amount of pleural effusion with pneumothorax and subcutaneous emphysema on the right side. The diffuse thin-walled cysts throughout both lungs were consistent with LAM. Several small lymph nodes in the aortopulmonic window and a small amount

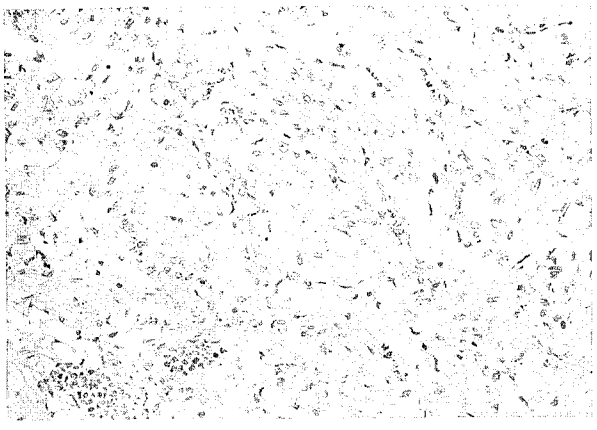

Fig. 2. Iliac node biopsy shows abnormal smooth muscle spindles (200x).

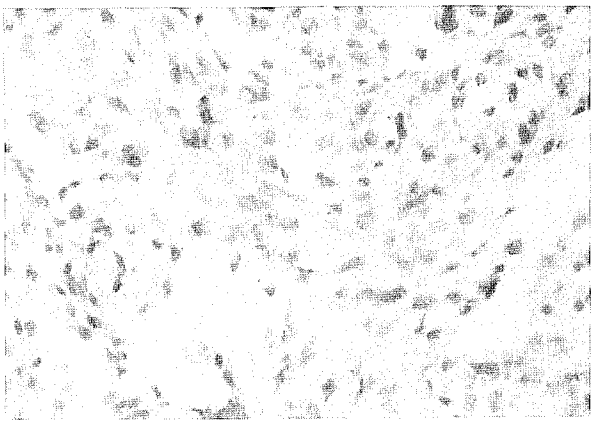

Fig. 3. Iliac lymph node biopsy shows abnormal smooth muscle cells with HMB-45 stain (brown colored) (+) (400x).

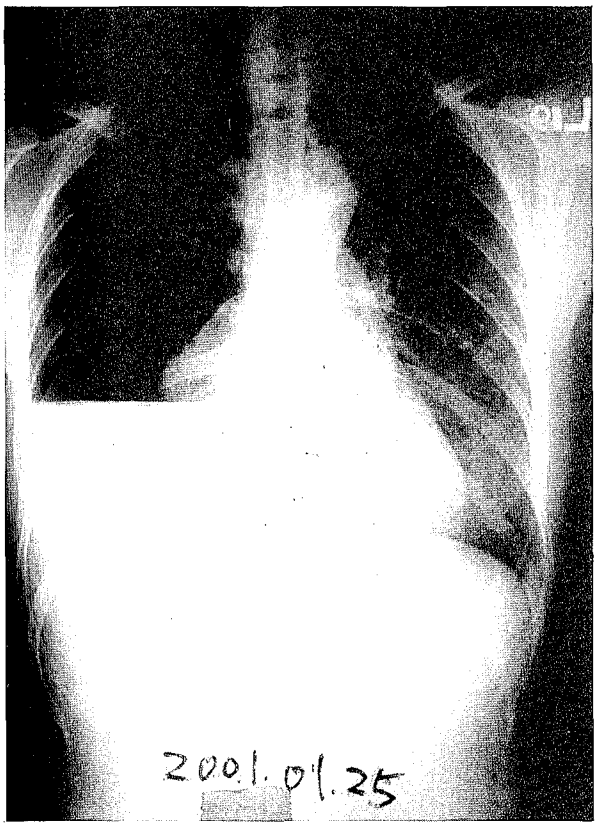

Fig. 4. Chest film revealed right chylopneumothorax and the same interstitial infiltration in the lower left lung as in Figure 1.

of ascites in the right subphrenic space were also noted (Figure 5). The patient then underwent chest tube drainage. With the poor reexpansion of her right lung, the patient asked to be transfered to Taipei Veterans General Hospital, at the end of January 2001, for further management.

At the second hospital, the physical examination was grossly normal except for mild tachycardia (HR= 107/min) and tachypnea (RR= 20/min). The biochemical data showed hypocholesteremia and hypoalbuminemia. After adjusting the position of the chest tube, the lung gradually reached full expansion. The pulmonary function test showed moderately obstructive ventilatory impairment with FVC= 2.22 L (67 % predict), FEV1= 1.34 L (47 % predict), and FEV1/FVC ratio= 60 %.

The patient was initially treated with nothing per os (NPO) and total parenteral nutrition to reduce the production of chylous pleural effusion. Later, she was put on a special diet with medium-chain triglycerides and hormonal therapy with Tamoxifen 20mg and Medroxyprogesterone 15mg prescribed daily. Two months later, the amount of pleural effusion had been reduced from 500cc to 100cc daily. The abdominal sonography showed a small amount of ascites. A chemical pleurodesis with a minocycline injection was also given. The chest tube was successfully removed, and the follow-up pulmonary function data showed some improvement, with FVC= 2.38 L (72 % predict), FEV1= 1.48 L (51 % predict), FEV1/FVC ratio= 62 %, TLC= 3.69 L (81 % predict), RV= 1.24 (96 % predict), and RV/TLC= 118 % predict. The

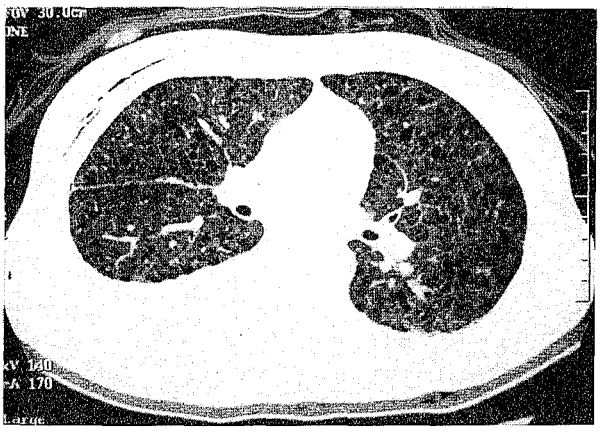

Fig. 5. High resolution computerized tomography shows typically variable-sized thin-walled cysts homogeneously throughout the bilateral whole lung fields, and bilateral chylous pleural effusions

DLCO indicated a severe reduction of gas exchange, with DLCO 26.34 ml/min/mmHg (24 % predict). A mild increase in airway resistance was noted, with Raw 2.26 (predict range: 1.078-1.736 cmH2O/L/sec). The follow-up CXR in July 2001 showed a right costophrenic angle blunting with a small amount of pleural effusion. There was no significant change from the chest film in April 2001, and the same interstitional-nodular infiltration was present in the bilateral lower lung fields.

Discussion

Lymphangioleiomyomatosis (LAM) is a rare disease found worldwide. Only few reports of LAM in the Chinese population are available [4,5]. LAM has been described as being highly associated with tuberous sclerosis complex (TSC) (26%) [6]. TSC is an autosomal dominant disorder characterized by seizures, mental retardation, and harmatomatous tumors of the brain, heart, kidney, lung, and skin. Among these characteristics, renal angiomyolipomas (harmatomas), a typical finding in the genetic disorder tuberous sclerosis, occur in 70% of TSC patients and in 33 to 63% of women with sporadic LAM [7]. Our patient didn't show evidence of tuberous sclerosis or renal angiomyolipoma. The coincident findings of abdominal tumor, ascites, and pneumothorax prompted us to suspect LAM. Because the disease may be diagnosed with a latent period of about 3-4 years, and half the patients can be stabilized with early treatment [2], early diagnosis is necessary. Diagnostic clues include interstitial infiltration on the chest film (CXR) and diffuse cystic lesions on high resolution computerized tomography (HRCT) [8]. In LAM, numerous thin-walled cysts of various sizes are present throughout the lungs, without any particular regional or lobar distribution; otherwise, the lung parenchyma appears relatively normal, although focal ground-glass opacities are occasionally noted.

To cysts have an appearance similar to other cystic lung diseases, such as histiocytosis X. However, the cysts are located primarily in the middle and upper lung zones, and are a prominent nodular component in the lung. In idiopathic pulmonary fibrosis, honeycombing cysts are a common feature. The cysts are usually located peripherally in a subpleural pattern, and areas of ground-glass opacification and other reticular or linear shadows are common. Alpha 1-antitrypsin deficiency emphysema is characterized by diffuse bullous and emphysematous changes on the CT scan. Because HRCT findings can confirm the diagnosis of LAM in a young woman with emphysema, recurrent pneumothrax, or chylous pleural effusion, tissue confirmation may not always be necessary [3]. The characteristic findings of HRCT and iliac node pathology can confirm this diagnosis. We were able to make the diagnosis of LAM in our patient without a lung biopsy.

The primary pathological abnormality is the proliferation of atypical smooth muscle cells around the bronchovascular structures and into the interstitium. The proliferating cells resemble vascular smooth muscle cells, but they are often somewhat shortened and pleomorphic, and stain positively with the monoclonal antibody HMB-45. Another unique pathologic feature is the occurrence of diffuse, cystic dilatation of the

terminal airspaces [9]. Hemosiderosis is common and is a consequence of clinically insignificant hemorrhage due to the rupture of dilated and tortuous venules. The normal architecture of the lung is distorted both grossly and microscopically by multiple small cysts, ranging from 0.1 cm to several centimeters in diameter. The interstitium is thickened, with evidence of smooth muscle-like proliferation around and within the pulmonary lymphatics, venules, and airways [2]. The lymphatic and venous vessels are often tortuous and dilated. Hilar, mediastinal, and retroperitoneal lymph nodes are regularly involved and enlarged. The thoracic duct is frequently thickened and dilated [10]. Extrapulmonary involvement with renal, retroperitoneal, intraabdominal, and pelvic angioleiomyomata is common. The pathogenesis of LAM is unknown, but data are accumulating which suggest a role for the loss of the tumor suppression functions of certain cellular enzymes, or abnormalities in proteins involved in the synthesis of catecholamine [1]. Many of these pathophysiologic features appear shared with tuberous sclerosis, a condition similar to LAM in terms of its lung pathology and the presence of renal angiomyolipomas [6-7]. It is not entirely clear how defects in these proteins or in catecholamine synthesis can produce the LAM phenotype. LAM cells stain with HMB-45, a monoclonal antibody derived from melanoma hybridomas and previously thought to be a specific marker for melanoma and immature melanocytes. The antigen to which HMB-45 binds has total cDNA homology with the gene Pmel 17, the product of which is involved in the synthesis of melanin and cathecholamine from the amino acid tyrosine [1]. The human Pmel 17 gene has been mapped to chromosome 12. One of the candidate gene loci for tuberous sclerosis has been mapped to a similar site on this chromosome. The gene for the enzyme phenylalanine hydroxylase is found at or near this tuberous sclerosis locus; this enzyme catalyzes the conversion of phenylalanine to tyrosine, the substrate for catecholamine synthesis. However, it should be emphasized that LAM and tuberous sclerosis are distinct syndromes, as the latter entity also affects the skin and central nervous system, and demonstrates clear Mendelian inheritance. It is possible that patients with LAM are mosaic, with TSC2 mutations in the lung (and sometimes the kidney) but not elsewhere, or that environmental factors play a critical role in the development of clinically apparent LAM [11].

The role of estrogen likely plays a central role in disease progression, since the disease does not present prior to menarche and only rarely after menopause. The disease is also known to accelerate during pregnancy and to abate after oophorectomy. Furthermore, estrogen and progesterone receptors have been demonstrated in a subpopulation of the abnormal smooth muscle cells that are characteristic of the disease. These receptors may be down-regulated following the institution of hormonal therapy [12]. Because of the impression that the disease progresses during pregnancy and because patients with LAM often suffer progressive declines and early death, thereby leaving the children without their mother [13], we cautioned our patient to avoid pregnancy.

Pulmonary function testing (PFT) usually reveals an obstructive or mixed pattern [14]. The lungs are often hyperinflated, with an increased total lung capacity (TLC) and increased thoracic gas volume. Gas trapping, as evident by an increase in residual volume (RV) and in the RV/TLC ratio, is commonly present. Airflow limitation and recoil is reduced, and that upstream resistance is increased. Both a loss of elastic recoil and an increase in airway resistance contribute to the observed airflow limitation. Gas exchange is often abnormal, with a markedly reduced DLCO and an increase in the alveolar-arterial oxygen difference. Diminished exercise performance is found in most patients. The follow-up PFT showed mildly obstructive and restrictive ventilatory impairment with an increased RV/TLC ratio. The hyperinflation did not show in our patient may have been due to the

early diagnosis while abdominal pain was present.

Treatment includes diet therapy, hormonal therapy, and medical pleurodesis. Recurrent chylopneumothorax has been reported in the literature, even with treatment, so thoracic duct ligation should be considered [10]. Our patient refused lung biopsy or any invasive procedure. We chose a medical pleurodesis in the right lung in light of the possibility of a reaccumulation of chylous fluid in a third space, including the abdominal cavity. Fortunately, this condition didn't occur. Because LAM may progress in a variable course to repiratory failure, we also advised the patient about the later possibility of lung transplantation. We will closely follow up any future complication in the patient. Left lung transplantation will be considered as a life-saving procedure if the patient does not respond to treatment and develops respiratory failure.

In conclusion, with the aid of HRCT, we believe that more LAM patients will be diagnosed in Taiwan in the near future. We have to keep the possibility of LAM in mind, especially in child-bearing woman with recurrent pneumothorax and chylothorax.

References

1. Johnson S. Rare diseases. 1. Lymphangioleiomyomatosis: clinical features,management and basic mechanisms. Thorax 1999; 54: 254-64.
2. Urban T, Lazor R, Lacronique J, *et al.* Pulmonary lymphangioleiomyomatosis. A study of 69 patients. Medicine 1999; 78: 321-37.
3. Chu SC, Horiba K, Usuki J, *et al.* Comprehensive evaluation of 35 patients with lymphangioleiomyomatosis. Chest 1999; 115: 1041-52.
4. Chuah KL, Tan PH. Multifocal micronodular pneumocyte hyperplasia, lymph-angiomyomatosis and clear cell micronodules of the lung in a Chinese female patient with tuberous sclerosis. Pathology 1998; 30: 242-6.
5. Peh WC, Law S, Fok M, *et al.* Case report: lymphangiomyomatosis with spon-taneous peritoneal rupture. British Journal of Radiology 1994; 67:605-8.
6. Costello LC, Hartman TE, Ryu JH. High frequency of pulmonary lymphan-gioleiomyomatosis in woman with tuberous sclerosis complex. Mayo Clin Proc 2000; 75:591-4.
7. Logginidou H, Ao X, Russo I, *et al.* Frequent estrogen and progesterone receptor immunoreactivity in renal angiomyolipomas from woman with pulmonary lymphangioleiomyomatosis. Chest 2000; 117: 25-30.
8. Trulock E. A 35-year-old woman with cough, dyspnea, and an abnormal chest radiograph. Chest 1998; 114: 1463-4.
9. Kitaichi M, Nishimura K, Itoh H, *et al.* Pulmonary lymphangioleiomyo-matosis: A report of 46 patients including a clinicopathologic study of prognostic factors. Am J Respir Crit care Med 1995; 151: 527-33.
10. Yildizeli B, Yuksel M. Chylothorax and lymphan-giomyomatosis. Ann Thorac Surg 2000; 69: 1640.
11. Smolarek TA, Wessner LL, McCormmack FX. Evidence that lymphangiomyo-matosis caused by TSC 2 mutations: Chromosome 16p13 loss of heterozygo-sity in angiomyolipomas and lymph nodes from woman with lymphangiomyomatosis. Am J Hum Genet 1998; 62: 810-5.
12. Matsui K, Takeda K, Yu ZX, *et al.* Downregulation of estrogen and progesterone receptors in the abnormal smooth muscle cells in pulmonary lymphangioleiomyomatosis following therapy. An immunohistochemical study. Am J Respir Crit Care Med 2000; 161: 1002-9
13. Warren SE, Lee D, Martin V, *et al.* Pulmonary lymphangiomyomatosis causing bilateral pneumothorax during pregnancy. Ann Thorac Surg 1993; 55: 998-1000.
14. Crausman RS, Jennings CA, Mortenson RL, *et al.* Lymphangioleiomyoma-tosis: the pathophysiology of diminished exercise capacity. Am J Respir Crit Care Med 1996; 153: 1368-76.

肺部淋巴血管肌肉增生症—病例報告

辛國輝　林明杰*　賴信良　蕭光明

淋巴血管肌肉增生症(LAM)是一個罕見的疾病，原因不明，幾乎全發生於生殖年齡的婦女。此病一向鮮少有中國人的報導，在此我們報告一位年輕女性，呈現左側卵巢囊腫、乳糜腹水、左側腸骨淋巴結腫大、右側乳糜胸及瀰漫性細網狀間質性肺病變。高解析度電腦斷層攝影及左腸骨淋巴切片檢查，確認 淋巴血管肌肉增生症的診斷。以全靜脈營養治療、中鏈三酸甘油脂飲食治療、胸管引流術及肋膜黏連術治療，再加上每日賀爾蒙治療(Tamoxifen 20mg & Medroxyprogesterone 15mg)，其肺部情況逐漸改善，胸管終於成功移除，胸部影像及肺功能也獲改善。因此，生殖年齡之國人婦女若合併有氣胸及乳糜胸時，LAM 也應列入鑑別診斷。*(胸腔醫學 2002; 17: 61-67)*

關鍵詞：淋巴血管肌肉增生症，乳糜胸

台北榮民總醫院　胸腔部　台大醫院　病理科*
索取抽印本請聯絡：辛國輝醫師，台北市石牌路二段 201 號

Lung Cancer with Complicating Chylothorax —A Case Report

Ai-Hsi Hsu, Jen-Jyh Lee, Gee-Gwo Yang

Lung cancer with complicating chylothorax is a rare clinical condition. In recent years, there have been only two published articles reporting the successful treatment of this condition. In the first one, which was published in Japan, the physicians announced a successful treatment using OK-432. The other case of lung cancer with complicating chylothorax was published in Poland, and reported that the leakage of chyle into the pleural cavity could be stopped after chemo- and radiotherapy. In this article, we present a case of pulmonary adenocarcinoma with complicating chylothorax. The patient died in spite of multiple modalities of treatment, including a low-fat and high-protein diet, chemotherapy with a regimen of gemcitabine plus cisplatin, and chemical pleurodesis. ***(Thorac Med 2002; 17: 68-72)***

Key words: lung cancer, chylothorax

Introduction

Chylothorax is a rare medical condition. In the past five years, there have been only six documented cases in our hospital. Variations in their causes have also been observed, as follows: In two cases, the cause was iatrogenic, after cardiovascular surgery in children; two cases were due to malignancy; one case was due to a bacterial infection of aeromonas hydrophilia-induced chylothorax; and one case was idiopathic. Herein, we review a case of chylothorax due to complicated bronchogenic carcinoma. This case, with chylous effusion complicated with malignant disease, did not have a common etiology.

Case Report

A 68-year-old male was admitted to our hospital due to an insidious onset of cough and exertional dyspnea, lasting for two weeks. A physical examination showed that his temperature was 36.5C, blood pressure 120/80 mmHg, and pulse rate 92 beats per minute. He was chronically ill-looking, though no neck mass was palpable. The heart rate had increased, but the breathing sound had decreased, especially in the right lung. There was neither abdominal distension, nor lower leg edema.

The complete blood count revealed WBC: 9400/ul with 87.3% neutrophils, Hb level: 10.7 g/dl, and Ht: 32.4%. The platelet count was

Division of Chest Medicine, Department of Internal Medicine, Buddhist Tzu-Chi Hospital, Hualien, Taiwan
Address reprint requests to: Dr. Ai-Hsi Hsu, Division of Chest Medicine, Department of Medicine, Buddhist Tzu-Chi Hospital, 707 Section 3, Chung-Yang Rd, Hualien, Taiwan

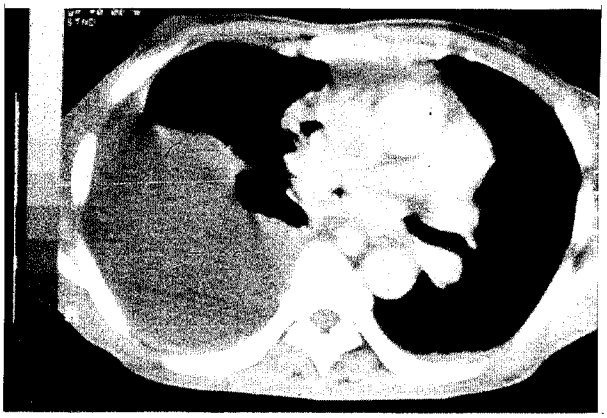

Fig. 1. Chest computed tomographic scan showing massive right pleural effusion on the first admisson.

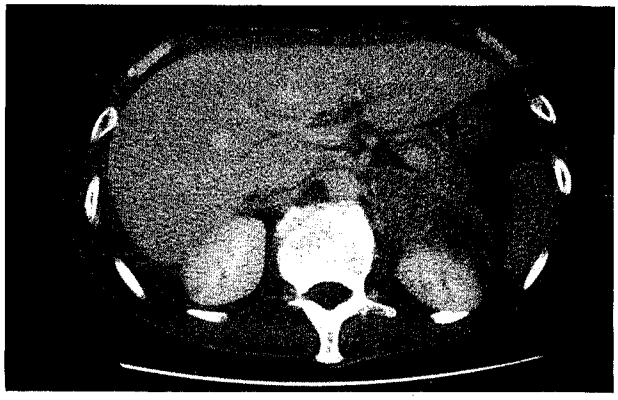

Fig. 2. Computed tomographic scan showing the left adrenal metastasis of lung cancer

299,000/ul. Blood sugar, liver function, and BUN/CREA ratio were all within the normal range.

A chest x-ray film revealed a large amount of right-side pleural effusion. Thoracentesis yielded a milky white fluid. The fluid analysis showed a white cell count: 3075/ul, lymphocyte count: 55%, sugar: 68mg/dl, LDH: 976 IU/L, triglycerides: 490 mg/dl and total cholesterol 70 mg/dl. The ACTH and cortisol level were within the normal range. The computerized tomographic scans of the chest (Figure 1)disclosed a massive right pleural effusion, and a passively collapsed right lung. Mediastinal lymphadenopathy and left adrenal gland metastasis (Figure 2) were also found. Bronchoscopic examination disclosed an external compression of the right bronchial trees. Although there was no visible endobronchial tumor, the tip of the bronchoscope cannot pass through the narrowed intermediate bronchus. Cytologic examination of the sputum reported a picture of adenocarcinoma. Repeated thoracentesis for symptom relief yielded about 4000 ml of chylous effusion. Then, chemotherapy with weekly gemcitabine plus cisplatin were given. After two doses of gemcitabine had been given, he was discharged. Unfortunately, he returned to our hospital 2 days later due to a rapid accumulation of the right-side effusion. A chest ultrasound revealed multi-loculated right-side pleural effusion (Figure 3). This was totally different (Figure 4) from that which was observed a week ago. Therefore, a 28-branch chest tube was inserted and an intrathoracic injection of streptokinase 250KE was administered for 7 consecutive days . In all, 4250 ml of fluid was drained out during that week. Then, the patient

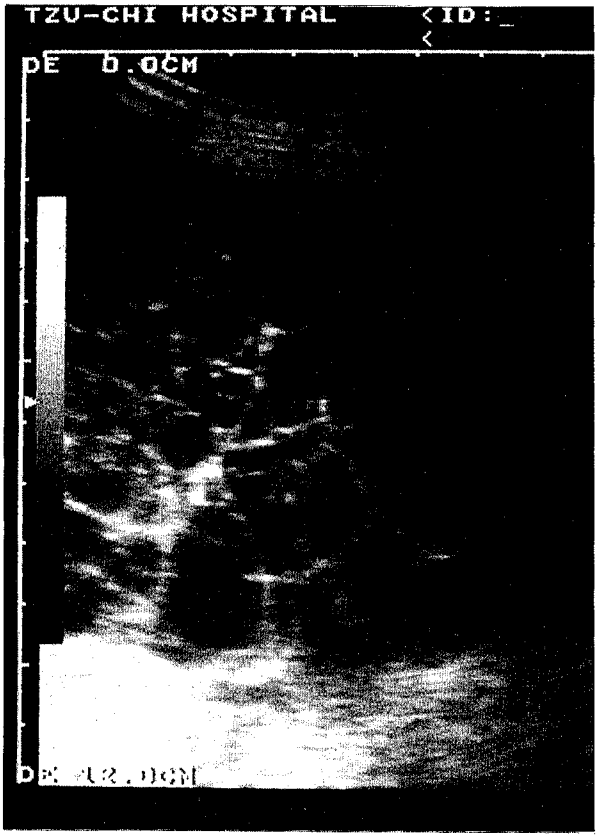

Fig. 3. Chest sonography showing the right pleural effusion becoming septated on the second admission.

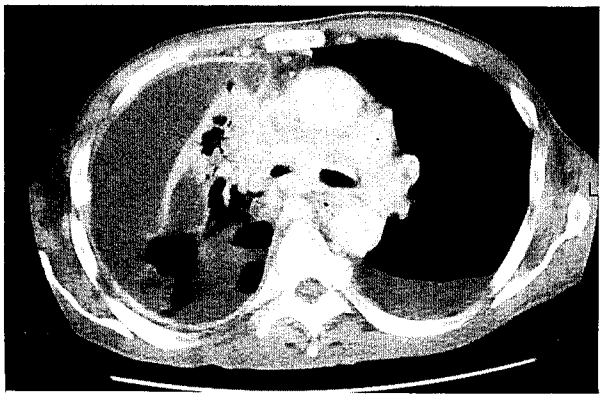

Fig. 4. Chest computed tomographic scan showing massive right pleural effusion with a loculated appearance, and left-side transudative pleural effusion noted on the second admission.

became more and more cachexic. Body weight decreased by 7 kg in the following 3 weeks. A chest surgeon was consulted to evaluate the possibility of surgical repair of the thoracic duct, and the management of the multi-loculated right side pleural effusion, as well. Due to the poor general condition of the patient, conservative treatment was advised by the surgeon. One week later, another fiberoptic bronchoscopic examination was performed, due to a delayed expansion of the middle right and lower right lobes of the lung, in spite of aggressive chest tube drainage with 15 cm H2O pressure suction. (Figure 5) There was still no endobrochial lesion, but the external compression of the right bronchial tree had improved. Chemical pleurodesis was performed with a minocycline 300 mg intrapleural injection . Unfortunately, six days after the pleurodesis, the pleural fluid had accumulated again. Furthermore, left-side transudative pleural effusion was also noted. Finally, the patient was admitted to the hospice care unit, and died 3 days later.

Discussion

Chylothorax is still not a common clinical problem. After a review of the literature, we found that nearly half of these cases had been associated with lymphomas, or other malignant tumors [1]. In a study conducted in India during 1972 [2], 34 of 150 cases of bronchogenic

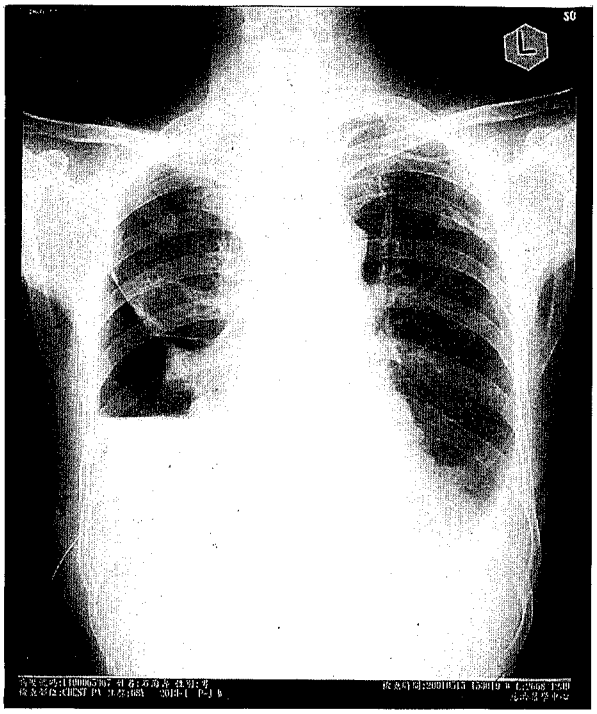

Fig. 5. Chest radiograph showing a chest tube inserted into the righ pleural cavity, the chylous effusion draining out, and the delaye full expansion of the right middle and lower lobes.

carcinoma were associated with pleural effusion, but there was no chylous effusion found.

In this most recent decade, chylothorax complicating bronchogenic carcinoma is still a very rare condition. Several published articles have discussed this entity, but none of them have mentioned the rapid septal formation of the chylous effusion, presenting as a complication of bronchogenic carcinoma. Various methods for the treatment of chylothorax have been discussed, including thoracic duct ligation, which was introduced in 1948 by Lampson [3], percutaneous catheterization and embolization of the thoracic duct [4], clipping of the thoracic duct with video assisted thoracic surgery [5], and using the octreotide, a long-acting somatostatin analog [6]. Recently, a published article reported a case of chylothorax complicating lung cancer, which was successfully treated by chemical pleurodesis with OK-432 [7].

In Finland, two cases of chylous pleural effusion complicating malignant disease were documented in 1983 [8]. The first was a case of

ovarian methothelioma, with mediastinal lymph node invasion. The chyle seemed to be leaking from the mediastinal lymph nodes. The second was a case of pancreatic carcinoma; the source of leakage was the enlarged and irregular retroperitoneal lymph nodes, then the chyle entered the pleural cavities through the diaphragm. Both cases failed to respond to a conservative treatment with a low-fat and high-protein diet. Due to a continuing loss of chyle in the first case, a thoracotomy was performed, and a mediastinal lymph nodes dissection and ligation of the thoracic duct was done, as well. Unfortunately, an additional 18 liters of chyle was yielded postoperatively. Six month later, the patient died. The second case, with pancreatic cancer, also died several months later, after only supportive treatment. There was another case of chylothorax complicating squamous cell lung cancer in Poland. The chylous effusion stopped progressing after the lung cancer had been controlled with chemo- and radiotherapy. [9]

Chylothorax due to iatrogenic, traumatic, and idiopathic etiologies responds well to conservative treatment. These treatment modalities include a low-fat and high- protein diet, or a surgical intervention with supra-diaphragmatic ligation of the thoracic duct, or even the removal of some large chylous cysts and lymph nodes. Chylothorax due to malignant cancer often responds poorly to dietary treatment and surgical intervention, except when the underlying malignant disease is controlled.

There was a report of a percutaneous catheterization and embolization of the thoracic duct for the treatment of chylothorax. This procedure requires a very experienced and skillful radiologist since it is difficult for clinical professionals to locate an approachable peripheral lymphatic channel. Another article reported a successful treatment of malignant chylothorax using chemical pleurodesis with OK-432.

After reviewing the current literature on malignant pleural chylous effusion, we can conclude that this medical condition remains a difficult task to solve clinically. With the current poor response to aggressive treatment modalities, we hope that the underlying malignancy can be controlled in the near future.

Reference

1. J. Ralph Macfarlane, Cranston W. Holman. Chylothorax. American review of Respiratory Disease 1972; 105: 287-91.
2. Jindal SK, Malik SK. Bronchogenic carcinoma: A review of 150 cases. Ind J Chest Dis and All Sci 1979; 21: 59.
3. Lampson RS. Traumatic chylothorax. J Thorac Surg 1948; 17: 778.
4. Eric K. Hoffer, Robert D. Bloch, *et al.* Treatment of chylothorax: percutaneous catheterization and embolization of the thoracic duct. AJR 2001; 176: 1040-2.
5. Tojo T, Nezu K, Kushibe K. Clipping of the thoracic duct with video-assisted thoracic surgery in the treatment of chylothorax after pulmonary resection. Nihon Kokyuki Gakkai Zasshi 1997 Aug; 45(8): 1102-6.
6. Nicholas J. Demos, Joseph Kozel, Joseph E. Scerbo. Somatostatin in the treatment of chylothorax. Chest 2001; 119:964-6.
7. Koga Y, Mita Y, *et al.* Lung cancer with chylothorax successfully treated by chemical pleurodesis with OK-432. Nihon Kokyuki Gakkai Zasshi 1999 Aug; 37(8); 627-30.
8. Seppo Kostiainen, Heikki Meurala. Chylothorax-clinical experience in nine cases. Scand J Thoracic Cardiovasc Surg 1983; 17: 79-83.
9. Witt M, Kurzawska-Firley D, *et al.* Chylothorax in the course of squamous cell lung cancer. Pneumonol Alergol Pol 1997; 65(5-6): 370-3.

肺癌合併乳糜胸水—病例報告

胥愛璽　李仁智　楊治國

肺癌合併乳糜胸水臨床上並不常見。文獻上近年只有兩例治療成功的報告。其中一例在日本用 OK-432 作肋膜沾粘術後，成功治療肺癌合併乳糜胸水。另外在波蘭亦報告一例經化學及放射療法後成功控制肺癌併乳糜胸水之病例。本篇報告一位六十八歲肺部腺癌合併右側大量乳糜胸水之男性病患，於今年四月中旬確立診斷後，經低脂高蛋白質飲食控制，化學藥物治療及肋膜沾粘術等方法處理後，病患仍持續產生大量乳糜胸水，併全身營養狀況持續惡化，於診斷後兩個月內死亡。本篇並就乳糜胸之致病因素及目前之處理方式做討論。 ***(胸腔醫學 2002; 17: 68-72)***

關鍵詞：肺癌，乳糜胸

花蓮慈濟醫院　胸腔內科
索取抽印本請聯絡：胥愛璽醫師，花蓮市中央路三段 707 號

Necrotizing Fasciitis as a Complication of Ultrasound-Guided Fine Needle Aspiration of a Lung Abscess—A Case Report

Chih-Yun Yang, Hong-Chung Wang*, Jau-Yoeng Lu*

Necrotizing fasciitis (NF) is a serious, rapidly progressive infection of the subcutaneous tissue and fascia, most often related to trauma or surgery. We report a rare case of NF which occurred as a complication of ultrasound (US) - guided transthoracic fine needle aspiration (TFNA) for lung cancer associated with an abscess formation. A standard US-guided TFNA for the lung abscess was performed for the purpose of cytological and bacterial analysis. Three days later, necrotizing fasciitis developed from the puncture site, with rapid extension to the upper lateral abdominal wall. A bacterial culture of the lung abscess isolated group D streptococcus, which is compatible with the culture of NF. Despite aggressive treatment, including emergency fasciectomy, the patient expired due to uncontrolled sepsis from a secondary wound infection 2 months after admission. ***(Thorac Med 2002; 17: 73-77)***

Key words: lung abscess, lung cancer, necrotizing fasciitis, transthoracic fine needle aspiration

Introduction

Necrotizing fasciitis (NF) is a rapidly progressive infection of the subcutaneous tissue and fascia, with widespread fascia necrosis and relative sparing of the skin and underlying muscle, usually caused by toxin-producing, virulent bacteria [1]. It is fatal unless promptly recognized and aggressively treated. The disease occurs more frequently in diabetics, alcoholics, immuno-suppressed patients, intravenous drug users, and patients with peripheral vascular diseases. There have been few reports of NF occurring as a complication of chest tube intubation [2]. Group A streptococci are the most common causative organisms. We herein report a case of NF which occurred as a complication of ultrasound (US) - guided transthoracic fine needle aspiration (TFNA) for a lung abscess caused by non-enterococcal group D streptococcus. Physicians should be aware of this potential complication, since mortality is high without definitive treatment, which requires not only antibiotics, but also surgical debridement.

Case Report

A 53-year-old man was admitted to the hospital because of productive cough, fever, and

Division of Respiratory, *Division of Chest Medicine, Department of Internal Medicine, Veterans General Hospital-Kaohsiung
Address reprint requests to: Dr. Hong-Chung Wang, No.386, Ta-chung 1st Rd., Kaohsiung, Taiwan

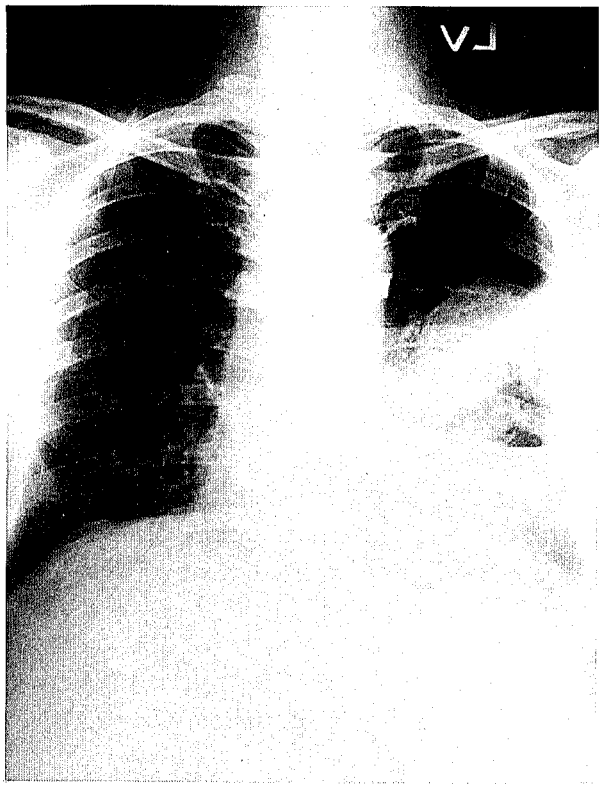

Fig. 1. Chest radiography showed a huge cavitary mass with an air-fluid level in the left lingular lobe.

chills. He had type 2 diabetes mellitus (DM), which had been treated with oral hypoglycemic agents for many years. Otherwise, he had no history of previous medical illnesses. He did have a 40-pack-a-year history of cigarette smoking. One week before the current admission, he developed a productive cough with copious dark sputum; these symptoms progressed over the next 3 days. Two days before admission, fever and chills developed. Upon admission, his temperature was 37.7℃, blood pressure 124/62 mmHg, and heart rate 112 beats per minute. On examination, his consciousness was clear. Fine crackles were heard in his left lung field, with diminished breathing sounds. The laboratory evaluation revealed a white blood cell count of 29530 per mm^3 with 86% neutrophils and 2% lymphocytes, a hemoglobin value of 9.5 gm/dL, and a platelet count of 236000 per mm^3. Other laboratory values were as follows: sodium, 127 mmol per L; potassium, 4.6 mmol per L; chloride, 92 mmol per L; and glucose, 361 mg per dL. The chest roentgenogram (Figure 1) showed a huge cavitary mass with an air-fluid level in the left lingular lobe. In addition, a minimal amount of left pleural effusion was also noted. The patient was given intravenous crystal penicillin and gentamicin under the suspicion of lung cancer complicated with an abscess formation.

A computerized tomographic (CT) scan of the chest revealed a poorly enhanced central mass in the lingular lobe, 7 x 8 cm in size, with an air-fluid level, and mediastinal lymphadenopathy. Under the guidance of ultrasound, a TFNA was performed for microbiological cultures and cytology. This procedure was done using a standard method, and the whole course was smooth. Thoracocentesis for the left pleural effusion was not done due to a minimal amount of pleural fluid. There were no significant abnormalities within the visible range of the bronchoscopy.

Three days after ultrasound-guided fine needle aspiration, he complained of left chest pain. Local tenderness of the chest wall with erythematous change of the skin around the puncture site was found, and cellulitis was diagnosed. In the next two days, the painful reddish macules extended rapidly, spreading from the puncture site to the abdomen, and at the same time, the patient also developed abdominal pain. *Streptococcus viridans*, group D streptococcus, and *Bacteroides stercoris* were isolated from cultures of the aspirated abscess. An urgent CT scan of the abdomen (Figure 2) showed the presence of soft tissue swelling with gas formation in the abdominal muscular layer, with communication to the chest wall and no direct invasion to the intra-abdominal organs, compatible with NF. A fasciectomy with debridement was performed immediately, along with a simultaneous thoracoscopic biopsy of the lung mass. The surgical pathologic reports were consistent with NF of the abdominal wall and squamous cell carcinoma of the lung. Group D streptococcus was isolated from the culture of specimens

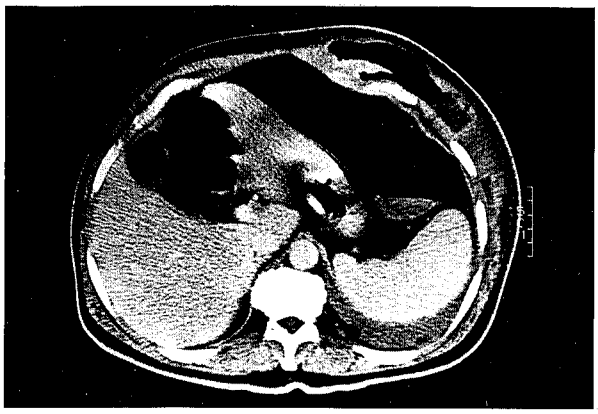

Fig. 2. Computerized tomography showed the presence of soft tissue swelling with a gas formation in the abdominal muscular layer, with some communication with the chest wall.

obtained intra-operatively, and this finding was compatible with the previous culture results from the ultrasound-guided aspiration of the lung abscess.

Unfortunately, after the fasciectomy with debridement of the NF, a superimposed surgical wound infection occurred. A secondary debridement and several broad-spectrum antibiotics, including crystal penicillin, clindamycin, and gentamicin, were given. Despite aggressive treatment, the patient eventually expired due to progressive lung cancer and uncontrolled sepsis.

Discussion

Necrotizing fasciitis is a rare and often fatal soft-tissue infection involving the superficial fascial layers of the extremities, abdomen, or perineum. It typically begins with trauma; however, the inciting event may be as seemingly innocuous as a simple contusion, minor burn, or insect bite.

The patient reported herein developed focal pain, swelling, and heating over a puncture site, with a rapid extension to the upper abdominal wall within three days after a TFNA procedure. The abdominal CT showed typical manifestations of NF in the abdominal wall, which was extended from the puncture, and communicated with the lung abscess. The NF culture result was group D streptococcus, which also grew in the culture of the lung abscess. The sensitivity tests of these two group D streptococci were similar. The clinical presentations, image and culture results implied that the NF was caused by the US – guided FNTA of the lung abscess.

Necrotizing fasciitis usually attacks 3-5 days after chest tube thoracostomy [2,4]. Susan KP and colleagues speculated that the difficult or traumatic tube insertion may play a role in the subcutaneous dissemination of the organism. This usually begins with the development of characteristic skin changes within 7 days of the inciting event [1]. Following the initial cellulitic skin changes, the skin darkens to a patchy, dusky blue, as blisters and bullae develop within a few days. By this time, the infection is well-established in the subcutaneous space, and necrosis of the fascia and fat begins to take place.

While group A streptococcus is the most common causative organism, predominant bacteria may include *Staphylococcus aureus,* group B Streptococcus, Enterococcus, coagulase-negative Staphylococcus, Bacillus, *Escherichia coli,* and *Bacteroides fragilis* [1,3,6,8]. The culture of our patient's necrotizing tissue demonstrated group D non-enterococcal streptococcus, a rarely reported pathogen in NF [1,3,5,7].

In our patient, the CT of the lung showed both a heterogenous mass in which a low density was easily identified with its thick and irregular wall consistent with lung cancer with central necrosis, and a not-well-defined and smooth wall, typical of simple lung abscess. Ultrasound-guided percutaneous lung aspiration for patients with lung abscess is done usually because of an unsatisfactory clinical or roentgenographic response, critical underlying diseases, or a poor general condition [10]. The role of drainage or surgery is based on serial clinical assessments of the patient. Bronchoscopic drainage may be most useful in the relief of abscess without air-fluid levels. In patients with coexistent empyema and lung abscesses, addressing the drainage of the empyema first is often useful. The surgical

resection of necrotic segments of the lung is helpful if the response to antibiotics is poor, the abscesses are large, or if ventilation-perfusion scans suggest little residual lung function in a limited necrotic region.

The treatment of NF includes antibiotics, surgery, supportive care, intravenous immunoglobulins, and hyperbaric oxygen [1,5,7]. The goal of the initial antibiotic therapy is to assure the broad coverage of aerobic Gram-positive and Gram-negative organisms and anaerobes. Penicillin or cephalosporin, and aminoglycosides and clindamycin or metronidazole are recommended [1,3,5]. Early and adequate surgical debridement and fasciotomy have been associated with improved survival, compared to delayed surgical intervention [6,8]. McHenry and colleagues found that delays in diagnosis and treatment (particularly adequate surgical debridement) correlated with a poor outcome. The critical period for diagnosing NF is within the first 24 to 48 hours after onset [2]. In our patient, broad-spectrum antibiotics were given at first, including clindamycin and gentamicin, and then crystal penicillin was prescribed based on the results of the bacterial sensitivity test. Surgical intervention was also undertaken as soon as possible. Unfortunately, a superimposed surgical wound infection after the fasciectomy, poorly controlled DM, and an underlying malignancy, led to death from sepsis. Mortality rates in NF are as high as 76% [6]. The risk factors that have been shown to correlate with increased mortality include an age over 50 years, diabetes mellitus, peripheral vascular disease and other systemic diseases, poor nutritional status, and an anatomic site of infection involving the trunk [9]. Our patient was an older male with DM, lung cancer, and NF involving the trunk, all of which were indicated as high risks for mortality.

The diagnosis of NF requires a high index of suspicion, especially when simple cellulitis becomes more severe. The complications of the fine-needle aspiration of a lung abscess should be kept in mind, especially when simple cellulitis becomes more severe, because early diagnosis and operative debridement may reduce the mortality rate.

References

1. Ronald JG, Donald CD, Thomas AR. Necrotizing fasciitis. Chest 1996; 110: 219-29.
2. Susan KP, John J. Necrotizing fasciitis as a complication of tube thoracostomy. Chest 1983; 83: 925-6.
3. Daniel LM, Martin K. Necrotizing fasciitis: a diagnostic challenge. Am Family Physician 1997; 56: 145-9.
4. Y.-M. Chen, M. F. Wu, P. Y. Lee, *et al.* Necrotizing fasciitis: is it a fetal complication of tube thoracostomy?-report of three cases. Resp Med 1992; 86: 249-51.
5. Roger AF, Christian MO, Theodore M. Necrotizing soft-tissue infections. J Am Acad Orthop Surg 2000; 8: 151-8.
6. McHenry CR, Piotrowski JJ, Petrinic D, *et al.* Determinants of mortality for necrotizing soft-tissue infections. Ann Surg 1995; 221: 558-65.
7. Heather AL, Anita P, Christopher M.B. Fernandes. Necrotizing fasciitis secondary to group A streptococcus. Canadian Family Physician 2000; 46: 1460-6.
8. Voros D, Pissiotis C, Georgantas D, *et al.* Role of early and extensive surgery in the treatment of severe necrotizing soft tissue infections. Br J Surg 1993; 80: 1190-1.
9. Rea WJ, Wyrick WJ. Necrotizing fasciitis. Ann Surg 1970; 172: 957-64.
10. Chung-Hua Chen, Ming-Long Kuo, Jen-Fu Shih, *et al.* Etiologic diagnosis of pulmonary infection by untrasonically guided percutaneous lung aspiration. Chin Med J 1993; 51: 333-9.

超音波指引之肺膿瘍抽吸術併發壞死性筋脈炎—病例報告

楊志勻　王鴻昌*　盧朝勇*

壞死性筋脈炎（necrotizing fasciitis）是一種嚴重而且惡化快速的皮下組織和筋脈感染症，大多與創傷或者手術有關。我們報告一個罕見在超音波指引之肺膿瘍抽吸術導致壞死性筋脈炎的病例。一個53歲男性肺癌合併肺膿瘍患者由於持續發燒，施予標準的超音波指引之肺膿瘍細針抽吸術。三天之後，從這個小針孔迅速擴展成為壞死性筋脈炎。肺膿瘍及壞死性筋脈炎之細菌培養均為D群鏈球菌。儘管施與包括抗生素治療及筋脈切除術等的積極處理，病人仍在兩個月後因為傷口感染導致敗血症而死亡。 ***(胸腔醫學 2002; 17: 73-77)***

關鍵詞：壞死性筋脈炎，肺膿瘍，細針抽吸術，肺癌

高雄榮民總醫院　內科部　呼吸治療科　胸腔內科*
索取抽印本請聯絡：王鴻昌醫師，高雄市左營區大中一路386號

Multicentric Desmoid Tumors—A Case Report and Literature Review

Pei-Ming Huang, Yih-Leong Chang*, Yung-Chie Lee

Aggressive fibromatosis (desmoid tumor) is a pathologic benign, uncommon, and often slowly growing fibrous tumor that is highly resistant to therapy. This type of tumor may arise in any musculoaponeurotic structure, and has a tendency to infiltrate adjacent tissues, become large in size, and cause functional limitation and/or pain, but does not metastasize.

We report a 48-year-old woman who underwent operation twelve times for recurrent and multicentric desmoid tumors, and briefly review the literature. The patient had an abdominal wall tumor 22 years ago, and has a hereditary desmoid disease which has affected a three generations in her family, but lacks the colonic features of familial adenomatous polyposis (FAP). In addition, a desmoid tumor at the mesentery involving the small intestine was also noted. The last operation, involving a wide excision of a right scapula tumor in the posterior area of the right chest wall, was performed in 1997. There is no local recurrence at present. Multiple episodes of recurrence (12 times), and multicentric occurrence, including an intra-abdominal presentation of the tumor, focal infiltration of the small bowel, and involvement of the chest wall, were unusual features for desmoid tumors. The clinical and histological features of desmoid tumors are presented here, with a discussion on management options. ***(Thorac Med 2002; 17: 78-83)***

Key words: desmoid tumor, multicentric, familial adenomatous polyposis

Introduction

Soft tissue tumors of the chest wall are uncommon lesions. While desmoid tumors are the most common histological subtype, they are highly resistant to treatment, and are relatively rare. Desmoid tumors may occur in a variety of sites, but most commonly arise in the extremities (42% to 51%). A chest wall site of origin has been reported in 10% to 28% of the cases, while an abdominal wall origin has been found in 12% to 22%. An increased risk has been associated with certain anatomical locations, especially the foot and calf, and with an intra-lesional or marginal resection [1]. Recurrence after incomplete surgical removal (18% to 54%) is usual, and death occurs as a result of the invasion of local structures [2]. Of several therapeutic approaches, no method to date has proven ideal

Division of Thoracic Surgery, Department of Surgery, National Taiwan University Hospital;
*Department of Pathology, National Taiwan University Hospital
Address reprint requests to: Dr. Yung-Chie Lee, Division of Thoracic Surgery, Department of Surgery, National Taiwan University Hospital, No 7, Chung-Shan S Rd, Taipei, Taiwan

for the treatment of recurrence, which aggravates the prognosis. With the availability of improved techniques in chest wall reconstruction, we recommend an aggressive wide resection of the tumor whenever possible.

Case Report

A 48-year-old woman came to our hospital in October of 1997 for a painful and slowly enlarging recurrent lump on her right shoulder. She has been operated on twelve times for multicentric desmoid tumors in the past 22 years.

Initially, she had had an abdominal wall tumor in her third decade. A biopsy confirmed the diagnosis of infiltrative fibromatosis. She underwent radical surgery, but the tumor recurred 3 years later. Another surgery was performed and the tumor was resected, but grew again over the course of only a few months. At 32 years of age, she had an abdominal wall tumor that had invaded the peritoneum, so, another operation was undertaken. Unfortunately, four years later, a tumor recurred and adhered to the peritoneum and mesentery. A CT scan of the abdomen revealed an intra-abdominal desmoid tumor. Her abdomen became protuberant, with masses extending from her mid-line incision. An excisional specimen (12 x 12 x 5cm) was composed of proliferating fibroblasts. The patient was again beginning to experience abdominal distension, nausea, and vomiting. A very large intra-abdominal desmoid involving the mesentery was resected, and necessitated the removal of her small bowel; another tumor rising from the nuchal fascia was resected at the same time. It has been noted that she did not have a previous colon polyp. At 42 years old, a tumor was found in the upper right back area. The lesion became ulcerative with pain, and was resected in 1991. She then developed a palpable breast lump at the age of 45, which later on proved to be a desmoid tumor. Anti-estrogen therapy failed to halt the progression of the disease. She also had two large firm deep lumps, one (10 x 8 x 6cm) overlaying the left lower ribs, and another (5 x 4 x 3cm) on the right scapular area. Two titanium plates conducted excision and reconstruction of the chest wall. A physical examination disclosed evidence of recurrent desmoid formation, most notably found at the right scapula. The patient also complained of right shoulder pain and weakness.

The examination showed that a firm, tender, subcutaneous 3 x 3cm plaque overlaid the right shoulder. Her range of motion was limited because of the pain. The remainder of her examination was unremarkable, except for old operative scars.

Laboratory studies revealed the following values: hemoglobin, 12.2 g/dL; and WBC count, 5360/ mm^3 (28% lymphocytes, 65.2% neutrophils, 4.1% monocytes) The results of a routine serum multichemistry screen and urinalysis were unremarkable. Chest radiographs did not disclose a defined density on the right chest wall, but a chest echo demonstrated a hypodensity lesion in the right scapular area. Fine needle aspiration was performed, although a cytology report was not made. A wide local excision of the tumor was performed.

Grossly, the soft tissue mass measuring 7 x 7 x 7 cm in size was firm. On the cut surface, it was white fibrous tissue with an irregular margin. Histologically, it was composed of proliferating fibroblasts with bland nuclei and rare mitoses. The skeletal muscle fibers were irregularly infiltrated or entrapped by the tumor, with section

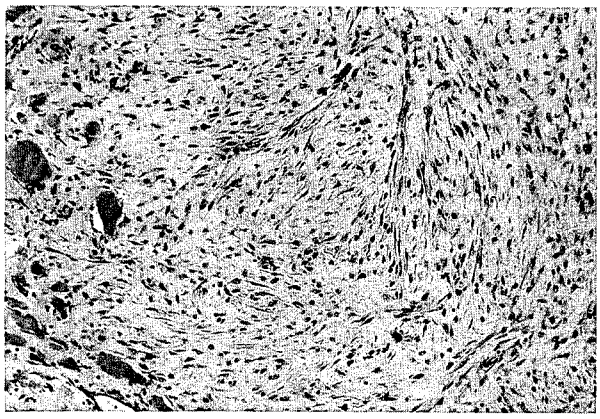

Fig. 1. Histological features of a desmoid tumor showing infiltrative scar-like fibrous tissue.

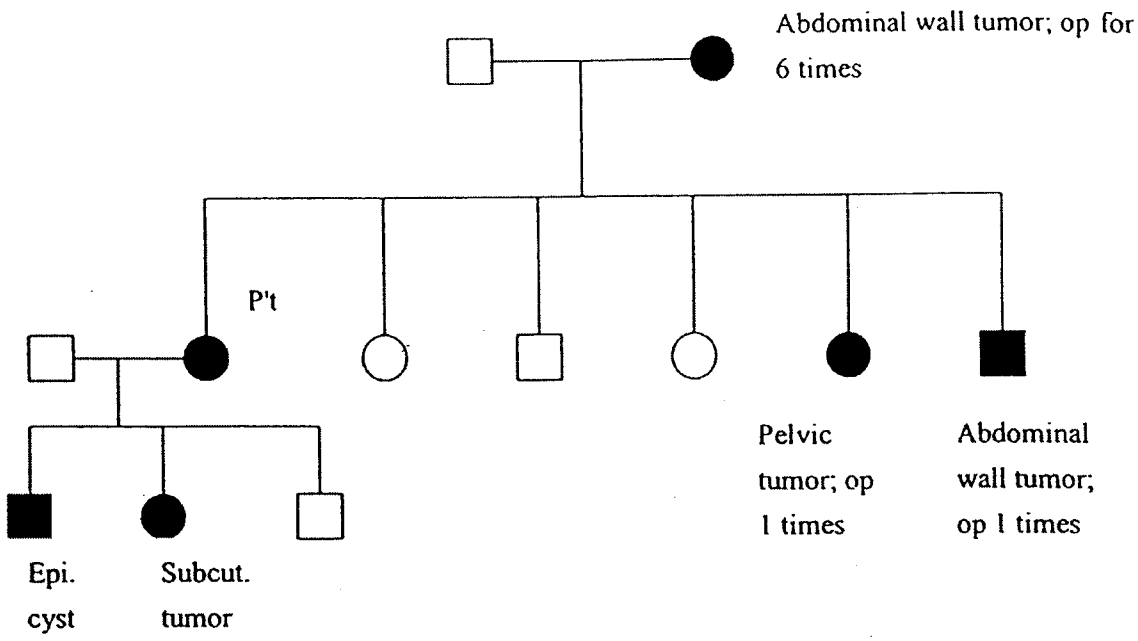

Fig. 2. Pedigree structure and disorders of the family members. op: operation, p't: patient, epi: epidermoid, subcut: subcutaneous

margin involvement (Figure 1). A diagnosis of fibromatosis of the chest wall was rendered. No evidence of recurrence has been noted until since the operation.

The family history showed that the patient's sister and brother had had pelvic and abdominal wall desmoid tumors. The patient's mother had similarly suffered from abdominal wall tumors, and was operated on six times for clinically palpable desmoid tumors. Moreover, her two daughters were clinically affected with small desmoid tumors of the skin. The structure and clinical features of the family are shown in Figure 2.

Discussion

Fibromatoses have been divided into superficial and deep-seated types. The deeper fibromatoses are termed desmoid tumors. Desmoid tumors derive from fascial or musculoaponeurotic soft-tissue structures. The term, "desmoid", was first applied by Muller in 1838. Histologically, the tumors are well-differentiated as intertwining fibroblasts and fibrocytes in variably loose or dense collagenous stroma, but their locally invasive and destructive manifestations are considered malignant soft-tissue tumors. However, they lack the pleomorphism of the nuclear and cytoplasmic features of cancer, and no metastases have been reported. Finger-like projections of the tumor frequently extend microscopically beyond their gross extent. This patient demonstrated the same pictures and multicentric involvement.

The incidence of these tumors is between 2 and 4 cases per million population per year, representing 3.6% of the neoplasms composed of fibrous tissues [3]. Approximately 58% of the desmoid tumors are extra-abdominal, 36% are abdominal, and 15% are intra-abdominal (mesenteric), with some overlap of categories [4]. Most extra-abdominal desmoid tumors originate from the extremities, the chest wall, and the head and neck. Intra-abdominal (mesenteric) and abdominal sites are associated with intrinsic genetic defects, such as FAP and Gardner variants [5]. Sen-Gupta et al. reported a somatic mutation of the adenomatous polyposis coli (APC) gene in the desmoid tumor tissue of a patient with polyposis coli caused by constitutional

chromosome 5q22 deletion [6]. These authors concluded that there is residual heterogeneity in the phenotypic expression of FAP, and suggested that the influence of other genes, as well as certain environmental factors or even chance, may be important. Affected individuals with hereditary desmoid disease kindred are characterized by multifocal fibromatosis of the paraspinal muscles, breast, occiput, arms, lower ribs, abdominal wall, and mesentery. Osteomas, epidermal cysts, and other congenital features have also been observed in these family members [7]. Riccardo et al. also reported a similar family, with a truncating mutation at the 3000'of the APC gene, resulting in a disease other than FAP. The site of desmoid tumors arising in the family members are unusual compared to the pattern observed in most FAP patients, such that the majority of FAP patients have the disease remotely from the abdominal wall and peritoneal cavity [7].

Several theories have been proposed for the origin of desmoid tumors, however, their pathogenesis and natural course still remain unclear. Pregnancy, estrogenic hormones, heredity, and trauma have been implicated in the development of desmoid tumors [8]. Patients are usually between twenty and forty years old, though all ages can be affected. Long-term follow-up suggests that the tumor's growth rate often decreases or ceases after an initial period of growth [9].

Early diagnosis and treatment are crucial to minimizing morbidity and mortality. Although an incisional biopsy is not always performed, there is no evidence that it is detrimental to the initial step of reaching a diagnosis [4]. Imaging is important for defining the extent of tissue involvement. Magnetic resonance imaging may prove to be the most effective method in evaluating both soft tissue extension and tumor recurrence.

Once the diagnosis is established, wide local excision is proposed as the definitive management of desmoid tumors. Most studies have suggested that the histopathological examination of the resectional margin can reflect the subsequent risk of local recurrence [2,10]. Adjuvant radiotherapy for positive, questionable, or reactive margins supplies good local control [11]. Radiotherapy or endocrine treatment is preferred for patients with an inoperable tumor or gross residual disease, after an operative management that might lead to major morbidity or loss of function. Adequate resection offers the best results, while adjuvant radiation therapy is probably beneficial. The use of chemotherapeutic agents may be grouped into four categories: traditional cytotoxic agents, non-steroidal anti-inflammatory drugs, cyclic-adenosine monophosphate, and anti-hormonal agents. The most frequently used chemotherapeutic agents appear to be doxorubicin, dactinomycin, and vincristine. The cAMP modulators include theophylline, chlorothiazide, ascorbic acid, and testolactone. NSAIDs may improve immune surveillance through prostaglandin suppression [12]. The preponderance of cases in women of childbearing age and reports of spontaneous tumor regression during menarche and menopause have raised the possibility of endocrine therapies [13].

Several interesting phenomena may be associated with this patient. Of particular interest with respect to her is the familial disorder and multicentric involvement with several operations. All of these features are classic. We conclude that our patient had either the same disorder of FAP or a very similar one. The present study provides evidence which shows that the ability to control local disease has improved. Better imaging techniques may have contributed to better preoperative planning. Surgical interventions have been accepted as a treatment for desmoid tumors, with survival rates close to 80%. Though not widely accepted for these patients, surgery can be an effective therapy. Adequate resection offers the best chance for a so-called cure. Adjuvant radiation therapy is probably beneficial, but the precise indication for its use is not well defined. However, it is clear that there is not one

method that is totally effective. Excision after the failure of medical therapy appears suitable, particularly for dysfunction patients. In conclusion, we believe this experience is the most significant observation ever reported indicting surgical intervention in the initiation of recurrence.

References

1. Rock MG, Pritchard DJ, Reiman HM, *et al.* Extra-abdominal desmoid tumors. J Bone and Joint Surg 1984; 66-A: 1369-74.
2. Posner MC, Shiu MH, Newsone JL, *et al.* The desmoid tumor: not a benign disease. Arch Surg 1989;124:191-6.
3. Welling RE, Hermann ME, Kasper GC. Experience with desmoid tumor in a community teaching hospital. J Surg Oncol 1992; 49: 113-5.
4. Mendez-Fernandez MA, Gard DA. The desmoid tumor: "benign' neoplasm, not a benign disease. Plast Reconstr Surg 1991; 87: 956-60.
5. Eagel BA, Zentler-Munro P, Smith IE. Mesenteric desmoid tumors in Gardner's syndrome: review of medical treatments. Postgrad Med J 1989; 65: 497-501.
6. Sen-Gupta S, Van der Lukt RB, Bowles LV, *et al.* Somatic mutation of APC gene in desmoid tumor in familial adenomatous polyposis. Lancet 1993;342:552-3.
7. Diana ME, Rob van der Luijt, Riccardo F, *et al.* Hereditary desmoid disease due to a frameshift mutation at codon 1924 of the APC gene. Am J Hum Genet 1996; 59: 1193-201.
8. Sweis IE, McHenry CR, Jordan RB. Limb- and life-threatening desmoid tumor of the neck. Plast Reconstr Surg 1993; 92: 335-9.
9. Winer-Muram HT, Borwman LC, Parham D. Intrathoracic desmoid tumor: CT and MRI appearance. South Med J 1994; 87: 1007-9.
10. Sherman NE, Romsdahl M, Evans H, *et al.* Desmoid tumors: a 20-year radiotherapy experience. Internat J Radiat Oncol Biol Phys 1990; 19: 37-40.
11. McCollough WM, Parsons JT, van der Griend R, *et al.* Radiation therapy for aggressive fibromatosis. The experience at the University of Florida. J Bone and Joint Surg 1991; 73-A: 717-25.
12. Waddell WR, Kirsch WM. Testolactone, sulindac, warfarin and vitamin K for unresectable desmoid tumors. Am J Surg 1991; 161: 416-21.
13. Wilcken N, Tattersol MHN. Endocrine therapy for desmoid tumors. Cancer 1991; 6: 1384-8.

多發家族性纖維瘤病——病例報告及文獻回顧

黃培銘　張逸良*　李元麒

侵犯性纖維瘤病是一種良性、罕見、及時常緩慢生長的腫瘤，對於化學及放射線療法常有抵抗性。他們常發生在任何肌肉筋膜層，且有向鄰接的組織侵潤，變大的趨勢，和引起機能的限制或者疼痛，但不轉移。

我們報告一個四十八歲的女性病例，在 22 年來她因為纖維瘤病接受了十二次的手術。之前她有腹壁的纖維瘤病，並且這個遺傳性的纖維瘤疾病影響到三代的親屬，但是並無家族性大腸息肉症的大腸息肉的特色。除此之外，此腹壁的纖維瘤病成腹內的纖維瘤病，最後一次的手術則於 1997 年 10 月因為長在腹部外靠在右側肩胛骨的纖維瘤病而開刀。我們對於腫瘤區域進行廣泛的切除，截至目前為止並無腫瘤再復發的情形發生。這種多發性且多次復發的纖維瘤病，由腹壁小腸發生，最後胸壁也發生是相當罕見的。本文針對纖維瘤病的臨床、組織學，及處理方法上加以討論說明。 ***(胸腔醫學 2002; 17: 78-83)***

關鍵詞：纖維瘤病，多發性，家族性大腸息肉症

台大醫院　胸腔外科　病理科*
索取抽印本請聯絡：李元麒醫師，台北市中山南路七號

Radiographic Manifestation of PCP in AIDS Patient

Ching-Ho Tsai, Shinn-Liang Lai

Pneumocystis carinii pneumonia (PCP) is the most common opportunistic infection in the immunocompromised host. However, early diagnosis is relatively difficult. The radiographic manifestations depend to a great extent, on the patient's state of immunosurveillance, and the duration of infection. There is no pathognomonic radiographic pattern for pneumocystis carinii pneumonia, though radiographic examination is still a reliable and useful diagnostic tool. Pneumocystis carinii pneumonia is manifested by a diffuse perihilar interstitial infiltration; other variable patterns have been observed in patients under prophylatic pentamidine treatment.

Herein, we present a case of PCP in an AIDS victim. He has had multiple sexual partners, and his girlfriend is also an AIDS patient. His major complaints included chronic cough, body weight loss, night sweating, and acute fever. Chest radiography showed a bilateral distribution of the diffuse interstitial infiltration. He was quickly diagnosed with a multiple infection, using a high index of suspicion, and received appropriate treatment. ***(Thorac Med 2002; 17: 84-88)***

Key words: pneumocystis carinii pneumonia, adult immune deficiency syndrome, interstitial infiltration, candidiasis

Introduction

Pneumocystis carinii is the most common opportunistic pathogen in the immunocompromised host [1,11]. The incidence of pneumocystis carinii pneumonia (PCP) has increased with the prolonged survival of immunocompromised patients and with improvements in the diagnostic techniques for this pathogen. In humans, three forms of the organism have been identified: the trophozoite, cyst, and sporozoite. The trophozoite, 2~5 μm in diameter, is either round or sickled-shaped. The cyst usually measures between 3 and 6 μm in diameter. Its cell wall consists of three layers, and its cytoplasma contains eight small pleomorphic intracystic bodies (sporozoites) [5,15].

The chest roentgenogram plays an important role in the diagnosis of PCP. No radiographic pattern is pathognomonic for pneumocystis infection, any more than for other "atypical" pneumonia. The radiographic pattern depends on the patient's underlying or accompanying disease, the state of immuno- suppression, and the duration of infection. In some cases, the chest roentgenogram is normal despite the clinical symptoms. Occasionally, the early stage of PCP is manifested by fine, bilateral, perihilar diffuse

Chest Department, Taipei Veterans General Hospital and Department of Internal Medicine, School of Medicine, National Yang-Ming University, Taipei, Taiwan
Address reprint requests to: Dr. Shinn-Liang Lai, Chest Department, Taipei Veterans General Hospital, 201, Section 2, Shih-Pai Road, Taipei 11217, Taiwan

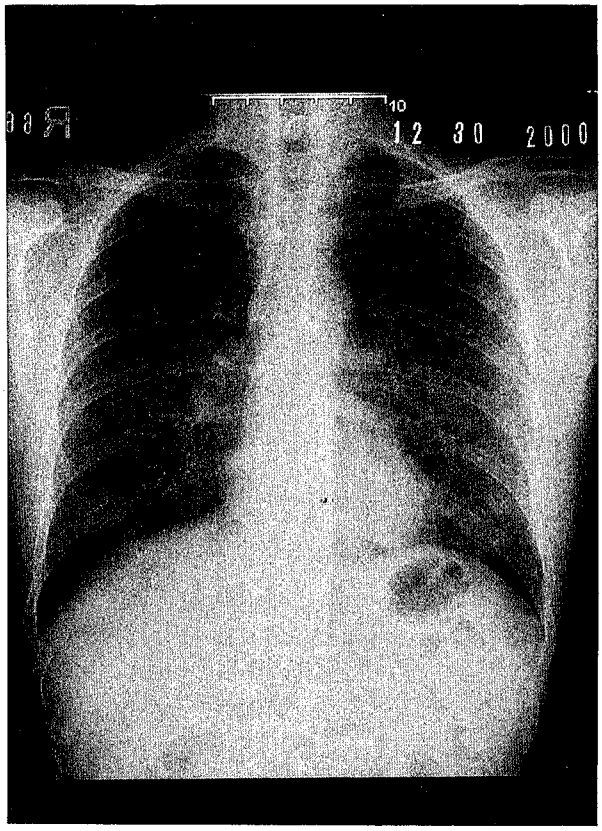

Fig. 1 CXR (admission): a bilateral diffuse reticulonodular pattern.

infiltrates that progress to an airspace pattern with a butterfly distribution. From the hilar region, the infiltrates spread to the apical or basal areas [1,9]. Similar to "atypical pneumonia", unusual manifestations and clinical courses are seen in the chest film, including nodules, unilateral infiltrates, and even lobar consolidation or minimal pleural effusion [8]. The distortions in the radiologic patterns are commonly due to prior radiation, drug-induced pulmonary injury, or concurrent infection with other organisms. The patient with recurrent pneumocystis infection may manifest chronic interstitial lesions, small cysts, or a honeycombing appearance on chest radiography [1].

Herein, we present a case of PCP in an AIDS patient who was quickly diagnosed using a high index of suspicion, then appropriately treated.

Case Report

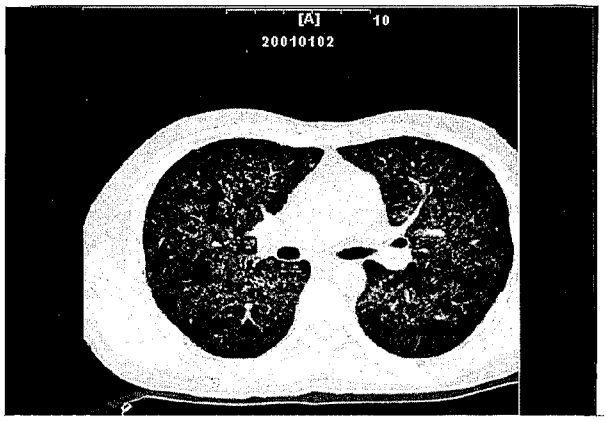

Fig. 2. Chest CT (admission): diffuse reticulonodular infiltration.

This 40-year-old male had been well until two months before this admission, when he became weak and suffered from cough, fever, and sweating, with a 9-Kg loss of body weight. He had travelled frequently in the most recent 2 years. The results of the laboratory studies in the medical emergency room were as follows: WBC: 7900/cumm; RBC: 5.84M/cumm; Band: 1%, Seg: 80%; Lym: 8.0%; Mono: 11%; PLT: 264000/cumm; ABG (O_2, 3 L/M) showed pH=7.442; $PaCO_2$=33.6 mmHg; PaO_2=135.6 mmHg; HCO_3^-=22.4 mm/l; and O_2Sat=98.8%. A long-term smoking history (1/2 PPD for 20+ years) was noted. He had traveled to China 2 weeks prior to the presence of these symptoms. In the emergency room, a CXR (Figure 1) showed diffuse reticulonodular infiltration in both lung fields. A high resolution chest CT (HRCT) scan (Figure 2) revealed diffuse reticulonodular inter- stitial infiltration in the bilateral lung fields, compatible with interstitial lung disease; no lymphadenopathy could be identified in the mediastinum.

After admission, oral candidiasis and a herpes simplex infection of the penis were found. According to his statement, his girlfriend is an AIDS victim, and he has had multiple sexual partners. A Gomori methenamine silver nitrite stain of the bronchoalveolar lavage (BAL) (Figure 3) showed pneumocystis carinii organisms. The laboratory examination showed CEA=12.29ng/ml; anti-HIV test EIA: positive; HIV-I Western blot test: positive; and CD4= lymphocytes 0.2%. A

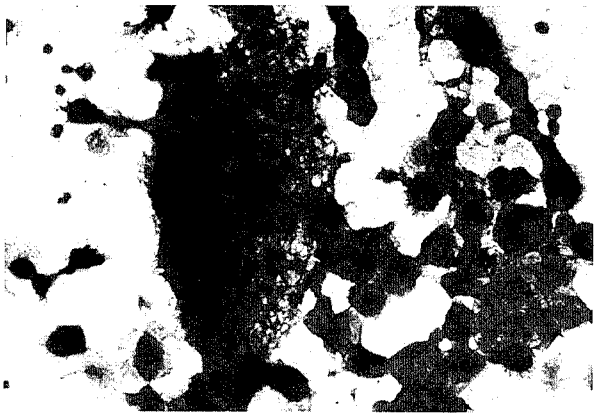

Fig. 3. GMS stain (original magnification x 400): many cysts are seen. (Gomori methenamine silver nitrite stain)

throat swab culture yielded a growth of candida albicans, and the blood cytomegalovirus ELISA Ig G test was positive. Immediate treatment with Septrin 20mg q6h and hydrocortisone 100mg q6h were given after the diagnosis was documented. An intensive surveillance for AIDS with an opportunistic infection was undertaken, then HAART (highly active anti-retrovirus therapy) was administered. Three weeks later, the patient's clinical and radiologic condition had improved (Figure 4), and the CBC showed WBC= 6400/cumm, seg=87.4%, and lym=9%.

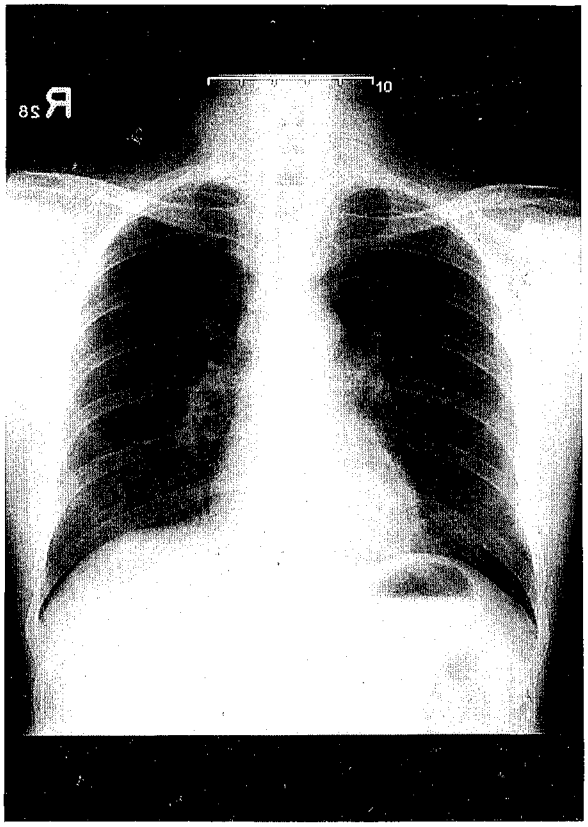

Fig. 4. CXR (recovery): the reticulonodular pattern disappeared.

Discussion

Pneumocystis carinii pneumonia is the most common and serious opportunistic pulmonary infection in patients with acquired immune deficiency syndrome (AIDS). It is estimated to occur in approximately 60% of patients with AIDS, and contributes significantly to the overall morbidity and mortality of these patients [1]. The roentgenographic manifestation of PCP in AIDS is most commonly described as a diffuse bilateral interstitial infiltration beginning in the perihilar regions. Other atypical patterns include a lobar distribution, pleural effusion, atelectasis, hilar adenopathy, and abscess formation. PCP is one of the five common HIV-associated opportunistic infections, along with oropharyngeal candidiasis, tuberculosis, mucocutaneous herpes simplex infection, and CMV infection. This case had a combined infection by several organisms: pneumocystis carinii, candida, herpes simplex, and possibly CMV, all at the same time. Impaired cellular immunity, which was disclosed by the very low level of CD4, may have contributed to the combined infections.

Lawrence *et al* studied 104 patients and found that bilateral diffuse interstitial infiltrates were seen in 99 patients, and was the most common CXR pattern. The others were unilateral infiltration in 5 patients; entire lung field involvement in 50 patients; localized infiltration involving the lower lungs in 35 patients; upper lung field involvement in 6 patients; the middle lung fields in 6 patients; and both middle and lower lung fields in 7 patients [1]. Atypical roentgenographic patterns, such as pulmonary air-filled cysts or pneumatoceles, which may lead to spontaneous pneumothorax, were indentified in

10% of the cases [2].

The differential diagnosis of pyogenic pulmonary infection (PPI) from PCP in AIDS patients is extremely important. The diffuse lung parenchymal pattern is much more common in PCP. On the other hand, lobar consolidation, the nodular pattern, round or patchy densities with pleural effusion, or pleural effusion alone, are noted mostly in the bacterial pneumonia group [3].

Janet categoriged three CT patterns in PCP: 26% ground-glass patterns, 56% patchwork patterns and 18% interstitial patterns. HRCT may allow the exclusion of PCP in patients with findings that are normal, equivocal, or nonspecific on the chest radiographs. HRCT has 100% sensitivity, 89% specificity, and 90% accuracy for the diagnosis of pneumocystis carinii pneumonia [12]. In summary, PCP is difficult to diagnose, and the diagnosis is usually delayed. A high index of suspicion of PCP is based on the patient's history, physical examination, and radiographic manifestations. A series survey should be arranged, and the appropriate treatment given as soon as possible.

Reference:

1. Lawrence J. DeLorenzo, Chin Tang Huang, George P. Maguire: Roentgenographic Patterns of Pneumocystis carii Pneumonia in 104 Patients with AIDS. Chest, 1987; 91: 323-25.
2. Sandhu JS, Goodman PC: Pulmonary cysts associated with Pneumocystis carinii pneumonia in patients with AIDS. Radiology, 1989; 173(1): 33-5.
3. Judith K. amorosa, Ronald G. Nahas, John L.Nosher, *et al*: Radiologic Distinction of Pyogenic Pulmonary Infection from Pneumocystis carinii Pneumonia in AIDS Patients. Radiology, 1990; 175: 721-24.
4. Janet E. Kuhlman, Madhav Kavuru, Elliot K. Fishman, *et al*: Pneumocystis carinii Pneumonia:Spectrum of Parenchymal CT Findings. Radiology, 1990; 175: 711-4.
5. Joy Alan Fishman: Pneumocystis carinii, Alfred p. Fishman, Jack A.Elias, Jay A. Fishman et al, Fishman's Pulmonary Disease and Disorders, 3rd, New York, McGraw-Hill company, 1998; 2313-32.
6. Peter Armstrong : Basic pattern in lung disease, Peter Armstrong, Alan G. Wilson, Paul Dee, *et al*: Imaging of Disease of the Chest, 3rd edition, London, Mosby Harcourt Publishers limited, 2000; 259-63.
7. John F. Murray, John Mills: Pulmonay Infection Complications of Human Immunodeficiency Virus Infection. AM REV RESPIR DIS, 1990; 141: 1356-72.
8. David P. Naidich, Stuart M. Garay, Barry S. Leitman, *et al*: Radiographic Manifestations of Pulmonary Disease in the Acquired Immunodeficiency Syndrome (AIDS). Seminars in Roentgenology, 1987; Vol XXII, No 1 (January): pp 14-30.
9. Bernard Suster, Michael Akerman, Marilyn Orenstein, *et al*: Pulmonary Manifestations of AIDS: Review of 106 Episodes. Radiology, 1986;161: 87-93.
10. Feurstein IM, Archer A, Pluda JM, *et al*: Thin-wall cavities, cysts, and pneumothorax in Pneumocystis carinii pneumonia: furthure observations with histopathologic correlation. Radiology, 1990; 174(3 Pt.1): 697-702.
11. Jedlovsky V, Fleischman JK: Pneumocystis carinii pneumonia as the first presentation of HIV infection in patients older than fifty. AIDS Patient Care & STDS, 2000; 14(5):247-9.
12. James F.Gruden, Laurence Huang, Jon Turner: High-Resolution CT in the Evaluation of Clinically Suspected Pneumocystis carinii Pneumonia in AIDS Patients with Normal, Equivocal, or Nonspecific Radiographic Findings. AJR 1997;169: 967-75.
13. Naresh G. Mansharamani, Robert Garland, David Delaney, *et al*: Management and Outcome Patterns for Adult Pneumocystis carinii Pneumonia, 1985 to 1995. Chest, 2000; 118:704-11.
14. Margarent H. Chaffey, Jeffrey S. Klein, Gordon Gamsu, et al: Radiographic Distribution of Pneumocystis carinii Peumonia in Patients with AIDS Treated with Prophylactic Inhaled Pentamidine. Radiology, 1990; 175: 715-9.
15. Laurence Huang, John D. Stansell: Pulmonary Complications of Human Immunodeficiency Virus Infection, John F Murray, Jay A Nadel, Mason Boushey, et al: Textbook of Respiratory Medicine, 3rd edition, Philadelphia, W.B. Saunders Company, 2000; 2187-96.

免疫不全病人卡氏肺囊蟲肺炎的胸部放射學表現

蔡清和　賴信良

卡氏肺囊蟲肺炎是免疫不全的人最常見的伺機性感染，但在診斷上常有困難；因在疾病不同時期或感染時間的長短，其胸部放射學表現會有差異。雖然胸部放射學的表現不能作確定的診斷，但其仍是最具有參考價值的。一般常見的胸部放射學表現為兩側瀰漫性間質型浸潤，但在接受預防性 Pentamidine 使用的病人，其胸部放射學的表現會有變化，增加診斷上的難度。

在此提出一個免疫不全病人卡氏肺囊蟲肺炎的病例，病患有多位性伴侶，且一位女友為後天免疫不全症候群患者。病患有慢性咳嗽、體重減輕、盜汗和急性發燒，胸部放射學上的表現為兩側瀰漫性間質型浸潤。在高度的警覺下，很快的診斷，並于治療。在此討論其胸部放射學上的表現，期能提高警覺，及早診斷，及早治療。 ***(胸腔醫學 2002; 17: 84-88)***

關鍵詞：卡氏肺囊蟲肺炎，成人免疫不全症候群，間質型浸潤

台北榮民總醫院　胸腔部
索取抽印本請聯絡：賴信良醫師，台北市北投區石牌路二段 201 號